A BIPARTITE SORTING SIGNAL ENSURES SPECIFICITY OF RETROMER COMPLEX IN MEMBRANE PROTEIN RECYCLING

A Dissertation

Presented to the Faculty of the Graduate School

Of Cornell University

In Partial Fulfillment of the Requirements for the Degree of

Doctor of Philosophy

by

Ya-Shan Chuang

August 2019

A Bipartite Sorting Signal Ensures Specificity of Retromer Complex in Membrane Protein Recycling

Ya-Shan Chuang, Ph.D.

Cornell University 2019

In the endosomal network, membrane proteins are either sorted into intraluminal vesicles for the lysosomal degradative pathway or exported from the endosome to the trans-Golgi network (TGN) via retrograde transport. Retromer is an evolutionarily conserved protein complex, which sorts functionally diverse membrane proteins into recycling tubules/vesicles from the endosome. Many of the identified cargos possess a recycling signal sequence defined as ØX[L/M/V], where Ø is a bulky aromatic residue and X could be any residue. However, this sequence is present in almost all proteins encoded in the genome. Also, several identified recycling sequences do not follow this rule. How retromer precisely selects its cargos remains unclear.

Here, we reveal that an additional motif is also required for cargo retrieval. The two distinct motifs form a bipartite recycling signal recognized by the retromer subunits, Vps26 and Vps35. Strikingly, Vps26 utilizes different binding sites depending on the

cargo, allowing retromer to recycle different membrane proteins. Thus, the complicated interaction between the retromer complex and cargoes increases the diversity and specificity in the recognition of cargo recycling.

BIOGRAPHICAL SKETCH of YA-SHAN CHUANG

Ya-Shan Chuang was born in Taichung City in Taiwan. He attended Taichung First Senior High School and received a Bachelor of Science in Life Science from National Tsing Hua University in 2006. After graduation, he joined Academia Sinica to do research on plant and immunobiology, followed by making the military service as a Second Lieutenant in Taiwan. In 2009, he went to University of Minnesota as a research assistant, studying embryonic stem cells, adipocytes, and immunology. In 2011, he came back to Taiwan and worked in the National Taiwan University Hospital to study induced pluripotent stem cells. In 2012 Ya-Shan accepted an offer from the graduate school of Cornell University and joined the Field of Biochemistry, Molecular, and Cell Biology in the Department of Molecular Biology and Genetics. In 2013, he was awarded the Government Scholarship to Study Abroad by the Ministry of Education, Republic of China (Taiwan). He then joined Dr. Scott Emr's lab and pursued the Ph.D. study to provide insight into how lysosomal membrane protein degradation is regulated and how cargos are precisely recognized for recycling. He has published his work in *Molecular Cell, eLife, and Journal of Cell Biology*.

This work is dedicated to my dear mother Bi E Lin.

此書獻給我親愛的母親林碧娥

ACKNOWLEDGMENTS

The journey to PhD is a long road. In front of me are countless challenges and uncertainties. This process is much more difficult than I thought in the beginning. I cannot imagine whether I will reach the end if there is nobody out there for me. There are lots of people I need to thank. And I am happy to show my gratitude to those who have helped me in this PhD journey.

First of all, I would like to thank my family, especially my mother and sister. Their unconditional support for me during the PhD is an important reason why I would continue in the face of many difficult times. Their care brings me great comfort and peace in my most anxious conditions. My success is also their success. I also believe that their love will continue to be important in my future career.

PhD training equips me to be critical thinkers, a fundamental skill in diverse careers. Studying with the great master of the field, I gained the preparation essential to my success. Thus, I am honored to thank my advisor, Scott Emr. He provided the environment where I can be trained to think critically and logically and also perform well under long-term pressure and uncertainties. “When one dares to try, rewards are not guaranteed, but at least it is an adventure." said Andre Geim, the 2010 Nobel Laureate. In this long road, I encountered great difficulties many times. After those years, I came to realize that adversity is common in reality, and that I needed to

learn how to live with that until I overcome it. I learned not to let my emotions cloud my judgements in my hard time. After all, anything that happens in the PhD is part of the training. There are so many times that I questioned myself whether I can make it. However, when I'm writing those words, I know that I do make it. None of these will not happen if I did not come here.

I also want to express my deep appreciation to Sho Suzuki and Ming Li. Without them, I don't think that I will have a chance to write this thesis today. Both Sho and Ming are highly talented scientists. It is very lucky for me to work with them so that I could learn so many things from them and also have an accomplishment in this research career. It would be another chapter if I write down everything they have helped me. I'll surely remember them in my future career.

Finally, I would like to thank God to bring me to Cornell, an extremely beautiful and fantastic school. There are only certain opportunities that come along in my life to be extraordinary, and this is one of them. This is really a once-in-a-lifetime opportunity. All the experience I had here is unforgettable in my life! I've heard that the Ivy League mentality includes mental toughness, perseverance, confidence, passion, and social responsibility. And now I can safely say that I am prepared well to face the future, no matter what will happen next.

TABLE OF CONTENTS

LIST OF FIGURES

LIST OF TABLES

Chapter I

Introduction

1.1 Membrane Trafficking System

In eukaryotic cells, proteins that follow the secretory and endocytic pathways are eventually either secreted or transported to one of several distinct organelles: the endoplasmic reticulum (ER), the Golgi complex, the endosome, the vacuole/lysosome, or the plasma membrane (PM). In the endosomal network, membrane protein cargos are either sorted from the endosomal membrane for transport into the lysosomal degradative pathway, or exported from the endosome to the Golgi via retrograde transport. The function of a particular organelle is mainly determined by the composition of the resident membrane proteins. Therefore, the trafficking of these integral membrane proteins must be well-regulated to maintain the integrity and homeostasis of individual organelles. The vacuole of the budding yeast *Saccharomyces cerevisiae*, for example, requires accurate trafficking of its resident proteins to maintain its normal function. Analogous to the lysosome of mammalian cells, the vacuole exerts multiple cellular functions, including macromolecular degradation, nutrient storage, and pH homeostasis (Klionsky et al., 1990). The normal operation of the vacuole requires vacuole-resident proteins such as proteases, hydrolases, and transporters. The vacuolar trafficking of these proteins involves multiple events, including cargo selection and vesicle formation from donor membranes, followed by the transport, docking and fusion of the

vesicular intermediates with the target organelle. Several genetic screens have been utilized to characterize mutants defective in vacuolar protein sorting (VPS), and nearly 50 VPS genes have been identified that function in the delivery of proteins from the trans-Golgi network to the vacuole (Bankaitis et al., 1986).

Protein trafficking to the vacuole in budding yeast is a valuable system for the study of vesicle-mediated protein transport. Investigation of the Golgi-to-vacuole transport revealed at least two distinct sorting pathways that deliver cargo proteins to the vacuole: the CPY and ALP pathways (Figure 1.1) (Odorizzi et al., 1998). The CPY pathway represents the major route of vacuolar trafficking by which many resident vacuolar proteins, such as the soluble hydrolase carboxypeptidase Y (CPY) and the vacuolar membrane protein carboxypeptidase S (CPS), are transported to the vacuole via an endosomal compartment. Golgi-to-endosome transport in the CPY pathway requires the Gga coat proteins for transport from the Golgi complex to the endosome, the guanine nucleotide exchange factor Vps9 for vesicle fusion, and the t-SNARE Pep12 at the endosome, while the endosome-to-vacuole transport of CPS in the CPY pathway requires the t-SNARE Vam3, the HOPS tethering complex, and the endosomal sorting complexes required for transport (ESCRTs), which are essential for the delivery of proteins destined for lysosomal/vacuolar degradation. In contrast, the vacuolar membrane protein alkaline phosphatase (ALP) and the vacuolar t-SNARE Vam3 are sorted from the Golgi to the vacuole via the ALP pathway, which depends on the AP-3 complex and bypasses the CPY pathway.

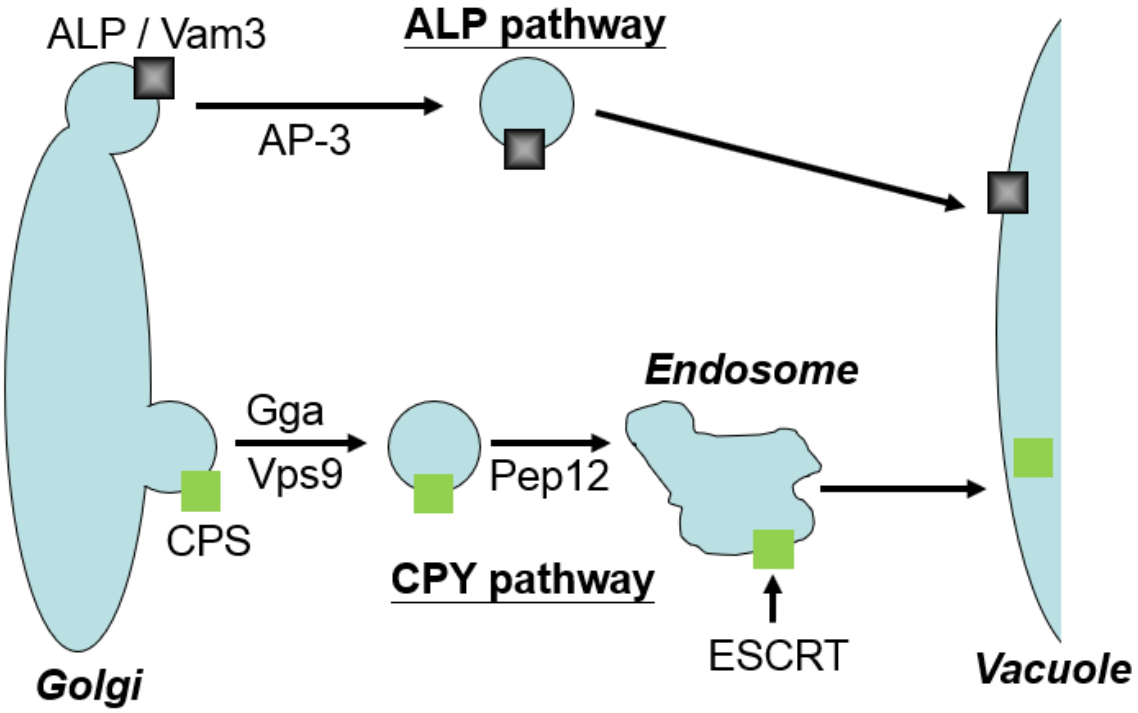
ALP / Vam3
ALP pathway
AP-3
Endosome
Gga
Vps9
Pep12
CPS
CPY pathway
ESCRT
Golgi
Vacuole

Figure 1.1

Figure 1.1. The ALP and CPY Pathways.

Proteins in the Golgi complex can be transported to the vacuole via two different pathways: the CPY and ALP pathways. In the CPY pathway, cargos such as the soluble hydrolase carboxypeptiase Y (CPY) and the vacuolar membrane protein carboxypeptidase S (CPS) are transported to the vacuole via an endosome. The Gga coat proteins are required for the vesicle formation in the Golgi complex, and the guanine nucleotide exchange factor Vps9, the Rab GTPase Vps21 as well as the t-SNARE Pep12 at the endosome are essential for the fusion of vesicles with the vacuole. In the ALP pathway, cargos such as the vacuolar membrane protein alkaline phosphatase (ALP) and the vacuolar t-SNARE Vam3 bypass the endosome and are transported from the Golgi complex to the vacuole. The AP-3 complex is required for the formation of ALP vesicles.

1.2 Protein Ubiquitination

Ubiquitination is a type of post-translational modification in which ubiquitin is covalently added to particular amino acids within a protein sequence. This modification regulates protein turnover, activity, and interactions. The conjugation of ubiquitin to a protein includes three main steps: activation, conjugation, and ligation, performed by ubiquitin-activating enzymes (E1s), ubiquitin-conjugating enzymes (E2s), and ubiquitin ligases (E3s), respectively (Kerscher et al., 2006). The E3 ubiquitin ligases interact with the substrate protein and therefore regulate the specificity of the ubiquitination reaction. E3 enzymes contain one of two domains: the Homologous to the E6-AP Carboxyl Terminus (HECT) domain and the Really Interesting New Gene (RING) domain (Pickart and Eddins, 2004). HECT E3s interact with the substrate and act through an E3-Ub intermediate for ubiquitin transfer. In humans, The Nedd4 family of E3 ubiquitin ligases plays an essential role in protein ubiquitination (Ingham et al., 2004). Nedd proteins possess a catalytic C-terminal HECT domain for ubiquitin transfer, a N-terminal C2 domain for lipid interaction, and WW domains for protein-protein interactions by recognizing proline-rich motifs such as PPxY motifs (Sudol, 1996; Rotin et al., 2000).

Rsp5 is the yeast equivalent of the human Nedd4 proteins and is essential for cell viability. Studies have clearly shown that Rsp5 plays a critical role in intracellular trafficking. For example, Rsp5-mediated ubiquitination is required for the endocytosis of the plasma membrane transporter Mup1 and the sorting of

carboxypeptidase S (CPS) from the Golgi to the vacuole by the multivesicular body (MVBs) pathway (Haguenauer-Tsapis and André, 2004; Dunn et al., 2004). Rsp5 has been found to use adaptor proteins for substrate recognition. For example, the PPxY motif-containing membrane adaptors Ssh4 and Ear1 interact with Rsp5 to regulate the ubiquitination and endocytosis of the uracil transporter Fur4 (Léon S et al., 2008).

1.3 Mechanisms of Protein Degradation

Many proteins are transported to the vacuole/lysosome for their turnover, which is the major degradative organelle in eukaryotic cells. It degrades PM proteins via endocytosis as well as intracellular components by autophagic and the MVB pathway (Figure 1.2). Furthermore, the vacuole also functions as a storage organelle for amino acids, ions, phosphate, and other small molecules. These molecules are transported into and out of the vacuole by a family of integral membrane transporters. This membrane transport system allows the cell to quickly adjust to changes in the nutrient level of the environment. Regulation of these vacuole membrane proteins is critical to maintain vacuolar integrity and functionality. In humans, defects of lysosomal membrane proteins can lead to lysosomal storage diseases. Mutation in the lysosomal cystine transporter cystinosin, for example, can cause cystinosis in humans (Kalatzis et al., 2004). Moreover, NPC1, the lysosomal cholesterol transporter, is mutated in type C Niemann – Pick disease, resulting in a dramatic accumulation of cholesterol within lysosomes (Carstea et al., 1997). It is therefore important to understand the regulation and turnover of lysosomal membrane proteins.

Despite their importance, the functional lifetime of vacuolar membrane proteins and the mechanisms that regulate their selective degradation are still poorly characterized. For PM proteins, environmental changes can induce the ubiquitination of those proteins and endocytosis for degradation. In the event of

endocytic turnover, both the internalization of ubiquitinated cargoes from the PM and their sorting at MVBs are dependent upon ubiquitin binding motifs present in trafficking regulators (Katzmann et al., 2001). The MVB pathway is mediated by the ESCRT machinery, which promotes the internalization of ubiquitinated cargoes into the lumen of endosomes. In contrast to PM protein turnover, little is known about the regulation of the quantity and quality of vacuolar membrane proteins. It remains elusive whether the cell has a protein quality control system to selectively down-regulate vacuolar membrane proteins.

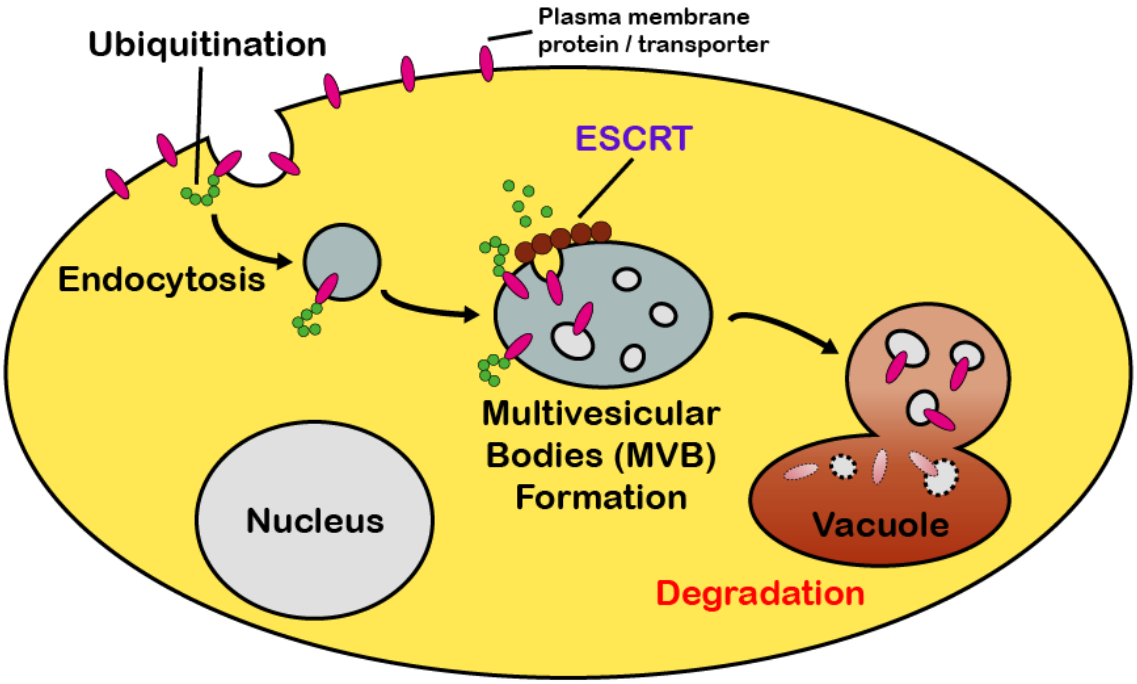
Ubiquitination
Plasma membrane
protein / transporter
ESCRT
Endocytosis
Multivesicular
Bodies (MVB)
Formation
Nucleus
Vacuole
Degradation

Figure 1.2

Figure 1.2. Plasma membrane protein degradation

Upon stimulation, plasma membrane proteins are ubiquitinated first by the E3 ubiquitin ligase and endocytosed to form a vesicle. The endocytosed vesicle fuses with the endosome. The ubiquitinated membrane proteins then recruit the ESCRT machinery, which promotes the internalization of ubiquitinated proteins into small vesicles that bud into the endosome forming multi-vesicular bodies (MVBs). The MVBs finally fuse with the vacuole to release the internal contents for degradation.

1.4 Mechanisms of Protein Recycling

In addition to the degradative pathway, some endosomal proteins can also be recycled to the plasma membrane or transported to the Golgi via retrograde trafficking. Retromer mediates the recycling of cargoes from the endosome to the Golgi (Seaman et al., 1997; Seaman et al., 1998; Cullen and Steinberg., 2018). In yeast, retromer is composed of five subunits that form two subcomplexes: a complex for cargo recognition, consisting of trimer of Vps26, Vps29, and Vps35, and the sorting nexins are composed of Vps5 and Vps17 for membrane association (Figure 1.3) (Seaman et al., 1998). Emr and colleagues have found that the retromer complex regulates the retrieval of the vacuolar hydrolase receptor Vps10 and the Golgi-resident proteases Kex2 and Ste13 from the endosome to the Golgi (Figure 1.4) (Marcusson et al., 1994). In mammals, retromer is required for diverse retrograde trafficking pathways such as the endosome-to-Golgi retrieval of cation-independent mannose-6-phosphate receptor (CI-M6PR), Wnt transport protein Wntless, and Sortilin-related receptor (SorL1). Retromer dysfunction is related to neurodegenerative disorders. For example, the VPS35-D620N mutation causes autosomal dominant Parkinson disease (McGough et al., 2014a; Zavodszky et al., 2014). The K297X mutation in VPS26A leads to atypical parkinsonism (Gustavsson et al., 2015; McMillan et al., 2016). Recycling defects of SorL1 are found to contribute to the development of Alzheimer disease due to its role as a receptor for amyloid-β precursor protein (AβPP).

The recycling signals recognized by retromer have not been clearly defined. The conserved sequences typically follow the ØX[L/M/V] rule, where Ø is F/Y/W. This type of motif contains at least one aromatic residue and another hydrophobic residue. It is unclear how the recycling motif of those cargos are recognized by the retromer complex. Maria Lucas et al. have shown that the YLL motif in DMT1-II can be recognized by Vps26 and Snx3, another sorting nexin (Lucas et al., 2016). However, the retromer might recognize cargos differentially and the detailed mechanism for precise and diverse recognition is still elusive.

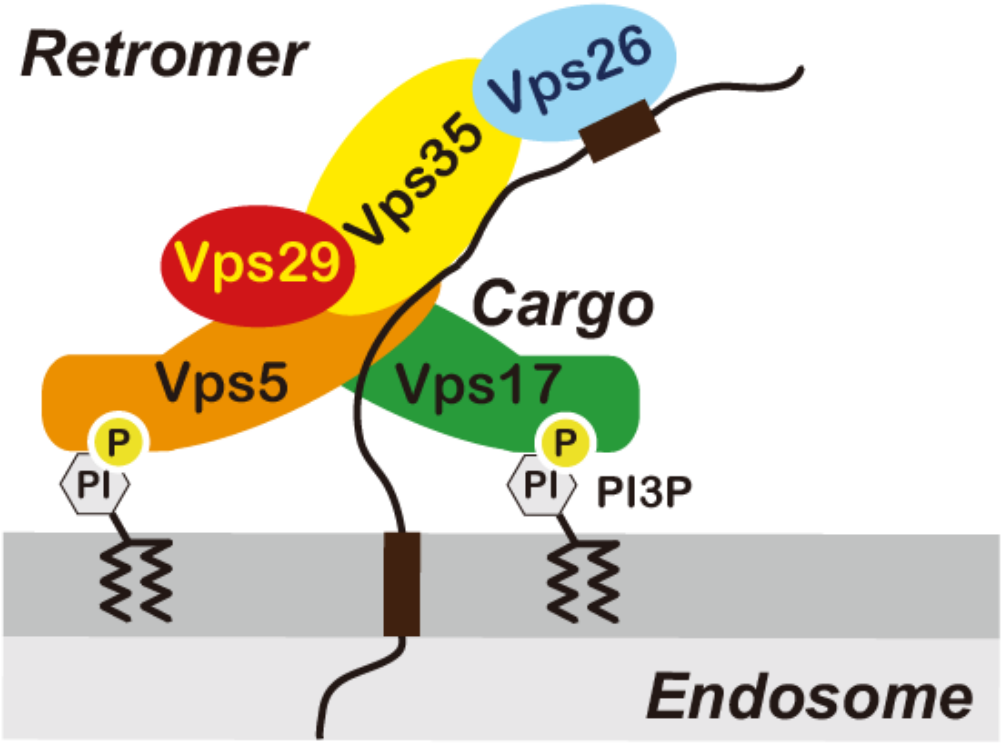
Retromer
Vps26
Vps35
Vps29
Cargo
Vps5
Vps17
P
PI
P
PI
PI3P
Endosome

Figure 1.3

Figure 1.3. The diagram of the retromer complex. Retromer consists of five subunits, including Vps26, Vps29, Vps35, Vps5, and Vps17. Vps26, Vps29, and Vps35 form the cargo selection complex, and Vps5 and Vps17 are sorting nexins for PI3P binding and membrane association.

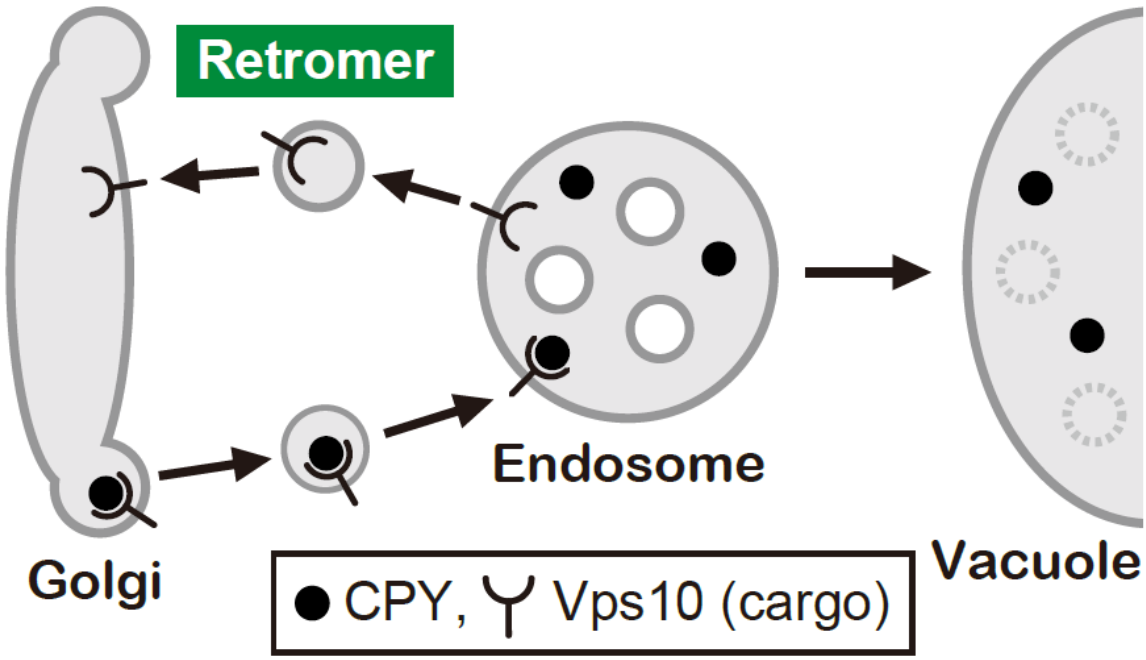

Figure 1.4

Figure 1.4. Retromer regulates Vps10 recycling. Vps10 is the sorting receptor of carboxypeptidase Y (CPY). Vps10 sorts CPY from the Golgi to the endosome, and retromer regulates the endosome-to-Golgi retrograde of Vps10.

Reference

Bankaitis VA, Johnson LM, Emr SD. Isolation of yeast mutants defective in protein targeting to the vacuole. Proc Natl Acad Sci U S A 1986; 83: 9075-9079.

Carstea ED, Morris JA, Coleman KG, Loftus SK, Zhang D, Cummings C, Gu J, Rosenfeld MA, Pavan WJ, Krizman DB, Nagle J, Polymeropoulos MH, Sturley SL, Ioannou YA, Higgins ME, Comly M, Cooney A, Brown A, Kaneski CR, Blanchette-Mackie EJ, Dwyer NK, Neufeld EB, Chang TY, Liscum L, Strauss JF, 3rd, Ohno K, Zeigler M, Carmi R, Sokol J, Markie D, O'Neill RR, van Diggelen OP, Elleder M, Patterson MC, Brady RO, Vanier MT, Pentchev PG, Tagle DA. Niemann-Pick C1 disease gene: homology to mediators of cholesterol homeostasis. Science 1997; 277: 228-231.

Cullen, P.J., and F. Steinberg. 2018. To degrade or not to degrade: mechanisms and significance of endocytic recycling. Nat. Rev. Mol. Cell Biol. 19(11): 679-696.

Dunn R., Klos D. A., Adler A. S., Hicke L. (2004). The C2 domain of the Rsp5 ubiquitin ligase binds membrane phosphoinositides and directs ubiquitination of endosomal cargo. J. Cell Biol 165, 135-144.

Gustavsson, E.K., I. Guella, J. Trinh, C. Szu-Tu, A. Rajput, A.H. Rajput, J.C. Steele, M.

McKeown, B.S. Jeon, J.O. Aasly, and M.J. Farrer. 2015. Genetic variability of the retromer cargo recognition complex in parkinsonism. Mov. Disord. 30:580–584. http ://dx .doi .org /10 .1002 /mds.26104

Haguenauer-Tsapis R., André B. (2004, Ed. E. BolesR. Krämer, Membrane trafficking of yeast transporters: mechanisms and physiological control of downregulation In: Molecular Mechanisms Controlling Transmembrane Transport, vol. 9 Berlin/Heidelberg, Germany: Springer, 273-323.

Ingham R. J., Gish G., Pawson T. (2004). The Nedd4 family of E3 ubiquitin ligases: functional diversity within a common modular architecture. Oncogene 23, 1972-1984.

Kalatzis V, Nevo N, Cherqui S, Gasnier B, Antignac C. Molecular pathogenesis of cystinosis: effect of CTNS mutations on the transport activity and subcellular localization of cystinosin. Hum Mol Genet 2004; 13: 1361-1371.

Katzmann DJ, Babst M, Emr SD. Ubiquitin-dependent sorting into the multivesicular body pathway requires the function of a conserved endosomal protein sorting complex, ESCRT-I. Cell 2001; 106: 145-155.

Kerscher O., Felberbaum R., Hochstrasser M. (2006). Modification of proteins by ubiquitin and ubiquitin-like proteins. Annu. Rev. Cell Dev. Biol 22, 159-180.

Klionsky DJ, Herman PK, Emr SD. The fungal vacuole: composition, function, and biogenesis. Microbiol Rev 1990; 54: 266-292.

Léon S, Erpapazoglou Z, Haguenauer-Tsapis R. Ear1p and Ssh4p are new adaptors of the ubiquitin ligase Rsp5p for cargo ubiquitylation and sorting at multivesicular bodies. Mol Biol Cell. 2008 Jun;19(6):2379-88. doi: 10.1091/mbc.E08-01-0068. Epub 2008 Mar 26.

Lucas M, Gershlick DC, Vidaurrazaga A, Rojas AL, Bonifacino JS, Hierro A. Structural Mechanism for Cargo Recognition by the Retromer Complex. Cell. 2016 Dec 1;167(6):1623-1635.e14. doi: 10.1016/j.cell.2016.10.056. Epub 2016 Nov 23.

Marcusson, E.G., B.F. Horazdovsky, J.L. Cereghino, E. Gharakhanian, and S.D. Emr. 1994. The sorting receptor for yeast vacuolar carboxypeptidase Y is encoded by the VPS10 gene. Cell. 77:579-586.

McGough, I.J., F. Steinberg, D. Jia, P.A. Barbuti, K.J. McMillan, K.J. Heesom, A.L. Whone, M.A. Caldwell, D.D. Billadeau, M.K. Rosen, and P.J. Cullen. 2014a. Retromer binding to FAM21 and the WASH complex is perturbed by the Parkinson disease-linked VPS35(D620N) mutation. Curr. Biol. 24:1670–1676. (published erratum appears in Curr. Biol. 2014. 14:1678) http ://dx .doi .org /10 .1016 /j .cub .2014 .06 .024

McMillan KJ, Gallon M, Jellett AP, Clairfeuille T, Tilley FC, McGough I, Danson CM, Heesom KJ, Wilkinson KA, Collins BM, Cullen PJ. Atypical parkinsonism-associated retromer mutant alters endosomal sorting of specific cargo proteins. J Cell Biol. 2016 Aug 15;214(4):389-99. doi: 10.1083/jcb.201604057.

Odorizzi G, Cowles CR, Emr SD. The AP-3 complex: a coat of many colours. Trends Cell Biol 1998; 8: 282-288.

Pickart C. M., Eddins M. J. (2004). Ubiquitin: structures, functions, mechanisms. Biochim. Biophys. Acta 1695, 55-72.

Rotin D., Staub O., Haguenauer-Tsapis R. (2000). Ubiquitination and endocytosis of plasma membrane proteins: role of Nedd4/Rsp5p family of ubiquitin-protein

ligases. J. Membr. Biol 176, 1-17.

Saksena S, Emr SD. ESCRTs and human disease. Biochem Soc Trans. 2009 Feb;37(Pt 1):167-72. doi: 10.1042/BST0370167. Review.

Seaman, M.N., E.G. Marcusson, J.L. Cereghino, and S.D. Emr. 1997. Endosome to Golgi retrieval of the vacuolar protein sorting receptor, Vps10p, requires the function of the VPS29, VPS30, and VPS35 gene products. J. Cell Biol. 137:79-92.

Seaman, M.N., J.M. McCaffery, and S.D. Emr. 1998. A membrane coat complex essential for endosome-to-Golgi retrograde transport in yeast. J. Cell Biol. 142:665-681.

Sudol M. (1996). Structure and function of the WW domain. Prog. Biophys. Mol. Biol 65, 113-132.

Zavodszky, E., M.N. Seaman, K. Moreau, M. Jimenez-Sanchez, S.Y. Breusegem, M.E. Harbour, and D.C. Rubinsztein. 2014. Mutation in VPS35 associated with Parkinson's disease impairs WASH complex association and inhibits autophagy. Nat. Commun.

5:3828. http ://dx .doi .org /10 .1038 /ncomms4828

Chapter II

A bipartite sorting signal ensures specificity of retromer complex in membrane protein recycling

Chapter II includes work of a publication in the ***Journal of Cell Biology***: A bipartite sorting signal ensures specificity of retromer complex in membrane protein recycling. The authors are Ya-Shan Chuang, Sho Suzuki, Ming Li, Matthew Seaman and Scott D. Emr (author name with underline contributed equally to this study). Ya-Shan's major contributions to this chapter are presented in Figure 2.1C-I, 2.2C D G, 2.3A-H J, 2.4B C E-J, 2.5C, 2.6C D, 2.7A-D, and Table 2.1 and 2.2.

Abstract

Retromer is an evolutionarily conserved protein complex, which sorts functionally diverse membrane proteins into recycling tubules/vesicles from the endosome. Many of the identified cargos possess a recycling signal sequence defined as ØX[L/M/V], where Ø is F/Y/W. However, this sequence is present in almost all proteins encoded in the genome. Also, several identified recycling sequences do not follow this rule. How then does retromer precisely select its cargos? Here, we reveal that an additional motif is also required for cargo retrieval. The two distinct motifs form a bipartite recycling signal recognized by the retromer subunits, Vps26 and Vps35. Strikingly, Vps26 utilizes different binding sites depending on the cargo, allowing retromer to recycle different membrane proteins. Thus, retromer interacts with cargos in a more complex manner than previously thought, which facilitates precise cargo recognition.

Introduction

Retromer is an evolutionally conserved protein coat complex that mediates recycling of endosomal membrane proteins (Seaman et al., 1997; Seaman et al., 1998; Cullen and Steinberg, 2018). Retromer is composed of 5 proteins; Vps5, Vps17, Vps26, Vps29, and Vps35, that together mediate the formation of cargo-containing recycling tubules/vesicles from the endosome (Seaman et al., 1998). The best characterized retromer cargo is yeast Vps10 (Marcusson et al., 1994). Vps10, the first member of the Sortilin receptor family, is a transmembrane protein receptor for carboxypeptidase Y (CPY), which sorts CPY into vesicles at the Golgi (Fig. 2.1A). After CPY-containing vesicles are transported to the endosome, the endosome matures and fuses with the vacuole, delivering soluble CPY to the vacuole lumen. Unlike CPY, which is released from the Vps10 receptor in the endosome, Vps10 is not delivered to the vacuole, but is recycled from the endosome back to the Golgi by the retromer complex, making Vps10 available for additional rounds of CPY sorting (Fig. 2.1A). In humans, loss of retromer function is associated with diseases such as Parkinson's disease. Certain familial Parkinson's disease patients have a mutation in VPS35 altering the localization of several retromer cargos (Vilariño-

Güell et al., 2011; Zimprich et al., 2011; Follett et al., 2014; McGough et al., 2014; Zavodszky et al., 2014; McMillan et al., 2017). Additionally, several viral and bacterial pathogen effectors target the retromer to promote replication during infection (Personnic et al., 2016). For instance, the Legionella effector RidL directly binds to Vps29 resulting in the inhibition of retrograde trafficking (Finsel et al., 2013; Romano-Moreno et al., 2017).

Retromer is composed of two subcomplexes, the cargo-selective complex (CSC) and the sorting nexin (SNX)-Bin, Amphiphysin, and Rvs (BAR) dimer (Seaman et al., 1998). The CSC consists of Vps26, Vps29, and Vps35. The SNX-BAR dimer consists of Vps5 and Vps17. During cargo recycling, retromer is recruited to the endosomal membrane via the specific interaction of the Vps5/Vps17 Phox homology (PX) domains with phosphatidylinositol 3-phosphate (PI3P) (Burda et al., 2002). Cargo recognition is thought to be mediated primarily through Vps26 (Lucas et al., 2016; Cui et al., 2017; Fjorback et al., 2012), but Vps35 could also play a role (Nothwehr et al., 2000). Finally, the BAR domains of Vps5/Vps17 deform the endosomal membrane to form cargo-containing recycling tubules/vesicles (Seaman and Williams, 2002; Peter et al., 2004).

Although a large number of transmembrane proteins are delivered to the endosomal membrane, retromer precisely selects its cargos and sorts them into recycling tubules/vesicles. The defined consensus sequence for retromer binding, ØX[L/M/V] where Ø is F/Y/W (Seaman, 2007; Cullen and Steinberg., 2018), is present on many proteins that are not retromer cargos. It is unlikely to mediate precise cargo recognition by itself. How retromer specifically recognizes each cargo is not known. Here, we reveal that an additional motif is required for cargo recycling, which explains the highly specific cargo recognition of the retromer complex.

Material and Methods

Yeast Strains and Plasmids.

S. cerevisiae strains used in this study are listed in Table 2.1. Plasmids used in this study are listed in Table 2.2. Standard protocols were used for yeast manipulation (Kaiser et al., 1994). Cells were cultured at 30°C to mid-log phase in YPD medium [1% (w/v) yeast extract, 2% (w/v) bacto peptone, and 2% (w/v) glucose] or YNB medium [0.17% (w/v) yeast nitrogen base w/o amino acids and ammonium sulfate, 0.5% (w/v) ammonium sulfate, and 2% (w/v) glucose] supplemented with the appropriate nutrients.

CPY sorting assay.

Cells were grown in YPD media for 3 hours at 30°C and separated to the intracellular (In.) and extracellular (Ex.) fractions by centrifugation. The fractions were mixed with trichloroacetic acid at a final concentration of 15%, and the mixtures were incubated for 30 min at 4°C. After centrifugation at 17,400 x g for 10 min at 4°C, the fractions were washed once with 100% acetone and then were lysed

in SDS-PAGE sample buffer [50 mM Tris-HCl (pH 7.5), 5% (w/v) SDS, 0.1 M EDTA, 10% glycerol, 100 mM DTT, and bromophenol blue] by beading with 0.5 mm YZB zirconire beads (Yasui Kikai) for 15 min. The lysates then were heated at 98°C for 5 min. After centrifugation at 10,000 x g for 1 min at room temperature, supernatants were analyzed by SDS-PAGE and immunoblotting using anti-CPY, and anti-Pgk1.

Antibodies.

For immunoblotting, mouse monoclonal anti-FLAG (clone 1E6; Wako), mouse monoclonal anti-HA (12CA5; Roche), rabbit polyclonal anti-Vps26 (Reddy and Seaman, 2001), rabbit polyclonal anti-Vps29 (Seaman et al., 1998), rabbit polyclonal anti-Vps35 (Seaman et al., 1998), rabbit polyclonal anti-G6PDH (Sigma-Aldrich), rabbit polyclonal anti-CPY (Klionsky et al., 1988), and mouse monoclonal anti-Pgk1 (no. 459250; Invitrogen) were used at dilution factors at 1:500, 1:1000, 1:2000, 1:5000, 1:5000, 1:20,000, 1:5000, and 1:10000 respectively.

Immunoprecipitation.

Anti-FLAG-conjugated magnetic beads were prepared according to the manufacture's protocol. In berief, NHS FG beads (Tamagawa Seiki) were treated with methanol, and then incubated with anti-DYKDDDK antibody (Wako) at 4°C for 30 min. The magnetic beads were mixed with 1.0 M 2-aminoethanol (pH 8.0) at 4°C for 16-20 hrs to quench the conjugation reaction, washed three times with the beads wash buffer [10 mM HEPES-NaOH (pH 7.2), 50 mM KCl, 1 mM EDTA, and 10% Glycerol], and stored in wash buffer containing 1 mg/ml bovine serum albumin (BSA) (A7030; Sigma-Aldrich).

To examine the retromer complex formation, cells expressing Vps5-FLAG and Vps17-HA grown to mid-log phase were washed twice with the wash buffer [20 mM Hepes-KOH (pH 7.2), 0.2 M Sorbitol, 50 mM AcOK, 2 mM EDTA] and harvested. The cells were lysed in IP buffer [20 mM Hepes-KOH (pH 7.2), 0.2 M Sorbitol, 50 mM AcOK, 2 mM EDTA, 1x protease inhibitor cocktail (Roche)] by beating with 0.5 mm YZB zirconia beads (Yasui Kikai) for 1 min. IP buffer containing 1.0% Triton X-100 was added to the lysate (final concentration of 0.5%), and the samples were rotated at 4°C for 10 min. The solubilized lysates were cleared at 500 x g for 5 min at 4°C, and the resultant supernatants were subjected to a high-speed centrifugation at

17,400 x g for 10 min. The cleared supernatants were incubated with pre-equilibrated anti-FLAG-conjugated magnetic beads and rotated at 4°C for 2 hours. After the beads were washed with wash buffer containing 0.5% Triton X-100, the bound proteins were eluted by incubating the beads in SDS-PAGE sample buffer at 98°C for 5 min.

To examine the cargo-retromer interaction, cells expressing Vps5-FLAG, Vps26-FLAG, or Vps35-FLAG grown to mid-log phase were washed twice with the wash buffer and harvested. The cells were lysed in IP buffer by beating with 0.5 mm YZB zirconia beads for 2 min. IP buffer containing 2.0% saponin was added to the lysate (final concentration of 1.0%), and the samples were rotated at 4°C for 60 min. The solubilized lysates were cleared at 500 x g for 5 min at 4°C, and the resultant supernatants were subjected to a high-speed centrifugation at 17,400 x g for 10 min. The cleared supernatants were incubated with pre-equilibrated anti-FLAG-conjugated magnetic beads and rotated at 4°C for 4 hours. After the beads were washed with wash buffer containing 1.0% saponin, the bound proteins were eluted by incubating the beads in Elution buffer [0.1M Glycine-HCl (pH 3.0), 1% Triton X-100] at 4°C for 30 min. Eluted samples was mixed with 2x SDS-PAGE sample buffer,

then incubated at 42°C for 5 min.

Fluorescence Microscopy.

Fluorescence microscopy was performed using a CSU-X spinning-disk confocal microscopy system (Intelligent Imaging Innovations) or a DeltaVision Elite system (GE Healthcare Life system).

A CSU-X spinning-disk confocal microscopy system is equipped with a DMI 6000B microscope (Leica), 100×/1.45 numerical aperture objective, and a QuantEM electron-multiplying charge-coupled device (CCD) camera (Photometrics). Imaging was done at room temperature in YNB medium using GFP and mCherry channels with different exposure times according to the fluorescence intensity of each protein. Images were analyzed and processed with SlideBook 6.0 software (Intelligent Imaging Innovations).

A DeltaVision Elite system is equipped with an Olympus IX-71 inverted microscope, DV Elite complementary metal-oxide semiconductor camera, a 100×/1.4 NA oil objective, and a DV Light SSI 7 Color illumination system with Live Cell Speed Option

with DV Elite filter sets. Imaging was done at room temperature in YNB medium using GFP and mCherry channels with different exposure times according to the fluorescence intensity of each protein. Image acquisition and deconvolution (conservative setting; five cycles) were performed using DeltaVision software softWoRx 6.5.2 (Applied Precision)

Quantitative analysis of Vps10-GFP and Ear1-mNeonGreen localizations

The Vps10-GFP or Ear1-mNeonGreen localizations were classified in two categories: punctate structures and the vacuole membrane localization. Cells having both punctate structures and the vacuole membrane localization were classified in the vacuole membrane localization category. For each experiment, at least 30 cells were classified and the data from three independent experiments were used for the statistical analysis. Error bars were obtained from three individual experiments.

Online supplemental material

Fig. 2.4 shows the localization of Vps10-GFP and Ear1-mNeonGreen mutants. Fig.

2.6 shows analysis of cargo recycling in retromer mutants. Fig. 2.8 shows analysis of cargo recognition by Vps26.

Results

Two distinct motifs in Vps10 serve as a bipartite recycling signal.

The retromer complex selectively recognizes cargos through a recycling sequence (Fig. 2.1A). In mammalian cells, ØX[L/M/V], where Ø is F/Y/W, is defined as a consensus sequence for recognition by retromer. However, several identified yeast recycling sequences such as YSSL of Vps10, FQFND of Ste13, YEF of Kex2, and WKY of Stv1 do not follow this rule (Fig. 2.4A; Cooper and Stevens, 1996; Nothwehr et al., 1993; Redding et al., 1996; Finnigan et al., 2012). Also, while there are less than thirty known cargos in yeast (Bean et al., 2017), the ØX[L/M/V] sequence was found in almost all proteins (99.6% of yeast proteins; 5841 out of 5916). We hypothesized that for retromer to specifically and accurately recognize the appropriate cargos, additional sequence information must be present. To test this idea, we performed mutational analysis of the CPY receptor Vps10 (Fig. 2.1B). When Vps10-GFP was expressed from its native promoter in WT cells, it localized on punctate structures, which were previously reported to be Golgi or endosomes (Marcusson et al., 1994; Fig. 2.1C). In the retromer-defective vps35Δ cells, retromer-mediated endosome-to-Golgi retrograde trafficking is impaired, and thus Vps10-GFP accumulated on the

vacuole membrane. Although CPY sorting is severely blocked in vps35Δ cells (Seaman et al., 1997), the Vps10 recycling sequence mutant, Y1492A, only exhibited a partial defect in CPY sorting (Cooper and Stevens, 1996). Consistent with this observation, replacing the Vps10 recycling signal (1492-YSSL-1496) with alanine residues (YSSL>AAAA) only showed a partial recycling defect (Fig. 2.1C), which raised the possibility that an additional sequence motif is required for its recycling. To define this motif, we first truncated the cytoplasmic tail of Vps10 and checked its localization (Fig. 2.1D and 2.1E). The Δ1419-1579 mutant stably localized on the vacuole membrane, whereas the Δ1517-1579 mutant localized to punctate structures, mimicking full length Vps10. This suggests that residues 1419-1516 on Vps10 are important for its retrieval. Next, we generated a series of Vps101417-1516 mutants in which ten consecutive amino acids were replaced with alanine residues (Fig. 2.1F, 2.1G, and 2.4B). 1417-1426A, 1427-1436A, and 1437-1446A mutants exhibited a severe defect in the Vps10 recycling. In contrast, 1487-1496A (which includes 1492-YSSL-1495) only showed a mild defect. The Δ1456-1459 mutant (1456-FYVF-1459) is known to cause the missorting of CPY (Cereghino et al., 1995). However, neither 1447-1456A nor 1457-1466A mutant exhibited striking

defects. Next, we mutated single residues in the region 1417-1446 to alanine. Of the mutants tested, F1428A, E1430A, I1431A, R1432A, and L1433A mutants stabilized Vps10-GFP on the vacuole membrane (Fig. 2.1H, 2.1I, and 2.4C), suggesting that the 1428-FGEIRL-1433 region of Vps10 is also important for its recycling.

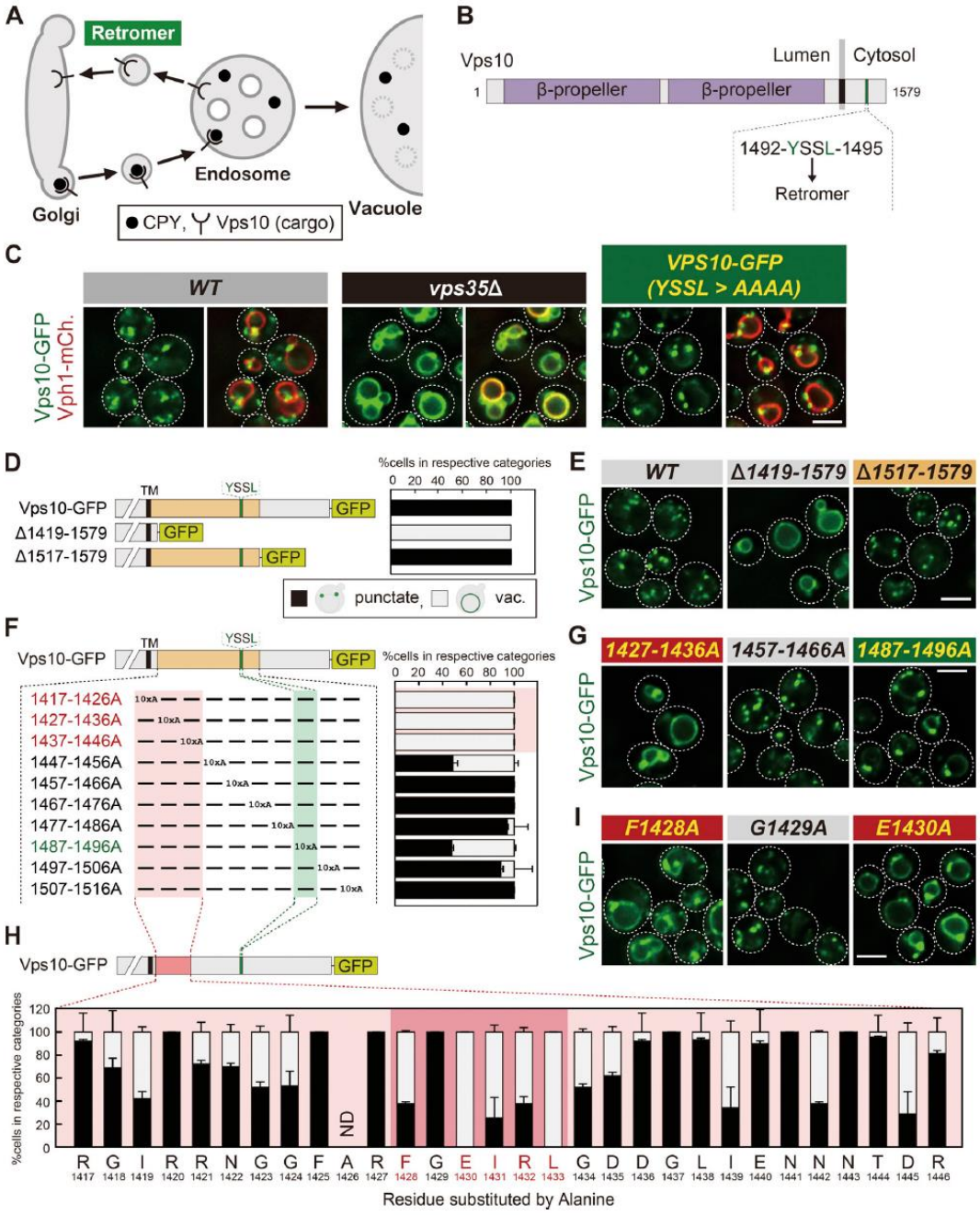
A
Retromer
Endosome
Golgi
Vacuole
CPY, Vps10 (cargo)
B
Vps10
Lumen
Cytosol
1
β-propeller
β-propeller
1579
1492-YSSL-1495
Retromer
C
WT
vps35Δ
VPS10-GFP
(YSSL > AAAA)
Vps10-GFP
Vph1-mCh.
D
%cells in respective categories
0 20 40 60 80 100
TM
YSSL
Vps10-GFP
Δ1419-1579
Δ1517-1579
GFP
punctate, vac.
E
WT
Δ1419-1579
Δ1517-1579
Vps10-GFP
F
Vps10-GFP
TM
YSSL
GFP
%cells in respective categories
0 20 40 60 80 100
1417-1426A
1427-1436A
1437-1446A
1447-1456A
1457-1466A
1467-1476A
1477-1486A
1487-1496A
1497-1506A
1507-1516A
10xA
G
1427-1436A
1457-1466A
1487-1496A
Vps10-GFP
I
F1428A
G1429A
E1430A
Vps10-GFP
H
Vps10-GFP
GFP
%cells in respective categories
120
100
80
60
40
20
0
ND
R G I R R N G G F A R F G E I R L G D D G L I E N N N T D R
1417 1418 1419 1420 1421 1422 1423 1424 1425 1426 1427 1428 1429 1430 1431 1432 1433 1434 1435 1436 1437 1438 1439 1440 1441 1442 1443 1444 1445 1446
Residue substituted by Alanine

Figure 2.1

Figure 2.1. The FGEIRL motif of Vps10 is also important for its recycling. (A) A model of Vps10 recycling. (B) Schematic of Vps10. (C, E, G, and I) Vps10-GFP localization. (D, F, and H) Schematic of Vps10 truncation analysis and the percentage of each category of Vps10-GFP mutant localization from E [D], from G and Fig. S1B [F], or from I and Fig. S1C [H]. Because the 1426th residue of Vps10 is Ala, A1426 was not substituted. ND means not determined. For all quantification shown in this figure, at least 30 cells were classified and the data from three independent experiments were used for statistical analysis. Scale bar: 2 μm.

Based on the mutational analysis of Vps10, in addition to 1492-YSSL-1495, 1428-FGEIRL-1433 is also required for its retrieval (Fig. 2.2A). Both sequences are highly conserved among Vps10 homologs from related species (Fig. 2.2B), suggesting that the cargo recognition mechanism via the two motifs is also conserved. To test the relationship of the two sequences, we replaced each sequence with alanine residues and examined Vps10-GFP localization (Fig. 2.2C and 2.2D). While the 1492-1495A mutant (YSSL>AAAA) mutant showed a partial defect in Vps10-GFP recycling, the 1428-1433A (FGEIRL>AAAAAA) mutant and the 1428-1433A/1492-1495A (FGEIRL>AAAAAA and YSSL>AAAA) double mutant exhibited a severe defect. To test whether these sequences are required for binding with the retromer, we performed co-immunoprecipitation experiments. While wild-type Vps10-GFP co-precipitated with Vps26-FLAG, the 1428-1433A/1492-1495A double mutant (Vps1010xAla-GFP) did not (Fig. 2.2E). We also examined the effect on CPY sorting in these mutants. CPY sorting to the vacuole can be monitored by the appearance of the mature form of CPY (mCPY). Consistent with Vps10-GFP localization, CPY maturation was moderately reduced in the 1492-1495A mutant, whereas it was strongly impaired in the 1428-1433A and 1428-1433A/1492-1495A mutants with

most of the precursor form of CPY (p2CPY) secreted to the extracellular space (Fig. 2.2F). Based on these observations, we propose that two distinct motifs in Vps10, 1428-FGEIRL-1433 and 1492-YSSL-1495, are both required for retromer recognition. However, the FGEIRL motif is essential for its recognition, whereas the YSSL enhances the recognition. Thus, these two distinct motifs form a bipartite recycling signal.

Finally, to address whether the bipartite recycling signal in Vps10 is sufficient for its recycling, we fused the C-tail of Vps10 (residues 1416-1523), which includes this recycling signal, to Ear1, an endosomal membrane protein (Léon et al., 2008). Truncation of the cytoplasmic tail of Ear1 (Ear1ΔC-GFP) resulted in its accumulation on the vacuole membrane, whereas fusion of the recycling sequences of Vps10 (Ear1ΔC-Vps10C-tail-GFP) restored its punctate localization (Fig. 2.2G), suggesting that the 1428-FGEIRL-1433 and 1492-YSSL-1495 motifs of Vps10 are sufficient for recognition by the retromer.

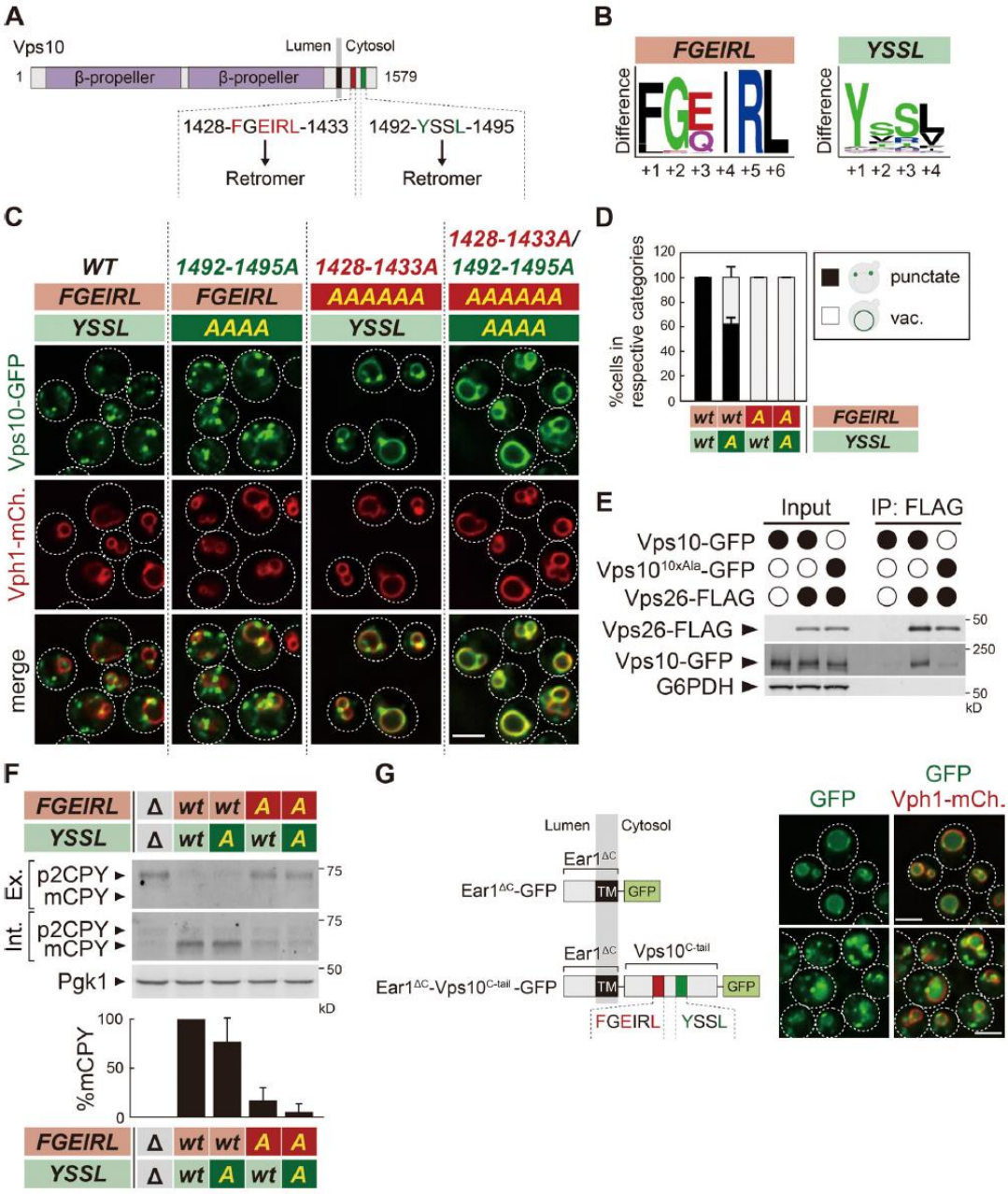
A
Vps10
Lumen
Cytosol
1
β-propeller
β-propeller
1579
1428-FGEIRL-1433
1492-YSSL-1495
Retromer
Retromer
B
FGEIRL
YSSL
Difference
+1 +2 +3 +4 +5 +6
+1 +2 +3 +4
C
WT
1492-1495A
1428-1433A
1428-1433A/
1492-1495A
FGEIRL
AAAAAA
YSSL
AAAA
Vps10-GFP
Vph1-mCh.
merge
D
%cells in respective categories
punctate
vac.
wt wt A A
wt A wt A
FGEIRL
YSSL
E
Input
IP: FLAG
Vps10-GFP
Vps10^10xAla-GFP
Vps26-FLAG
Vps26-FLAG ►
Vps10-GFP ►
G6PDH ►
50
250
50
kD
F
FGEIRL
YSSL
Δ wt wt A A
Δ wt A wt A
Ex.
Int.
p2CPY ►
mCPY ►
Pgk1 ►
75
75
50
kD
%mCPY
100
50
0
G
Lumen
Cytosol
Ear1^ΔC
Ear1^ΔC-GFP
TM
GFP
Vps10^C-tail
Ear1^ΔC-Vps10^C-tail-GFP
FGEIRL
YSSL
GFP
GFP
Vph1-mCh.

Figure 2.2

Figure 2.2. Two distinct sequences of Vps10 serve as a bipartite recycling signal. (A) Schematic of Vps10. (B) Weblogo residue conservation of 1428-FGEIRL-1433 and 1492-YSSL-1495 of Vps10 among 85 Vps10 homologs from related species. (C) Vps10-GFP localization. (D) The percentage of each category of Vps10-GFP mutant localization from C. (E) The Vps26-Vps10 interaction in Vps10-GFP mutants. Vps26-FLAG was immunoprecipitated from cells expressing Vps10-GFP or Vps10-GFP with a mutation in a bipartite recycling signal (Vps1010xAla-GFP), and interacting Vps10-GFP was detected by immunoblotting using antibodies against FLAG, GFP, and G6PDH. (F) CPY sorting in vps10Δ cells expressing Vps10-GFP mutants. CPY sorting is examined by immunoblotting against CPY and Pgk1. Mature form of CPY in WT was set to 100%. “Ex.” and “Int.” indicate extracellular and intracellular space, respectively. (G) Ear1ΔC-GFP and Ear1ΔC-Vps10C-tail-GFP localization. For all quantification shown in this figure, at least 30 cells were classified and the data from three independent experiments were used for statistical analysis. Scale bar: 2 μm.

Two separate motifs are also important for Ear1 retrieval.

To assess if the two distinct motifs are also important for other retromer cargos, we performed mutational analysis of Ear1. Ear1 is a transmembrane protein that localizes to the endosomal membrane (Léon et al., 2008; Fig. 2.3A). The region 456-FEF-458 of Ear1 was previously identified as a recycling signal, which is required for its endosomal localization (Bean et al., 2017). Ear1 serves as an adaptor that recruits the E3 ubiquitin ligase Rsp5 to the endosome via its PY motifs (Fig. 2.4D; Léon et al., 2008), allowing the ubiquitination of mislocalized membrane proteins on the endosomal membrane (Sardana et al., 2019). Since Ear1 itself is also ubiquitinated by Rsp5, leading to its degradation (Léon et al., 2008), we expressed Ear1-mNeonGreen in the rsp5(G747E) hypomorphic mutant (Fisk and Yaffe, 1999; Fig. 2.4E). Ear1-mNeonGreen mainly localized to the endosomes in the rsp5(G747E) mutant, but accumulated on the vacuole membrane in a rsp5(G747E) vps35Δ double mutant (Fig. 2.4F), confirming that the endosomal localization of Ear1-mNeonGreen, is maintained due to its recycling by the retromer.

For mutational analysis of Ear1, we constructed a series of C-terminally truncated Ear1-mNeonGreen mutants and expressed them in the rsp5(G747E)

strain. Ear1 Δ511-550 and Δ491-550 mutants localized to the endosome, whereas the Δ471-550 mutant accumulated on the vacuole membrane, even though this mutant still contains the previously identified Ear1 recycling signal (456-FEF-458) (Fig. 2.3A, 2.3B, and 2.4G). The Δ451-550 mutant lacking 456-FEF-458 also localized to the vacuole membrane. Next, we generated a series of Ear1 mutants by replacing five consecutive amino acids with alanines in the region 452-486 and examined their localization. Among these, the 452-456A, 457-461A, and 472-476A mutants were blocked on the vacuole membrane (Fig. 2.3C, 2.3D and 2.4H). Furthermore, mutating single residues to alanine in the region 452-461, revealed that in addition to the F456A and F458A mutations, the P453A mutant also localized to the vacuole membrane (Fig. 2.3E, 2.3F and 2.4I), suggesting that the 453-PPGFEF-458 motif serves as the recycling signal in Ear1. Additionally, mutagenesis of the residues in the region 472-476 showed that the I473A and L475A mutants also exhibited vacuole membrane localization (Fig. 2.3E, 2.3G, and 2.4J), suggesting that 473-INL-475 is another motif required to maintain Ear1 localization to the endosome. To test whether both of these two discontinuous motifs were required for its endosomal localization in cells expressing wild-type Rsp5, we investigated the localization of

Ear1 by using a pH sensitive green fluorescence protein, pHluorin, whose fluorescence is quenched in the acidic pH of the vacuole lumen (Miesenböck et al., 1998). While wild-type Ear1-pHluorin localized to the endosome, the F456A and L475A mutants were blocked on the vacuole membrane (Fig. 2.3H). Not surprisingly, both these motifs in Ear1 are strictly conserved across multiple fungal species (Fig. 2.3I). Finally, to determine whether these two motifs are sufficient for Ear1 retrieval, we fused the C-tail of Ear1 (residues 451-550) to the truncated C-tail of Vps10 (Vps10ΔC). The Vps10ΔC-GFP truncation mutant localized to the vacuole membrane, whereas Vps10ΔC-Ear1C-tail-GFP restored the punctate localization of Vps10 (Fig. 2.3J). We conclude that two discontinuous motifs in Ear1, 453-PPGFEF-458 and 473-INL-475, are sufficient for its recycling mediated by the retromer complex (Fig. 2.3K). Interestingly, both of these motifs are essential for retromer recognition unlike Vps10.

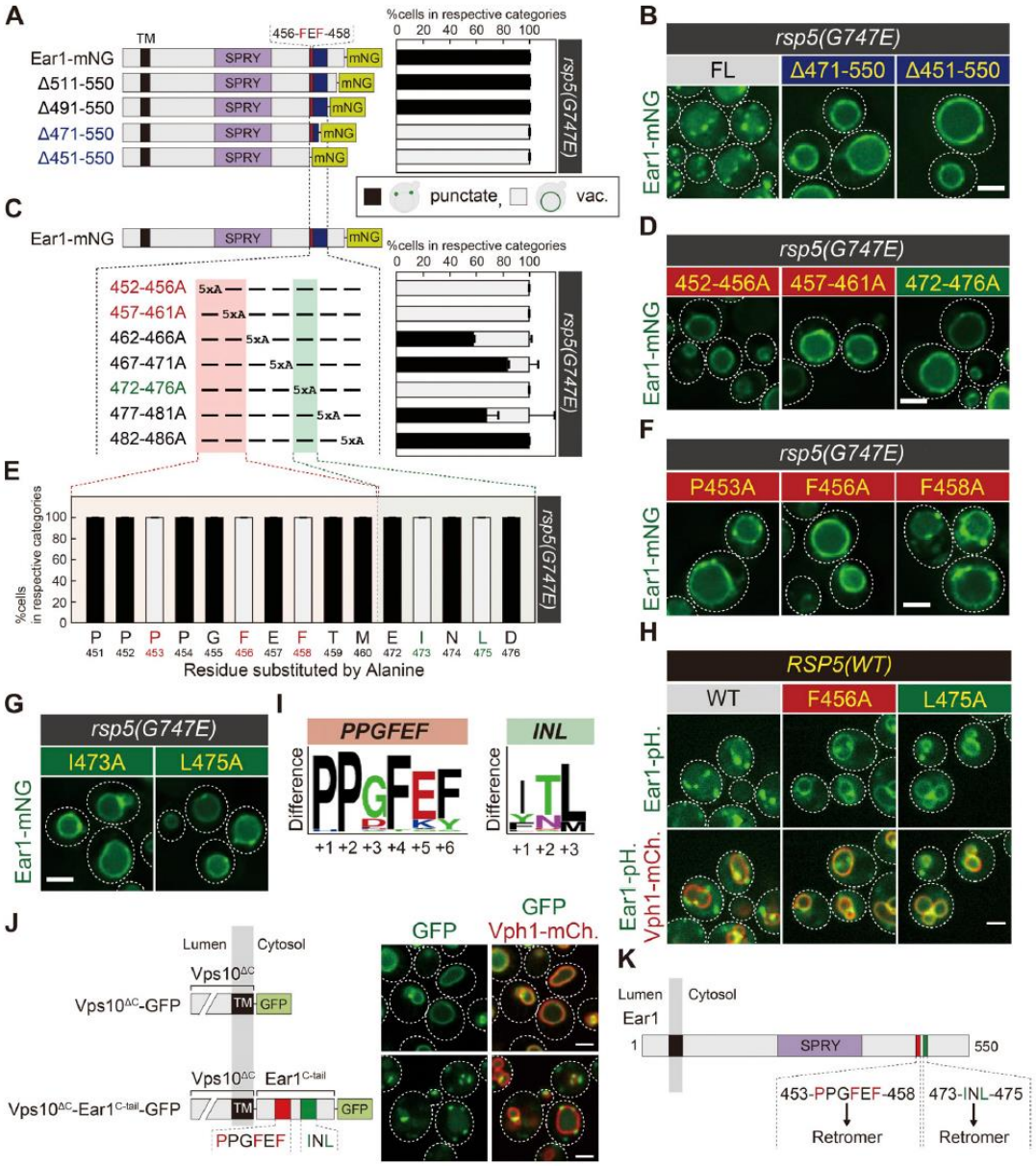
A
TM
456-FEF-458
Ear1-mNG
Δ511-550
Δ491-550
Δ471-550
Δ451-550
SPRY
mNG
%cells in respective categories
0 20 40 60 80 100
rsp5(G747E)
punctate, vac.
B
rsp5(G747E)
FL
Δ471-550
Δ451-550
Ear1-mNG
C
452-456A
457-461A
462-466A
467-471A
472-476A
477-481A
482-486A
5xA
D
452-456A
457-461A
472-476A
E
%cells in respective categories
P P P P G F E F T M E I N L D
451 452 453 454 455 456 457 458 459 460 472 473 474 475 476
Residue substituted by Alanine
F
P453A
F456A
F458A
G
I473A
L475A
H
RSP5(WT)
WT
F456A
L475A
Ear1-pH.
Ear1-pH. Vph1-mCh.
I
PPGFEF
INL
Difference
+1 +2 +3 +4 +5 +6
+1 +2 +3
J
Lumen
Cytosol
Vps10ΔC
Vps10ΔC-GFP
TM
GFP
Vps10ΔC Ear1C-tail
Vps10ΔC-Ear1C-tail-GFP
PPGFEF
INL
GFP
Vph1-mCh.
K
Lumen
Cytosol
Ear1
1
SPRY
550
453-PPGFEF-458
473-INL-475
Retromer
Retromer

Figure 2.3

Figure 2.3. Two separate sequences are also important for Ear1 retrieval. (A, C, and E) Schematic of Ear1-mNeonGreen truncation analysis and the percentage of each category of Ear1-mNeonGreen mutant localization in rsp5(G747E) mutants from B and Fig. S1G [A], from D and Fig. S1H [C], or from F, G, S1I, and S1J [E]. (B, D, F, and G) Ear1-mNeonGreen localization in rsp5 (G747E) mutants. (H) Ear1-pHluorin localization in cells expressing WT Rsp5. (J) Vps10ΔC-GFP and Vps10ΔC-Ear1C-tail-GFP localization. (I) Weblogo residue conservation of 453-PPGFEF-458 and 473-INL-475 of Ear1 among 37 Ear1 homologs from related species. (K) Schematic of Ear1. For all quantification shown in this figure, at least 30 cells were classified and the data from three independent experiments were used for statistical analysis. Scale bar: 2 μm.

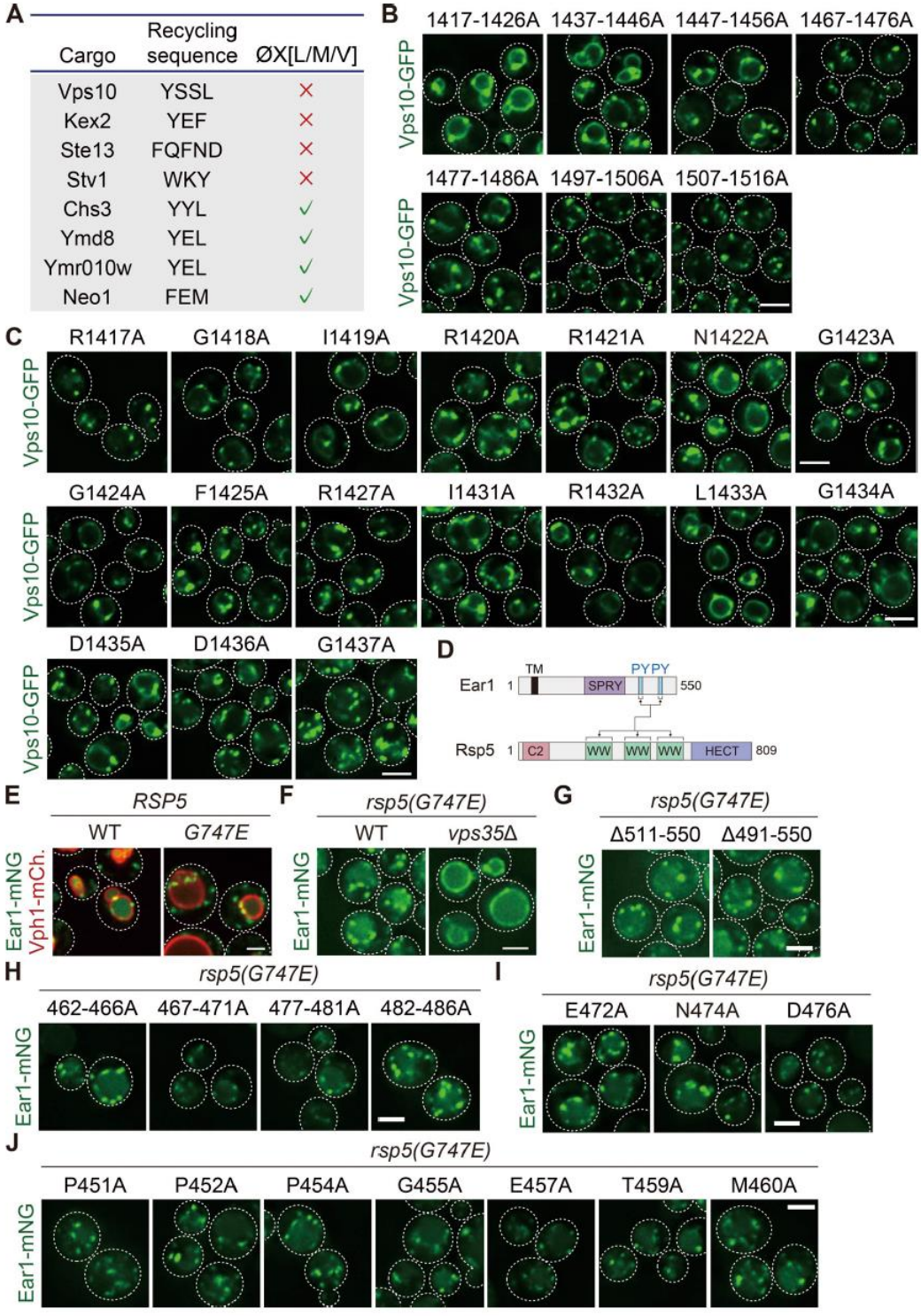
A
Cargo
Recycling sequence
ØX[L/M/V]
Vps10 YSSL ×
Kex2 YEF ×
Ste13 FQFND ×
Stv1 WKY ×
Chs3 YYL ✓
Ymd8 YEL ✓
Ymr010w YEL ✓
Neo1 FEM ✓
B
1417-1426A
1437-1446A
1447-1456A
1467-1476A
1477-1486A
1497-1506A
1507-1516A
Vps10-GFP
C
R1417A
G1418A
I1419A
R1420A
R1421A
N1422A
G1423A
G1424A
F1425A
R1427A
I1431A
R1432A
L1433A
G1434A
D1435A
D1436A
G1437A
D
TM
PY PY
Ear1
SPRY
550
Rsp5
C2
WW
HECT
809
E
RSP5
WT
G747E
Ear1-mNG
Vph1-mCh.
F
rsp5(G747E)
WT
vps35Δ
G
rsp5(G747E)
Δ511-550
Δ491-550
H
rsp5(G747E)
462-466A
467-471A
477-481A
482-486A
I
rsp5(G747E)
E472A
N474A
D476A
J
rsp5(G747E)
P451A
P452A
P454A
G455A
E457A
T459A
M460A

Figure 2.4

Figure 2.4. The localization of Vps10-GFP and Ear1-mNeonGreen mutants. (A) Schematic of the recycling sequence in yeast. (B, C) The localization of Vps10-GFP mutants. (D) Schematic of the Ear1-Rsp5 interaction. (E) Ear1-mNeonGreen localization in WT or rsp5 (G747E) cells. (F) Ear1-mNeonGreen localization in rsp5 (G747E) or rsp5 (G747E) vps35Δ cells. (G, H, I, and J) The localization of Ear1-mNeonGreen mutants in rsp5 (G747E) cells. Scale bar: 2 μm.

Retromer recognizes the endosomal cargo through Vps26 and Vps35.

In yeast, retromer is composed of the CSC (Vps26-Vps29-Vps35 complex) and the SNX-BAR dimer (Vps5-Vps17 complex) (Seaman et al., 1998; Fig. 2.5A). Two models have been proposed for the assembly of the retromer complex (Fig. 2.6A). Previous reports show that the CSC interacts with the SNX-BAR dimer through Vps29 and Vps35 (Reddy and Seaman, 2001; Seaman and Willliams, 2002; Collins et al., 2005). Indeed, a Vps29 (L252E) mutant fails to interact with the SNX-BAR dimer, although it assembles normally with Vps26 and Vps35 (Collins et al., 2005). However, recent work based on the Cryo-EM structure of C. thermophilum Vps5-Vps5-Vps26-Vps29-Vps35 complex by Kovtun et al. proposed another model where the CSC interacts with the SNX-BAR through Vps26 (Kovtun et al., 2018). In the latter model, Vps26 forms the sole contact between the CSC and SNX-BAR dimer. Vps29 and Vps35 have no interaction with the SNX-BAR dimer. To explore this apparent discrepancy, we examined retromer assembly using yeast cells expressing genomically tagged functional Vps5-FLAG and Vps17-HA. In WT cells, Vps17-HA, Vps26, Vps29, and Vps35 co-immunoprecipitated with Vps5-FLAG (Fig. 2.5B). Strikingly, we still observed coimmunoprecipitation of Vps29 and Vps35 with Vps5-FLAG in vps26Δ

cells. On the other hand, the Vps26 association with Vps5-FLAG was abolished in vps29Δ or vps35Δ cells. These results support the previously published findings (Seaman and Williams, 2002; Collins et al., 2005) and demonstrate that the CSC interacts with the SNX-BAR dimer through Vps29 and Vps35, but not through Vps26. Based on this finding as well as the work by Collins and others, we conclude that retromer assembly in S. cerevisiae and in C. thermophilum may be rather different.

In mammalian cells, the CSC and the SNX-BAR dimer do not form a stable complex (Harbour and Seaman, 2011; Cullen and Steinberg, 2018). Also, recycling of the mannose-6-phosphate receptor requires the SNX-BAR dimer, but not the CSC (Simonetti et al., 2017; Kvainickas et al., 2017). Hence, we re-evaluated the requirement of each retromer subunit for the retrieval of yeast retromer cargos. For this purpose, we examined Vps10-GFP or Ear1-pHluorin localization in cells lacking Vps5, Vps17, Vps26, Vps29, or Vps35. In vps26Δ, vps29Δ, and vps35Δ mutants, Vps10-GFP and Ear1-pHluorin accumulated on the vacuole membrane (Fig. 2.5C), implying that the CSC is required for cargo recycling in yeast. Since the vacuole morphology is extremely fragmented in vps5Δ or vps17Δ cells (Köhrer and Emr,

1993; Nothwehr and Hindes, 1997; Horazdovsky et al., 1997), it was difficult to determine cargo localization in these mutants (Fig. 2.6B). However, the vacuole fragmentation phenotype in vps5Δ or vps17Δ cells was partially rescued under osmotic stress (Fig. 2.5D). By using these conditions, we found that Vps10-GFP required both Vps5 and Vps17 for its recycling, however Ear1-pHluorin only required Vps5, but not Vps17.

Since Vps17 is not required for Ear1 retrieval, we tested if Vps10 and Ear1 are recycled by the same or distinct retromer complexes in WT cells (retromer complex with or without Vps17). For this purpose, we overexpressed Ear1 in Vps10-GFP expressing cells and examined whether Ear1 competes with Vps10-GFP. In WT cells, overexpressing Ear1 led to missorting of Vps10-GFP to the vacuole membrane (Fig. 2.6C and D). When we overexpressed the Ear1 PY motif mutant (Ear1PYmut. OE), Vps10-GFP still mislocalized to the vacuole membrane, implying that Ear1 binding with Rsp5 is dispensable to compete with Vps10-GFP. On the other hand, upon overexpression of the Ear1 recycling defective mutant (F456A), Vps10-GFP exhibited punctate localization, suggesting that Vps10 and Ear1 are recycled by the same retromer complex in WT cells, although Ear1 is recycled even in the absence of

Vps17. Based on these observations, we confirmed that yeast endosomal cargo retrieval requires both the CSC and the SNX-BAR dimer.

To determine which retromer subunits recognize cargos, we examined the Vps10-Vps26 interaction in cells lacking Vps5, Vps17, Vps29, or Vps35. Vps10-GFP co-precipitated with Vps26-FLAG in vps5Δ, vps17Δ, and vps29Δ cells, but not in vps35Δ cells (Fig. 2.5E). To test whether Vps26 is also required, we examined the Vps10-Vps35 interaction in vps26Δ cells. Vps10-GFP co-precipitated with Vps35-FLAG, but not in vps26Δ cells (Fig. 2.5F). We also asked whether the SNX-BAR dimer requires the association with the CSC for cargo binding. We analyzed the Vps5-Vps10 interaction in vps29Δ cells. The binding of Vps5-FLAG with Vps10-GFP was abolished in vps29Δ cells (Fig. 2.6E and F). From these results, we propose that cargo recognition by the yeast retromer is mediated through Vps26 and Vps35.

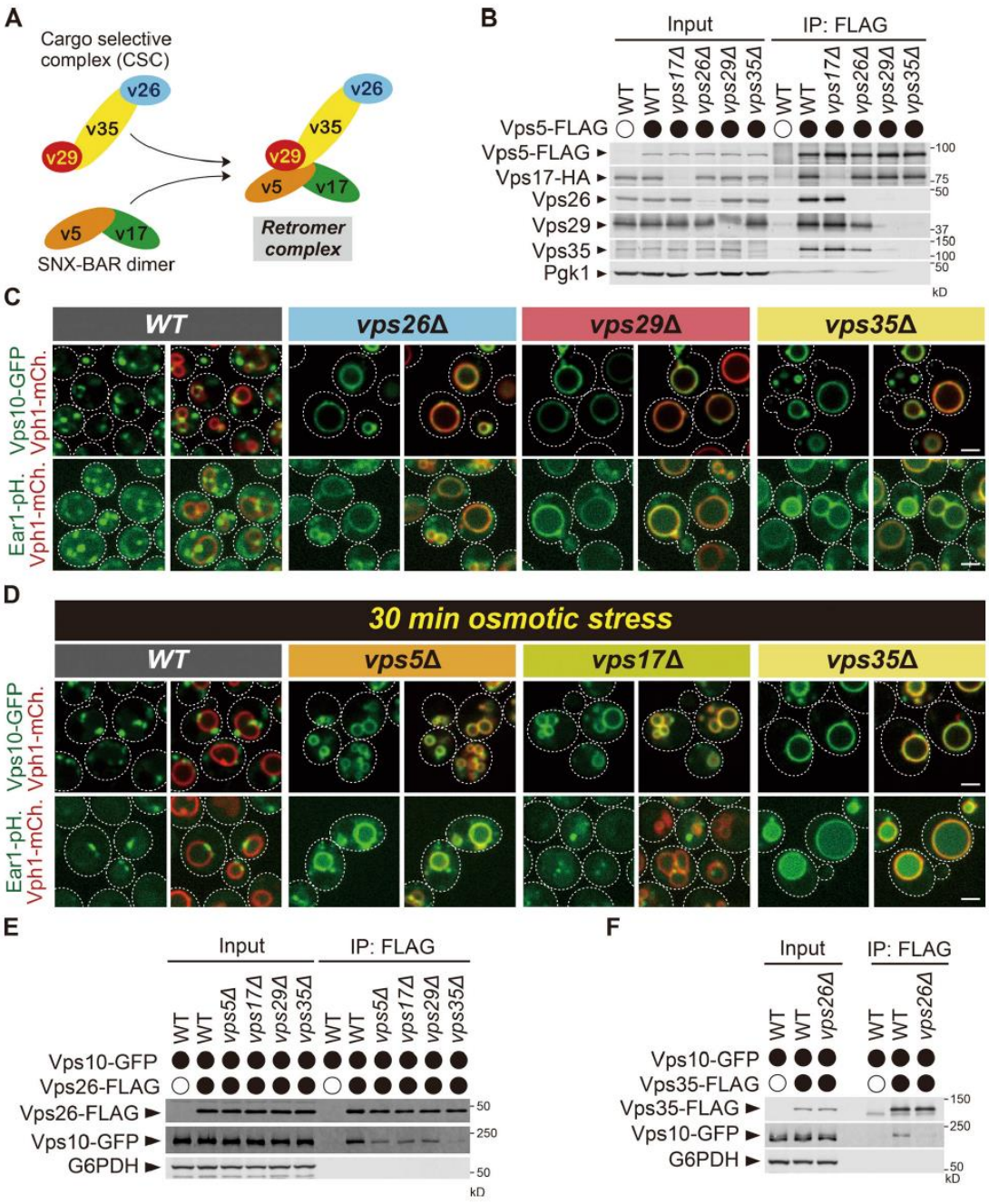
A
Cargo selective complex (CSC)
v26
v35
v29
v5
v17
SNX-BAR dimer
Retromer complex
B
Input
IP: FLAG
WT
vps17Δ
vps26Δ
vps29Δ
vps35Δ
Vps5-FLAG
Vps17-HA
Vps26
Vps29
Vps35
Pgk1
kD
C
WT
vps26Δ
vps29Δ
vps35Δ
Vps10-GFP Vph1-mCh.
Ear1-pH. Vph1-mCh.
D
30 min osmotic stress
WT
vps5Δ
vps17Δ
vps35Δ
E
Input
IP: FLAG
Vps10-GFP
Vps26-FLAG
G6PDH
F
Vps35-FLAG

Figure 2.5

Figure 2.5. The retromer complex recognizes the endosomal cargo through Vps26 and Vps35. (A) Model of the retromer complex in yeast. (B) The retromer assembly in retromer subunit mutants. Vps5-FLAG was immunoprecipitated from cells lacking Vps17, Vps26, Vps29, or Vps35, and interacting Vps17-HA, Vps26, Vps29, and Vps35 were detected by immunoblotting using antibody against FLAG, HA, Vps26, Vps29, Vps35, and Pgk1. (C) The localization of Vps10-GFP or Ear1-pHluorin (Ear1-pH.) in WT, vps26Δ, vps29Δ, and vps35Δ cells. (D) The localization of Vps10-GFP or Ear1-pHluorin (Ear1-pH.) in WT, vps5Δ, vps17Δ, and vps35Δ cells under osmotic stress. Cells expressing Vps10-GFP grown in YPD media were resuspended in water and incubated for 30 min. (E) The Vps26-Vps10 interaction in retromer subunit mutants. Vps26-FLAG was immunoprecipitated from Vps10-GFP expressing cells lacking Vps5, Vps17, Vps29, or Vps35, and interacting Vps10-GFP was detected by immunoblotting using antibody against FLAG, GFP, and G6PDH. (F) The Vps35-Vps10 interaction in vps26Δ cells. Vps35-FLAG was immunoprecipitated from WT or vps26Δ cells, and interacting Vps10-GFP was detected by immunoblotting using antibody against FLAG, GFP, and G6PDH. Scale bar: 2 μm.

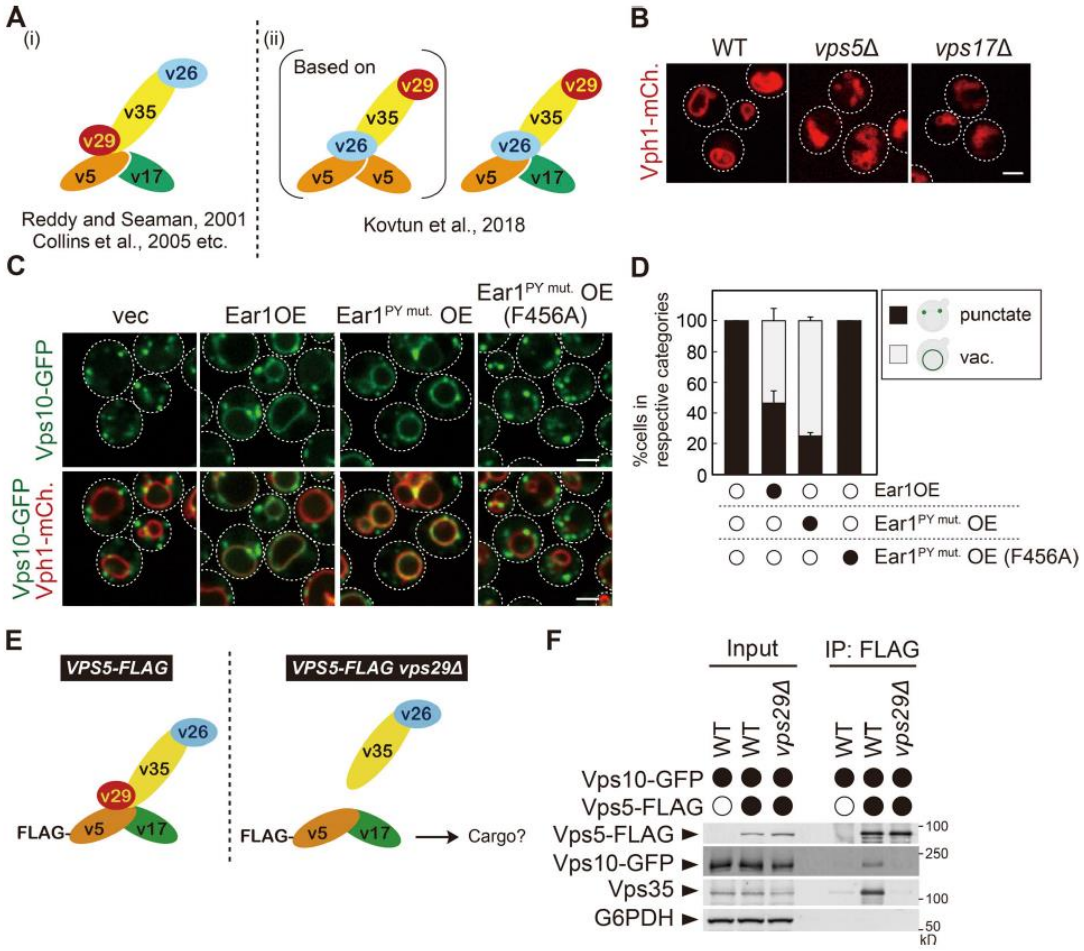
A
(i)
v26
v35
v29
v5
v17
Reddy and Seaman, 2001
Collins et al., 2005 etc.
(ii)
Based on
Kovtun et al., 2018
B
WT
vps5Δ
vps17Δ
Vph1-mCh.
C
vec
Ear1OE
Ear1PY mut. OE
Ear1PY mut. OE (F456A)
Vps10-GFP
Vps10-GFP Vph1-mCh.
D
%cells in respective categories
punctate
vac.
Ear1OE
Ear1PY mut. OE
Ear1PY mut. OE (F456A)
E
VPS5-FLAG
VPS5-FLAG vps29Δ
FLAG-
Cargo?
F
Input
IP: FLAG
WT
vps29Δ
Vps10-GFP
Vps5-FLAG
Vps35
G6PDH
kΩ

Figure 2.6

Figure 2.6. Analysis of cargo recycling in retromer mutants.

(A) Two models for the retromer assembly. (B) The vacuole morphology in WT, vps5Δ or vps17Δcells. (C) Vps10-GFP localization in cells overexpressing Ear1 mutants. (D) The percentage of each category of Vps10-GFP mutant localization from C. (E, F) The Vps5-Vps10 interaction in vps29Δ cells. Vps5-FLAG was immunoprecipitated from cells lacking Vps29 and interacting Vps10-GFP was detected by immunoblotting using antibody against FLAG, GFP, Vps35 and G6PDH. For all quantification shown in this figure, at least 30 cells were classified and the data from three independent experiments were used for statistical analysis. Scale bar: 2 μm.

Different sites in Vps26 are required for Vps10 or Ear1 recognition.

Since the recycling sequences identified in Vps10 and Ear1 are not similar to each other (Fig. 2.4A), we wondered how retromer recognizes these different sequences. Our biochemical analysis revealed that both Vps26 and Vps35 are required for cargo recognition. Since the crystal structure of the mammalian Vps26-Vps35-Snx3 complex with its cargo, DMT1-II, is solved (Lucas et al., 2016), we further analyzed cargo recognition by Vps26. In the crystal structure, V168 and F287 residues of human Vps26 (I251 and F368 in yeast Vps26, respectively) recognize the human DMT1-II recycling signal sequence YLL. To test the function of the corresponding residues in yeast, we replaced the corresponding I251 and F368 to Glu in yeast Vps26 (Fig. 2.8A) and examined the localization of Vps10-GFP (Fig. 2.7A and B) and Ear1-mNeonGreen (Fig. 2.7C and D). The I251E/F368E mutant exhibited a defect in Ear1-mNeonGreen recycling, but not Vps10-GFP. Since Vps26 is required for Vps10 binding (Fig. 2.5F), we mutated multiple conserved surface residues on Vps26 to identify residues required for cargo recognition (Collins et al., 2008), and found two mutants (F334E and L285E) that affect cargo localization. In the F334E mutant, Vps10-GFP localized to the vacuole membrane, whereas Ear1-mNeonGreen retained

its punctate localization. The L285E mutant exhibited a defect in the recycling of both Vps10-GFP and Ear1-mNeonGreen. Co-immunoprecipitation experiments confirmed that these Vps26 mutants can still form a stable retromer complex (Fig. 2.7E). To address whether these residues are required for cargo recognition, we examined cargo binding of retromer in vps26 mutants and found that while I251/F368E mutants only slightly decrease an affinity for Vps10-GFP, F334E and L285E mutants severely impaired binding (Fig. 2.7F). These data indicate that Vps10 recycling requires an interaction with Vps26 residues L285 and F334, whereas Ear1 requires an interaction with I251, L285, and F368. Based on these findings, we conclude that different sites on Vps26 are required for Vps10 or Ear1 recognition and recycling. The residues of Vps26 required for cargo recognition, (I251, L285, F334, and F368) are evolutionally conserved from yeast to humans (Fig. 2.8B and C), raising the possibility that a similar mechanism is present in higher eukaryotes. Since both Vps10 and Ear1 require L285, they can compete for Vps26 binding (Fig. 2.6C and D).

A bipartite recycling signal sequence ensures precise cargo recognition by the retromer complex.

It had been believed that retromer recognizes its cargo through the consensus sequence defined as ØX[L/M/V] (Cullen and Steinberg, 2018). However, since almost all proteins coded in the yeast genome have this sequence, how the retromer complex selectively recognizes its cargo remained elusive. In the present study, we reveal that in addition to the previously defined recycling sequence, a second recognition motif is also important for cargo retrieval. These two sequences form a bipartite recycling signal recognized by the retromer subunits Vps26 and Vps35 (Fig. 2.7G). Thus, retromer interacts with its cargo more specifically than previously thought, which explains the selectivity of cargo recognition by the retromer.

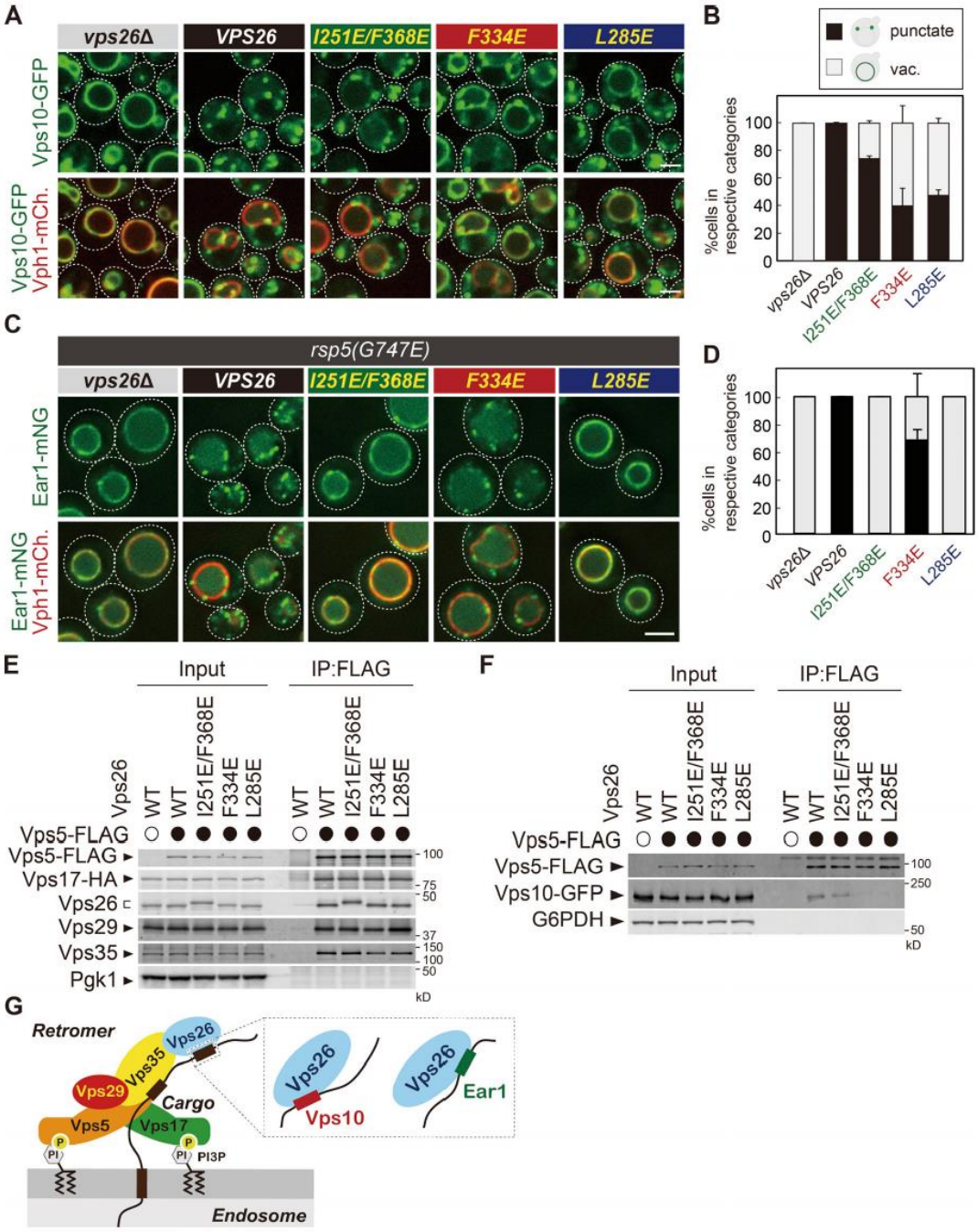
A
vps26Δ
VPS26
I251E/F368E
F334E
L285E
Vps10-GFP
Vps10-GFP Vph1-mCh.
B
punctate
vac.
%cells in respective categories
vps26Δ
VPS26
I251E/F368E
F334E
L285E
C
rsp5(G747E)
Ear1-mNG
Ear1-mNG Vph1-mCh.
D
E
Input
IP:FLAG
Vps26
Vps5-FLAG
Vps17-HA
Vps29
Vps35
Pgk1
kD
F
Vps10-GFP
G6PDH
G
Retromer
Vps26
Vps35
Vps29
Cargo
Vps5
Vps17
PI3P
Endosome
Vps10
Ear1

Figure 2.7

Figure 2.7. Different sites in Vps26 are required for Vps10 or Ear1 recognition. (A) The localization of Vps10-GFP in vps26 mutants. (B) The percentage of each category of Vps10-GFP mutant localization from A. (C) The localization of Ear1-mNeonGreen (Ear1-mNG) in rsp5(G747E) vps26 mutants. (D) The percentage of each category of Ear1-mNeonGreen mutant localization from C. (E) The retromer assembly in vps26 mutants. Vps5-FLAG was immunoprecipitated from cells expressing vps26 mutants, and interacting Vps17-HA, Vps26, Vps29, and Vps35 were detected by immunoblotting using antibody against FLAG, HA, Vps26, Vps29, Vps35, and Pgk1. (F) The Vps5-Vps10 interaction in vps26 mutants. Vps5-FLAG was immunoprecipitated from cells expressing vps26 mutants, and interacting Vps10-GFP was detected by immunoblotting using antibody against FLAG, GFP, and G6PDH. (G) The model of retromer cargo recognition. For all quantification shown in this figure, at least 30 cells were classified and the data from three independent experiments were used for statistical analysis. Scale bar: 2 μm.

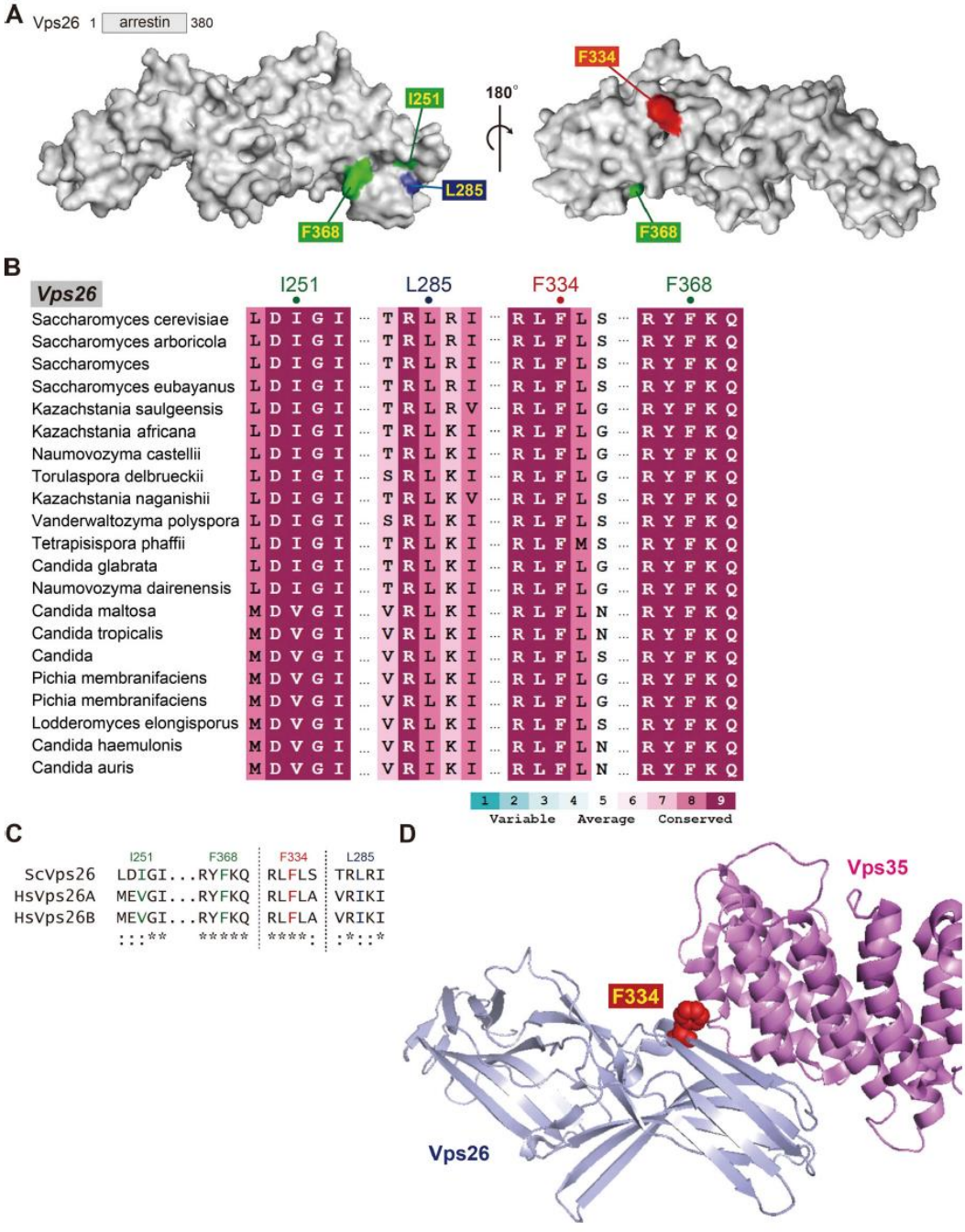
A
Vps26 1 arrestin 380
I251
L285
F368
180°
F334
F368
B
Vps26
I251
L285
F334
F368
Saccharomyces cerevisiae L D I G I ... T R L R I ... R L F L S ... R Y F K Q
Saccharomyces arboricola L D I G I ... T R L R I ... R L F L S ... R Y F K Q
Saccharomyces L D I G I ... T R L R I ... R L F L S ... R Y F K Q
Saccharomyces eubayanus L D I G I ... T R L R I ... R L F L S ... R Y F K Q
Kazachstania saulgeensis L D I G I ... T R L R V ... R L F L G ... R Y F K Q
Kazachstania africana L D I G I ... T R L K I ... R L F L G ... R Y F K Q
Naumovozyma castellii L D I G I ... T R L K I ... R L F L G ... R Y F K Q
Torulaspora delbrueckii L D I G I ... S R L K I ... R L F L G ... R Y F K Q
Kazachstania naganishii L D I G I ... T R L K V ... R L F L S ... R Y F K Q
Vanderwaltozyma polyspora L D I G I ... S R L K I ... R L F L S ... R Y F K Q
Tetrapisispora phaffii L D I G I ... T R L K I ... R L F M S ... R Y F K Q
Candida glabrata L D I G I ... T R L K I ... R L F L G ... R Y F K Q
Naumovozyma dairenensis L D I G I ... T R L K I ... R L F L G ... R Y F K Q
Candida maltosa M D V G I ... V R L K I ... R L F L N ... R Y F K Q
Candida tropicalis M D V G I ... V R L K I ... R L F L N ... R Y F K Q
Candida M D V G I ... V R L K I ... R L F L S ... R Y F K Q
Pichia membranifaciens M D V G I ... V R L K I ... R L F L G ... R Y F K Q
Pichia membranifaciens M D V G I ... V R L K I ... R L F L G ... R Y F K Q
Lodderomyces elongisporus M D V G I ... V R L K I ... R L F L S ... R Y F K Q
Candida haemulonis M D V G I ... V R I K I ... R L F L N ... R Y F K Q
Candida auris M D V G I ... V R I K I ... R L F L N ... R Y F K Q
1 2 3 4 5 6 7 8 9
Variable Average Conserved
C
I251 F368 F334 L285
ScVps26 LDIGI...RYFKQ RLFLS TRLRI
HsVps26A MEVGI...RYFKQ RLFLA VRIKI
HsVps26B MEVGI...RYFKQ RLFLA VRIKI
:::** ***** ****: :*::*
D
Vps35
F334
Vps26

Figure 2.8

Figure 2.8. Analysis of cargo recognition by Vps26.

(A) Mutation sites used in this study are shown on the crystal structure of Mus musculus Vps26 [Protein Databank ID code: 2R51]. (B) Sequence comparison of Vps26 residues required for cargo retrieval among Vps26 homologs from related species. (C) Sequence comparison of Vps26 residues required for cargo retrieval in Saccharomyces cerevisiae Vps26, Homo sapiens Vps26A, and Homo sapiens Vps26B. (D) F334 on Vps26 are shown on the crystal structure of Homo sapiens Vps26A-Vps35 complex [Protein Databank ID code: 5F0L].

Discussion

In this study, we demonstrate that a bipartite recycling signal is recognized by Vps26 and Vps35. Strikingly, I251 and F368 on Vps26, which recognizes DMT1-II (Lucas et al., 2016), are required for Ear1 recycling, but dispensable for Vps10 recycling. Alternatively, Vps10 requires F334 on Vps26. Thus, the retromer complex has multiple cargo binding sites for interacting with different cargos. Interestingly, F334 on Vps26 locates close to Vps35 (Fig. 2.8D). Vps10 might interact with Vps26 and Vps35, coincidently. There are several questions to be answered. (1) How many cargo binding sites does the retromer have? (2) How does Vps35 interact with the cargo? (3) Which sequences are recognized by each binding pocket? Further studies will be necessary to address these questions.

Reference

Bean, B.D., M. Davey, and E. Conibear. 2017. Cargo selectivity of yeast sorting nexins. Traffic. 18:110-122.

Burda, P., S.M. Padilla, S. Sarkar, and S.D. Emr. 2002. Retromer function in endosome-to-Golgi retrograde transport is regulated by the yeast Vps34 PtdIns 3-kinase. J. Cell Sci. 115: 3889-3900.

Cereghino, J.L., E.G. Marcusson, and S.D. Emr. 1995. The cytoplasmic tail domain of the vacuolar protein sorting receptor Vps10p and a subset of VPS gene products regulate receptor stability, function, and localization. Mol. Biol. Cell 6(9): 1089-1102.

Collins, B.M., C.F. Skinner, P.J. Watson, M.N. Seaman, and D.J. Owen. 2005. Vps29 has a phosphoesterase fold that acts as a protein interaction scaffold for retromer assembly. Nat. Struct. Mol. Biol. 12(7): 594-602.

Collins, B.M., S.J. Norwood, M.C. Kerr, D. Mahony, M.N. Seaman, R.D. Teasdale, and D.J. Owen. 2008. Structure of Vps26B and mapping of its interaction with the retromer protein complex. Traffic. 9(3): 366-379.

Cooper, A.A., and T.H. Stevens. 1996. Vps10p cycles between the late-Golgi and prevacuolar compartments in its function as the sorting receptor for multiple yeast vacuolar hydrolases. J. Cell Biol. 133(3): 529-541.

Cui, T.Z., T.A. Peterson, and C.G. Burd. 2017. A CDC25 family protein phosphatase gates cargo recognition by the Vps26 retromer subunit. Elife. 6: e24126.

Cullen, P.J., and F. Steinberg. 2018. To degrade or not to degrade: mechanisms and significance of endocytic recycling. Nat. Rev. Mol. Cell Biol. 19(11): 679-696.

Finnigan, G.C., G.E, Cronan, H.J. Park, S. Srinivasan, F.A. Quiocho, and T.H. Stevens. 2012. Sorting of the yeast vacuolar-type, proton-translocating ATPase enzyme complex (V-ATPase): identification of a necessary and sufficient Golgi/endosomal retention signal in Stv1p. J. Biol Chem. 287(23):19487-19500.

Finsel, I., C. Ragaz, C. Hoffmann, C.F. Harrison, S. Weber, V.A. van Rahden, L. Johannes, and H. Hilbi. 2013. The Legionella effector RidL inhibits retrograde trafficking to promote intracellular replication. Cell Host Microbe. 14(1): 38-50.

Fisk, H.A., and M.P. Yaffe. 1999. A role for ubiquitination in mitochondrial inheritance in Saccharomyces cerevisiae. J. Cell Biol. 145(6): 1199-1208.

Fjorback, A.W., M. Seaman, C. Gustafsen, A. Mehmedbasic, S. Gokool, C. Wu, D. Militz, V. Schmidt, P. Madsen, J.R. Nyengaard, T.E. Willnow, E.I. Christensen, W.B. Mobley, A. Nykjær, and O.M. Andersen. 2012. Retromer binds the FANSHY sorting motif in SorLA to regulate amyloid precursor protein sorting and processing. J. Neurosci.

32(4): 1467-1480.

Follett, J., S.J. Norwood, N.A. Hamilton, M. Mohan, O. Kovtun, S. Tay, Y. Zhe, S.A. Wood, G.D. Mellick, P.A. Silburn, B.M. Collins, A. Bugarcic, and S.D. Teasdale. 2014. The Vps35 D620N mutation linked to Parkinson's disease disrupts the cargo sorting function of retromer. Traffic 15(2):230-244.

Harbour, M.E., and M.N. Seaman. 2011. Evolutionary variations of VPS29, and their implications for the heteropentameric model of retromer. Commun. Integr. Biol. 4(5):619-622.

Horazdovsky, B.F., B.A. Davies, M.N. Seaman, S.A. McLaughlin, S. Yoon, and S.D. Emr. 1997. A sorting nexin-1 homologue, Vps5p, forms a complex with Vps17p and is required for recycling the vacuolar protein-sorting receptor. Mol. Biol. Cell. 8:1529-1541.

Kaiser, C., S. Michaelis, and A. Mitchell. 1994. Methods in Yeast Genetics: A Cold Spring Harbor Laboratory Course Manual (Cold Spring Harbor Lab Press, Cold Spring Harbor, NY).

Klionsky, D.J., L.M. Banta, and S.D. Emr. 1988. Intracellular sorting and processing of a yeast vacuolar hydrolase: proteinase A propeptide contains vacuolar targeting information. Mol. Cell Biol. 8(5): 2105-2116.

Kovtun, O., N. Leneva, Y.S. Bykov, N. Ariotti, R.D. Teasdale, M. Schaffer, B.D. Engel, D.J. Owen, J.A. G. Briggs, and B.M. Collins. 2018. Structure of the membrane-assembled retromer coat determined by cryo-electron tomography. Nature 561(7724): 561-564.

Köhrer, K., and S.D. Emr. 1993. The yeast VPS17 gene encodes a membrane-

associated protein required for the sorting of soluble vacuolar hydrolases. J. Biol. Chem. 268(1): 559-569.

Kvainickas, A., A. Jimenez-Orgaz, H. Nägele, Z. Hu, J. Dengjel, and F. Steinberg. 2017. Cargo-selective SNX-BAR proteins mediate retromer trimer independent retrograde transport. J. Cell Biol. 216(11): 3677-3693.

Léon, S., Z. Erpapazoglou, and R. Haguenauer-Tsapis. 2008. Ear1p and Ssh4p are new adaptors of the ubiquitin ligase Rsp5p for cargo ubiquitylation and sorting at multivesicular bodies. Mol. Biol. Cell. 19(6): 2379-2388.

Lucas, M., D.C. Gershlick, A. Vidaurrazaga, A.L. Rojas, J.S. Bonifacino, and A. Hierro. 2016. Structural Mechanism for Cargo Recognition by the Retromer Complex. Cell. 167(6): 1623-1635.

Marcusson, E.G., B.F. Horazdovsky, J.L. Cereghino, E. Gharakhanian, and S.D. Emr. 1994. The sorting receptor for yeast vacuolar carboxypeptidase Y is encoded by the VPS10 gene. Cell. 77: 579-586.

McGough, I.J., F. Steinberg, D. Jia, P.A. Barbuti, K.J. McMillan, K.J. Heesom, A.L. Whone, M.A. Caldwell, D.D. Billadeau, M.K. Rosen, and P.J. Cullen. 2014. Retromer binding to FAM21 and the WASH complex is perturbed by the Parkinson disease-linked VPS35(D620N) mutation. Curr Biol. 24(14): 1670-1676.

McMillan, K.J., H.C. Korswagen, and P.J. Cullen. 2017. The emerging role of retromer in neuroprotection. Curr. Opin. Cell Biol. 47: 72-82.

Miesenböck, G., D.A. De Angelis, and J.E. Rothman. 1998. Visualizing secretion and synaptic transmission with pH-sensitive green fluorescent proteins. Nature. 394(6689): 192-195.

Nothwehr, S.F., C. J. Roberts, and T.H. Stevens. 1993. Membrane protein retention in the yeast Golgi apparatus: dipeptidyl aminopeptidase A is retained by a cytoplasmic signal containing aromatic residues. J. Cell Biol. 121(6): 1197-1209.

Nothwehr, S.F., and A.E. Hindes. 1997. The yeast VPS5/GRD2 gene encodes a sorting nexin-1-like protein required for localizing membrane proteins to the late Golgi. J. Cell Sci. 110: 1063-1072.

Nothwehr, S.F., S.A. Ha, and P. Bruinsma. 2000. Sorting of yeast membrane proteins into an endosome-to-Golgi pathway involves direct interaction of their cytosolic domains with Vps35p. J. Cell Biol. 151(2): 297-310.

Personnic, N., K. Bärlocher, I. Finsel, and H. Hilbi. 2016. Subversion of Retrograde Trafficking by Translocated Pathogen Effectors. Trends Microbiol. 24(6): 450-462.

Peter, B.J., H.M. Kent, I.G. Mills, Y. Vallis, P.J. Butler, P.R. Evans, and H.T. McMahon. 2004. BAR domains as sensors of membrane curvature: the amphiphysin BAR structure. Science 303(5657): 495-499.

Redding, K., J.H. Brickner, L.G. Marschall, J.W. Nichols, and R.S. Fuller. 1996. Allele-specific suppression of a defective trans-Golgi network (TGN) localization signal in Kex2p identifies three genes involved in localization of TGN transmembrane proteins. Mol. Cell Biol. 16(11): 6208-6217.

Reddy, J.V., and M.N. Seaman. 2001. Vps26p, a component of retromer, directs the interactions of Vps35p in endosome-to-Golgi retrieval. Mol Biol Cell 12(10): 3242-3256.

Romano-Moreno, M., A.L, Rojas, C.D. Williamson, D.C. Gershlick, M. Lucas, M.N.

Isupov, J.S. Bonifacino, M.P. Machner, and A. Hierro. 2017. Molecular mechanism for the subversion of the retromer coat by the Legionella effector RidL. Proc. Natl. Acad. Sci. U.S.A. 114(52): E11151-E11160.

Sardana, R., L. Zhu, and S.D. Emr. 2019. Rsp5 Ubiquitin ligase-mediated quality control system clears membrane proteins mistargeted to the vacuole membrane. J. Cell Biol. 218(1): 234-250.

Seaman, M.N., E.G. Marcusson, J.L. Cereghino, and S.D. Emr. 1997. Endosome to Golgi retrieval of the vacuolar protein sorting receptor, Vps10p, requires the function of the VPS29, VPS30, and VPS35 gene products. J. Cell Biol. 137: 79-92.

Seaman, M.N., J.M. McCaffery, and S.D. Emr. 1998. A membrane coat complex essential for endosome-to-Golgi retrograde transport in yeast. J. Cell Biol. 142: 665-681.

Seaman, M.N., and H.P. Williams. 2002. Identification of the functional domains of yeast sorting nexins Vps5p and Vps17p. Mol. Biol. Cell. 13(8): 2826-2840.

Seaman, M.N. 2007. Identification of a novel conserved sorting motif required for retromer-mediated endosome-to-TGN retrieval. J. Cell Sci. 120(Pt 14): 2378-2389.

Simonetti, B., C.M. Danson, K.J. Heesom, and P.J. Cullen. 2017. Sequence-dependent cargo recognition by SNX-BARs mediates retromer-independent transport of CI-MPR. J. Cell Biol. 216(11): 3695-3712.

Vilariño-Güell, C., C. Wider, O.A. Ross, J.C. Dachsel, J.M. Kachergus, S.J. Lincoln, A.I. Soto-Ortolaza, S.A. Cobb, G.J. Wilhoite, J.A. Bacon, B. Behrouz, H.L. Melrose, E. Hentati, A. Puschmann, D.M. Evans, E. Conibear, W.W. Wasserman, J.O. Aasly, P.R. Burkhard, R. Djaldetti, J. Ghika, F. Hentati, A. Krygowska-Wajs, T. Lynch, E. Melamed,

A. Rajput, A.H. Rajput, A. Solida, R.M. Wu, R.J. Uitti, Z.K. Wszolek, F. Vingerhoets, and M.J. Farrer. 2011. VPS35 mutations in Parkinson disease. Am. J. Hum. Genet. 89: 162-167.

Zavodszky, E., M.N. Seaman, K. Moreau, M. Jimenez-Sanchez, S.Y. Breusegem, M.E. Harbour, and D.C. Rubinsztein. 2014. Mutation in VPS35 associated with Parkinson's disease impairs WASH complex association and inhibits autophagy. Nat. Commun. 5: 3848.

Zimprich, A., A. Benet-Pagès, W. Struhal, E. Graf, S.H. Eck, M.N. Offman, D. Haubenberger, S. Spielberger, E.C. Schulte, P. Lichtner, S.C. Rossle, N. Klopp, E. Wolf, K. Seppi, W. Pirker, S. Presslauer, B. Mollenhauer, R. Katzenschlager, T. Foki, C. Hotzy, E. Reinthaler, A. Harutyunyan, R. Kralovics, A. Peters, F. Zimprich, T. Brücke, W. Poewe, E. Auff, C. Trenkwalder, B. Rost, G. Ransmayr, J. Winkelmann, T. Meitinger, and T.M. Strom. 2011. A mutation in VPS35, encoding a subunit of the retromer complex, causes late-onset Parkinson disease. Am. J. Hum. Genet. 89:168-175.

Table 2.1. Yeast strains used in the Chapter II

Strain	Genotype	Source
SEY6210	*MATα ura3-52 his3-200 leu2-3,112 trp1-901 lys2-801 suc2-9*	(1)
SEY6210.1	*MATa ura3-52 his3-200 leu2-3,112 trp1-901 lys2-801 suc2-9*	(1)
YCY220	SEY6210, *VPH1-mCherry::TRP1*	This study
YCY950	SEY6210, *VPH1-mCherry::HIS3, vps10Δ::TRP1*	This study
YCY951	SEY6210, *VPH1-mCherry::HIS3*, *vps10Δ::TRP1, vps35Δ::KanMX6*	This study
YCY856	SEY6210, *rsp5Δ::HIS3, VPH1-mCherry::TRP1, pRS415-rsp5(G747E)*	This study
YCY755	SEY6210, *rsp5Δ::HIS3, EAR1-mNeonGreen::TRP1, pRS415-rsp5(G747E)*	This study
YCY722	SEY6210, *rsp5Δ::HIS3, EAR1-mNeonGreen::TRP1, vps35Δ::KanMX6, pRS415-rsp5(G747E)*	This study
YCY730	SEY6210, *rsp5Δ::HIS3, EAR1(Δ511-550)-mNeonGreen::TRP1, pRS415-rsp5(G747E)*	This study
YCY729	SEY6210, *rsp5Δ::HIS3, EAR1(Δ491-550)-mNeonGreen::TRP1, pRS415-rsp5(G747E)*	This study
YCY728	SEY6210, *rsp5Δ::HIS3, EAR1(Δ471-550)-mNeonGreen::TRP1, pRS415-rsp5(G747E)*	This study
YCY673	SEY6210, *rsp5Δ::HIS3, EAR1(Δ451-550)-mNeonGreen::TRP1, pRS415-rsp5(G747E)*	This study
YCY948	SEY6210.1, *VPS10-GFP::HIS3, VPH1-mCherry::TRP1, vps26Δ::KanMX6*	This study
YCY946	SEY6210, *EAR1-pHluorin::natMX6, Vph1-mCherry::TRP1, vps26Δ::KanMX6*	This study
YCY960	SEY6210, *rsp5Δ::HIS3, VPH1-mCherry::TRP1, pRS415-rsp5(G747E), vps26Δ::hphNT1*	This study
SSY896	SEY6210, *VPH1-mCherry::TRP1, vps5Δ::LEU2*	This study
SSY897	SEY6210, *VPH1-mCherry::TRP1, vps17Δ::KanMX6*	This study
SSY894	SEY6210, *VPH1-mCherry::TRP1, vps26Δ::LEU2*	This study
SSY895	SEY6210, *VPH1-mCherry::TRP1, vps29Δ::HIS3*	This study
SSY216	SEY6210, *VPH1-mCherry::TRP1, vps35Δ::KanMX6*	This study
SSY933	SEY6210, *VPS10-GFP::KanMX6, VPH1-mCherry::TRP1*	This study
SSY934	SEY6210, *VPS10-GFP::KanMX6, VPH1-mCherry::TRP1, vps5Δ::LEU2*	This study
SSY935	SEY6210, *VPS10-GFP::KanMX6, VPH1-mCherry::TRP1, vps17Δ::HIS3*	This study
SSY936	SEY6210, *VPS10-GFP::KanMX6, VPH1-mCherry::TRP1, vps35Δ::HIS3*	This study
SSY924	SEY6210, *VPS17-3xHA::TRP1*	This study
SSY926	SEY6210, *VPS5-3xFLAG::HIS3, VPS17-3xHA::TRP1*	This study
SSY923	SEY6210, *VPS5-3xFLAG::HIS3, vps17Δ::TRP1*	This study
SSY987	SEY6210, *VPS5-3xFLAG::HIS3, VPS17-3xHA::TRP1, vps26Δ::hphNT1*	This study
SSY1047	SEY6210, *VPS5-3xFLAG::HIS3, VPS17-3xHA::TRP1, vps29Δ::KanMX6*	This study
SSY1048	SEY6210, *VPS5-3xFLAG::HIS3, VPS17-3xHA::TRP1, vps35Δ::KanMX6*	This study
SSY970	SEY6210, *pep4Δ::LEU2, prb1Δ::LEU2*	This study
SSY981	SEY6210, *pep4Δ::LEU2, prb1Δ::LEU2, VPS5-3xFLAG::hphNT1*	This study

SSY1042	SEY6210, *pep4Δ::LEU2, prb1Δ::LEU2, VPS5-3xFLAG::hphNT1, vps29Δ::KanMX6*	This study
SSY982	SEY6210, *pep4Δ::LEU2, prb1Δ::LEU2, VPS26-3xFLAG::hphNT1*	This study
SSY1043	SEY6210, *pep4Δ::LEU2, prb1Δ::LEU2, VPS26-3xFLAG::hphNT1, vps5Δ::KanMX6*	This study
SSY1044	SEY6210, *pep4Δ::LEU2, prb1Δ::LEU2, VPS26-3xFLAG::hphNT1, vps17Δ::KanMX6*	This study
SSY1045	SEY6210, *pep4Δ::LEU2, prb1Δ::LEU2, VPS26-3xFLAG::hphNT1, vps29Δ::KanMX6*	This study
SSY1046	SEY6210, *pep4Δ::LEU2, prb1Δ::LEU2, VPS26-3xFLAG::hphNT1, vps35Δ::KanMX6*	This study
SSY983	SEY6210, *pep4Δ::LEU2, prb1Δ::LEU2, VPS35-3xFLAG::hphNT1*	This study
SSY1049	SEY6210, *pep4Δ::LEU2, prb1Δ::LEU2, VPS35-3xFLAG::hphNT1, vps26Δ::KanMX6*	This study
SSY1050	SEY6210, *VPS17-3xHA::TRP1, pep4Δ::KanMX6*	This study
SSY1051	SEY6210, *VPS5-3xFLAG::HIS3, VPS17-3xHA::TRP1, pep4Δ::KanMX6*	This study
SSY1052	SEY6210, *VPS5-3xFLAG::HIS3, VPS17-3xHA::TRP1, vps26Δ::hphNT1 pRS305-VPS26(I251E/F368E), pep4Δ::KanMX6*	This study
SSY1053	SEY6210, *VPS5-3xFLAG::HIS3, VPS17-3xHA::TRP1, vps26Δ::hphNT1, pRS305-VPS26(F334E) , pep4Δ::KanMX6*	This study
SSY1054	SEY6210, *VPS5-3xFLAG::HIS3, VPS17-3xHA::TRP1, vps26Δ::hphNT1, pRS305-VPS26(L285E), pep4Δ::KanMX6*	This study

Table 2.2. Plasmids used in the Chapter II

Name	Genotype	Source
pRS416 [vec]	*CEN URA3*	(2)
pRS416-VPS10-GFP	*pRS416-VPS10-GFP*	Lab stock
pRS416-VPS10(ΔC)-GFP	*pRS416-VPS10(2-1418)-GFP*	This study
pRS416-VPS10(ΔC)-EAR1(C-tail)-GFP	*pRS416-VPS10(2-1418)-EAR1(451-550)-GFP*	This study
pRS416-VPS10(Δ1517-1579)-GFP	*pRS416-VPS10(2-1516)-GFP*	This study
pRS416-VPS10(1417-1426A)-GFP	*pRS416-VPS10(1417-1426A)-GFP*	This study
pRS416-VPS10(1427-1436A)-GFP	*pRS416-VPS10(1427-1436A)-GFP*	This study
pRS416-VPS10(1437-1446A)-GFP	*pRS416-VPS10(1437-1446A)-GFP*	This study
pRS416-VPS10(1447-1456A)-GFP	*pRS416-VPS10(1447-1456A)-GFP*	This study
pRS416-VPS10(1457-1466A)-GFP	*pRS416-VPS10(1457-1466A)-GFP*	This study
pRS416-VPS10(1467-1476A)-GFP	*pRS416-VPS10(1467-1476A)-GFP*	This study
pRS416-VPS10(1477-1486A)-GFP	*pRS416-VPS10(1477-1486A)-GFP*	This study
pRS416-VPS10(1487-1496A)-GFP	*pRS416-VPS10(1487-1496A)-GFP*	This study
pRS416-VPS10(1497-1506A)-GFP	*pRS416-VPS10(1497-1506A)-GFP*	This study
pRS416-VPS10(1507-1516A)-GFP	*pRS416-VPS10(1507-1516A)-GFP*	This study
pRS416-VPS10(R1417A)-GFP	*pRS416-VPS10(R1417A)-GFP*	This study
pRS416-VPS10(G1418A)-GFP	*pRS416-VPS10(G1418A)-GFP*	This study
pRS416-VPS10(I1419A)-GFP	*pRS416-VPS10(I1419A)-GFP*	This study
pRS416-VPS10(R1420A)-GFP	*pRS416-VPS10(R1420A)-GFP*	This study
pRS416-VPS10(R1421A)-GFP	*pRS416-VPS10(R1421A)-GFP*	This study
pRS416-VPS10(N1422A)-GFP	*pRS416-VPS10(N1422A)-GFP*	This study
pRS416-VPS10(G1423A)-GFP	*pRS416-VPS10(G1423A)-GFP*	This study
pRS416-VPS10(G1424A)-GFP	*pRS416-VPS10(G1424A)-GFP*	This study
pRS416-VPS10(F1425A)-GFP	*pRS416-VPS10(F1425A)-GFP*	This study
pRS416-VPS10(R1427A)-GFP	*pRS416-VPS10(R1427A)-GFP*	This study
pRS416-VPS10(F1428A)-GFP	*pRS416-VPS10(F1428A)-GFP*	This study
pRS416-VPS10(G1429A)GFP	*pRS416-VPS10(G1429A)GFP*	This study
pRS416-VPS10(E1430A)-GFP	*pRS416-VPS10(E1430A)-GFP*	This study
pRS416-VPS10(I1431A)-GFP	*pRS416-VPS10(I1431A)-GFP*	This study
pRS416-VPS10(R1432A)-GFP	*pRS416-VPS10(R1432A)-GFP*	This study
pRS416-VPS10(L1433A)-GFP	*pRS416-VPS10(L1433A)-GFP*	This study
pRS416-VPS10(G1434A)-GFP	*pRS416-VPS10(G1434A)-GFP*	This study

pRS416-VPS10(D1435A)-GFP	*pRS416-VPS10(D1435A)-GFP*	This study
pRS416-VPS10(D1436A)-GFP	*pRS416-VPS10(D1436A)-GFP*	This study
pRS416-VPS10(G1437A)-GFP	*pRS416-VPS10(G1437A)-GFP*	This study
pRS416-VPS10(L1438A)-GFP	*pRS416-VPS10(L1438A)-GFP*	This study
pRS416-VPS10(I1439A)-GFP	*pRS416-VPS10(I1439A)-GFP*	This study
pRS416-VPS10(E1440A)-GFP	*pRS416-VPS10(E1440A)-GFP*	This study
pRS416-VPS10(N1441A)-GFP	*pRS416-VPS10(N1441A)-GFP*	This study
pRS416-VPS10(N1442A)-GFP	*pRS416-VPS10(N1442A)-GFP*	This study
pRS416-VPS10(N1443A)-GFP	*pRS416-VPS10(N1443A)-GFP*	This study
pRS416-VPS10(T1444A)-GFP	*pRS416-VPS10(T1444A)-GFP*	This study
pRS416-VPS10(D1445A)-GFP	*pRS416-VPS10(D1445A)-GFP*	This study
pRS416-VPS10(R1446A)-GFP	*pRS416-VPS10(R1446A)-GFP*	This study
pRS416-EAR1(ΔC)-GFP	*pRS416-EAR1(2-67)-GFP*	This study
pRS416-EAR1(ΔC)-VPS10(C-tail)-GFP	*pRS416-EAR1(2-67)-VPS10(1416-1523)-GFP*	This study
pRS416-VPS10(1492-1495A)-GFP	*pRS416-VPS10(1492-1495A)-GFP*	This study
pRS416-VPS10(1428-1433A)-GFP	*pRS416-VPS10(1428-1433A)-GFP*	This study
pRS416-VPS10(1428-1433A/1492-1495A)-GFP	*pRS416-VPS10(1428-1433A+1492-1495A)-GFP*	This study
pRS416-EAR1-mNeonGreen-3xHA	*pRS416-EAR1-mNeonGreen-3xHA*	This study
pRS416-EAR1(Δ511-550)-mNeonGreen-3xHA	*pRS416-EAR1(2-510)-mNeonGreen-3xHA*	This study
pRS416-EAR1(Δ491-550)-mNeonGreen-3xHA	*pRS416-EAR1(2-490)-mNeonGreen-3xHA*	This study
pRS416-EAR1(Δ471-550)-mNeonGreen-3xHA	*pRS416-EAR1(2-470)-mNeonGreen-3xHA*	This study
pRS416-EAR1(Δ451-550)-mNeonGreen-3xHA	*pRS416-EAR1(2-450)-mNeonGreen-3xHA*	This study
pRS416-EAR1(452-456A)-mNeonGreen-3xHA	*pRS416-EAR1(452-456A)-mNeonGreen-3xHA*	This study
pRS416-EAR1(457-461A)-mNeonGreen-3xHA	*pRS416-EAR1(457-461A)-mNeonGreen-3xHA*	This study
pRS416-EAR1(462-466A)-mNeonGreen-3xHA	*pRS416-EAR1(462-466A)-mNeonGreen-3xHA*	This study
pRS416-EAR1(467-471A)-mNeonGreen-3xHA	*pRS416-EAR1(467-471A)-mNeonGreen-3xHA*	This study
pRS416-EAR1(472-476A)-mNeonGreen-3xHA	*pRS416-EAR1(472-476A)-mNeonGreen-3xHA*	This study
pRS416-EAR1(477-481A)-mNeonGreen-3xHA	*pRS416-EAR1(477-481A)-mNeonGreen-3xHA*	This study
pRS416-EAR1(482-486A)-mNeonGreen-3xHA	*pRS416-EAR1(482-486A)-mNeonGreen-3xHA*	This study
pRS416-EAR1(P451A)-mNeonGreen-3xHA	*pRS416-EAR1(P451A)-mNeonGreen-3xHA*	This study
pRS416-EAR1(P452A)-mNeonGreen-3xHA	*pRS416-EAR1(P452A)-mNeonGreen-3xHA*	This study
pRS416-EAR1(P453A)-mNeonGreen-3xHA	*pRS416-EAR1(P453A)-mNeonGreen-3xHA*	This study
pRS416-EAR1(P454A)-mNeonGreen-3xHA	*pRS416-EAR1(P454A)-mNeonGreen-3xHA*	This study
pRS416-EAR1(G455A)-mNeonGreen-3xHA	*pRS416-EAR1(G455A)-mNeonGreen-3xHA*	This study
pRS416-EAR1(F456A)-mNeonGreen-3xHA	*pRS416-EAR1(F456A)-mNeonGreen-3xHA*	This study

Name	*Genotype*	Source
pRS416-EAR1(E457A)-mNeonGreen-3xHA	*pRS416-EAR1(E457A)-mNeonGreen-3xHA*	This study
pRS416-EAR1(F458A)-mNeonGreen-3xHA	*pRS416-EAR1(F458A)-mNeonGreen-3xHA*	This study
pRS416-EAR1(T459A)-mNeonGreen-3xHA	*pRS416-EAR1(T459A)-mNeonGreen-3xHA*	This study
pRS416-EAR1(M460A)-mNeonGreen-3xHA	*pRS416-EAR1(M460A)-mNeonGreen-3xHA*	This study
pRS416-EAR1(E472A)-mNeonGreen-3xHA	*pRS416-EAR1(E472A)-mNeonGreen-3xHA*	This study
pRS416-EAR1(I473A)-mNeonGreen-3xHA	*pRS416-EAR1(I473A)-mNeonGreen-3xHA*	This study
pRS416-EAR1(N474A)-mNeonGreen-3xHA	*pRS416-EAR1(N474A)-mNeonGreen-3xHA*	This study
pRS416-EAR1(L475A)-mNeonGreen-3xHA	*pRS416-EAR1(L475A)-mNeonGreen-3xHA*	This study
pRS416-EAR1(D476A)-mNeonGreen-3xHA	*pRS416-EAR1(D476A)-mNeonGreen-3xHA*	This study
pRS416-EAR1(PY mut.)-mNeonGreen-3xHA	*pRS416-EAR1(P398A/Y400A/P483A/Y485A)-mNeonGreen-3xHA*	This study
pCM189	*pCM189-TETOFFpro-CYC1pro*	This study
pCM189-EAR1 OE	*pCM189-TETOFFpro-CYC1pro-EAR1*	This study
pCM189-EAR1(PY mut.) OE	*pCM189-TETOFFpro-CYC1pro-EAR1(P398A/Y400A/P483A/Y485A)*	This study
pCM189-EAR1(PY mut./F456A) OE	*pCM189-TETOFFpro-CYC1pro-EAR1(P398A/Y400A/F456A/P483A/Y485A)*	This study
pRS416-CPYpro-mCherry-PHO8	*pRS416-CPYpro-mCherry-PHO8*	This study
pRS305-VPS26	*pRS305-VPS26*	This study
pRS305-VPS26(I251E/F368E)	*pRS305-VPS26(I251E/F368E)*	This study
pRS305-VPS26(F334E)	*pRS305-VPS26 (F334E)*	This study
pRS305-VPS26(L285E)	*pRS305-VPS26(L285E)*	This study
pRS416-VPS26	*pRS416-VPS26*	This study
pRS416-VPS26(I251E/F368E)	*pRS416-VPS26(I251E/F368E)*	This study
pRS416-VPS26(F334E)	*pRS416-VPS26 (F334E)*	This study
pRS416-VPS26(L285E)	*pRS416-VPS26(L285E)*	This study

Supplemental References

1. Robinson, J.S., Klionsky, D.J., Banta, L.M., Emr, S.D. (1988) Protein sorting in Saccharomyces cerevisiae: isolation of mutants defective in the delivery and processing of multiple vacuolar hydrolases. Mol. Cell Biol. *8*, 4936-4948.

2. Sikorski RS, Hieter P (1989) A system of shuttle vectors and yeast host strains designed for efficient manipulation of DNA in Saccharomyces cerevisiae. Genetics *122*, 19-27.

Chapter III

Ubiquitin-Dependent Lysosomal Membrane Protein Sorting and Degradation

Chapter III is the paper currently in press in ***Molecular Cell*** : Ubiquitin-Dependent Lysosomal Membrane Protein Sorting and Degradation. Ming Li, Yueguang Rong, Ya-Shan Chuang, Dan Peng, Scott D. Emr. Ya-Shan's contribution to this chapter is confirming the interaction between the E3 ubiquitin ligase Rsp5 and the adaptor Ssh4 by co-immunoprecipitation and also proves that Ypq1 is an AP3 cargo. His work is presented in Figure 3.8G and 3.4C.

Abstract

As an essential organelle in the cell, the lysosome is responsible for digestion and recycling of intracellular components, storage of nutrients, and pH homeostasis. The lysosome is enclosed by a special membrane to maintain its integrity, and nutrients are transported across the membrane by numerous transporters. Despite their importance in maintaining nutrient homeostasis and regulating signaling pathways, little is known about how lysosomal membrane protein lifetimes are regulated. We identified a yeast vacuolar amino acid transporter, Ypq1, that is selectively sorted and degraded in the vacuolar lumen following lysine withdrawal. This selective degradation process requires a vacuole anchored ubiquitin ligase (VAcUL-1) complex composed of Rsp5 and Ssh4. We propose that after ubiquitination, Ypq1 is selectively sorted into an intermediate compartment. The ESCRT machinery is then recruited to sort the ubiquitinated Ypq1 into intraluminal vesicles (ILVs). Finally, the compartment fuses with the vacuole and delivers ILVs into the lumen for degradation.

Introduction

The lysosome (or vacuole in yeast and plants) is an essential organelle in all eukaryotic cells. As the primary digestive organelle, it is responsible for the turnover of extracellular materials and plasma membrane (PM) proteins (e.g., EGFR) that have been internalized by phagocytosis or endocytosis. It is also responsible for the degradation of cytosolic components and organelles that are engulfed and delivered to the lysosome by various types of autophagy. Proteins, polysaccharides, lipids, nucleic acids, as well as other intracellular macromolecules are digested within the lysosome, and the products (such as amino acids, sugars, and fatty acids) are transported out for reuse by the cell. In addition, lysosomes also serve as storage organelles for excess nutrients such as amino acids, ions, and many secondary metabolites. Toxic compounds and heavy metals are also accumulated in the lysosome to detoxify the compounds and protect the cell from damage. Furthermore, the lysosome is an important signaling hub to control cell growth and numerous other intracellular processes. The target of rapamycin complex 1 (TORC1) is localized on the lysosomal membrane, where it phosphorylates downstream substrates to regulate growth (Laplante and Sabatini, 2009). Amino

acid levels within the lysosome can be sensed by the Rag GTPase and thereby affect its GTP/GDP state to recruit the downstream TORC1 complex (Bar-Peled and Sabatini, 2014).

Because the lysosome is acidic and filled with digestive enzymes, it is enclosed by a special membrane that resists digestion and maintains a proton gradient. To maintain the nutrient homeostasis between the lysosome and cytoplasm, many membrane transporters are present in the lysosomal membrane that can transport nutrients in and out of lysosome. Remarkably, most of these membrane transporters are structurally and functionally related to PM transporters. Some of them are even paralogues derived from the same origin. For example, Ftr1, the high-affinity iron permease, forms a complex with Fet3 in the yeast PM where it transports iron into the cell (Stearman et al., 1996). Paralogues of this complex, Fth1 and Fet5, are localized in the vacuole membrane (VM) to mediate the efflux of Fe^{2+} from the vacuole lumen (Urbanowski and Piper, 1999). Other examples include the cationic amino acids transporters. While Lyp1, Can1, and Alp1 mediate the uptake of cationic amino acids in the yeast PM, two other families of amino acid transporters, including

the PQ-loop-containing transporters (Ypq1–3) (Jézégou et al., 2012) and the vacuole basic amino acids transporter family (Vba1–4) (Shimazu et al., 2005), reside in the vacuole membrane to transport cationic amino acids. These two distinct membrane (PM and VM) transporting systems enable the cell to quickly adapt to changes of nutrient concentrations in the environment. Misregulation or malfunction of lysosomal membrane transporters leads to storage diseases in humans. For example, mutations in the lysosomal cholesterol transporter, NPC1, disrupt intracellular lipid homeostasis, resulting in a massive accumulation of lipids within lysosomes, leading to the type C1 Niemann-Pick disease (Platt et al., 2012). In addition, mutations in cystinosin, the lysosomal cystine transporter that is also a PQ-loop-containing protein (Jézégou et al., 2012), result in the accumulation of free cystine within the lysosome and cause cystinosis in humans (Platt et al., 2012). Finally, defects in the cationic amino acid transporters such as PQLC2, the human homolog of Ypq1, have been implicated in Batten disease because of the low cationic amino acid levels in the patients' fibroblasts (Jézégou et al., 2012; Ramirez-Montealegre and Pearce, 2005).

Despite their importance in maintaining nutrient homeostasis and regulating signaling pathways, little is known about the regulation of the quantity and quality of these lysosomal membrane proteins. What controls their lifetime in the membrane, and how are they degraded? For PM receptors, ion channels, and transporters, interaction with ligands or changes in their substrate concentration triggers selective ubiquitination and endocytosis (Doherty and McMahon, 2009). Endocytosed cargoes then follow the endomembrane trafficking pathway and are sent to the lysosomal lumen for degradation. However, it is unclear whether cells can downregulate lysosomal membrane proteins. Given the harsh environment of the lysosomal lumen, many lysosomal membrane proteins may be damaged and must be cleared from the membrane to maintain the integrity of the organelle. It remains to be addressed whether the cell has a protein quality control system to cope with these stresses and, if so, what the molecular machinery is. One example of a retro-grade trafficking pathway from the vacuole membrane to the TGN was reported using an artificial chimeric protein. However, the recycling mechanism was not determined (Bryant et al., 1998).

In this study, we report that lysosomal membrane proteins are subject to tight regulation in response to changes of their substrate concentration. Using budding yeast as a model system, we found that the vacuolar cationic amino acid transporter, Ypq1, is selectively sorted and degraded inside the vacuole lumen following lysine withdrawal. This selective degradation process requires ubiquitination by a Nedd4 family E3 ubiquitin ligase, Rsp5. Recruitment of Rsp5 to the vacuole requires a PY-motif-containing adaptor, Ssh4, which resides in the vacuole membrane. Strikingly, after ubiquitination, Ypq1 is selectively sorted off the vacuole membrane to initiate a process similar to endo-membrane trafficking. The ESCRT (endosomal sorting complex required for sorting) machinery is then recruited to these compartments, and the ubiquitinated Ypq1 is sorted into the intraluminal vesicles (ILVs) before it is delivered into the vacuole for degradation. We name this process as the vacuole membrane protein recycling and degradation (vReD) pathway.

Material and Methods

Yeast Strains, Plasmids, and Growth Conditions

All yeast strains and plasmids used in this study are listed in Table 3.1. For the Ypq1 degradation assay, yeast cells were grown in YPD media or YNB media containing 23 μg/ml lysine to mid-log phase (optical density 600 [OD600]: 0.4~0.8) before being collected at 2,500 × g for 5 min. After wash with water twice, the yeast cells were immediately resuspended in YNB media without lysine and incubated for an appropriate amount of time (typically 2–6 hr) before being collected for further analysis. Most experiments were performed at 26°C. For the temperature-sensitive mutants, after yeast cells reached the mid-log phase at 26°C, the culture was shifted to 37°C for 20 min before being exchanged into the lysine minus media (pre-incubated at 37°C) to induce the degradation. All later experiments were performed at 37°C.

Microscopy and Image Processing

Most microscopy, except the split GFP assay in Figure 3.5H, was performed with a

DeltaVision RT system (Applied Precision), equipped with a Photometrics CoolSNAP HQ Camera, a 100× objective, and a DeltaVision RT Standard Filter Set (FITC for GFP/pHluorin and RD-TR-Cy3 for mCherry). Image acquisition, deconvolution, and maximum projection analysis were performed in the program Softworx. The line-scan analysis and image cropping were performed using the ImageJ software (NIH). For the split GFP assay, images were acquired using a 100× objective on an inverted Olympus IX3 spinning-disc confocal microscope equipped with an EM CCD camera (iXon Ultra, Andor Technology). The GFP emission was collected with the 520/28 nm filter set.

Immunoprecipitation (IP) assay

The IP assay was adapted from Breslow *et al* (Breslow *et al*., 2010), with some modifications. Essentially, yeast cells were grown into the mid-log phase in YPD media, before being shifted to YNB minus lysine media for 30 min or 2 hours. ~ 40 OD600 cells were collected, washed once with water at 4 oC, and resuspended in 500 µl IP buffer (50 mM HEPES-KOH, pH 6.8, 150 mM KOAc, 2mM MgOAc, 1mM

CaCl2, and 15% glycerol) with 0.1% digitonin, supplemented with protease inhibitors and 20 mM NEM (n-ethylmalemide). Whole cell lysates were prepared by bead beating at 4 oC for 10 min, followed by addition of 500 µl 1.9% digitonin in IP buffer. Membranes were solubilized by nutating lysates at 4 oC for 50 min. The insolubile material was removed by spinning at 100,000g for 20 min. The resulting lysate was incubated with 25 µl GFP-TRAP resin (Chromo Tek) at 4 oC for 2 hours. The GFP-TRAP resin was then washed four times with 0.1% digitonin in IP buffer, and bound proteins were eluted by boiling resin with SDS-PAGE sample buffer.

Western Blot and Antibodies

Total cell lysates were prepared from 7 OD600 cultures by incubating on ice 1 hr in 10% TCA. Following two acetone wash-sonication cycles, samples were bead-beated 5 min in 2x urea buffer (150mMTris [pH 6.8], 6Murea, 6%SDS) and incubated 5 min at 37˚C. After addition of 2x sample buffer (150mMTris [pH 6.8], 2%SDS, 100mM DTT and bromophenol blue), samples were bead-beated for 5

min and heated 5 min at 37˚C. Samples were run on 10% polyacrylamide gels and

transferred to nitrocellulose membranes. Antibodies used for blotting were G6PDH, GFP (B2, Santa Cruz Biotech.), and Vph1 (10D7, Invitrogen).

Table 3.1. Yeast Strains and Plasmids Used in the Chapter III

S. cerevisiae strains			
strain	***name***	***genotype***	***reference/source***
SEY6210	*wild type*	*Mata, leu1-3, 112 ura3-52 his3-200, trp1-901 lys2-801 suc2-D9*	(Robinson et al., 1988)
YYR5	*vam3tsf, YPQ1-GFP*	6210, *vam3tsf, YPQ1-GFP::TRP1*	this study
YYR6	YPQ1-GFP	6210, *YPQ1-GFP::TRP1*	this study
YYR13	*vps4tsf, YPQ1-GFP*	6210.1, *vps4Δ::TRP1, vps4ts::LEU2, YPQ1-GFP::HIS3*	this study
YYR16	*atg1 Δ, YPQ1-GFP*	6210, *atg1Δ::KAN, YPQ1-GFP::TRP1*	this study
YYR17	*atg5 Δ, YPQ1-GFP*	6210, *atg5Δ*::HIS3, *YPQ1-GFP::TRP1*	this study
YYR18	*atg7 Δ, YPQ1-GFP*	6210, *atg7Δ::LEU2, YPQ1-GFP::TRP1*	this study
YYR31	*pep4Δ, YPQ1-GFP*	6210, *pep4Δ::LEU2, YPQ1-GFP::TRP1*	this study
YYR35	*pep12tsf, YPQ1-GFP, VPH1-mCherry*	6210, *pep12tsf::LEU2, YPQ1-GFP::TRP1, VPH1-mCherry::HIS3*	this study
YYR36	*YPQ1-GFP , VPH1-mCherry*	6210,*VPH1-mCherry::HIS3, YPQ1-GFP::TRP1*	this study
YYR44	*SSH4-3XGFP*	6210, *SSH4-3XGFP::NAT*	this study
YYR51	*ssh4 Δ,* YPQ1-GFP	6210, *ssh4Δ::TRP1, YPQ1-GFP::KAN*	this study
YML428	*YPQ1-nGFP, VPS23-cGFP*	6210.1, *YPQ1-nGFP::TRP1, VPS23-cGFP::HIS3*	this study
YML457	*PMC1-GFP, VPH1-mCherry*	6210,*VPH1-mCherry::HIS3, PMC1-GFP::TRP1*	this study
YML471	*GFP-RSP5*	6210.1, *GFP-RSP5::LEU2*	this study
YML522	*doa4 Δ, YPQ1-GFP*	6210, *doa4Δ*::HIS3, *YPQ1-GFP::TRP1*	this study
YML535	*EAR1-GFP*	6210.1, *EAR1-GFP::TRP1*	this study
YML536	*vps18tsf, YPQ1-GFP*	6210, *vps18tsf, YPQ1-GFP::KAN*	this study
YML540	*ear1Δ, YPQ1-GFP*	6210, *ear1Δ*::HIS3, *YPQ1-GFP::TRP1*	this study
YML547	*ssh4 Δ, doa4 Δ YPQ1-GFP*	6210, *ssh4Δ*::TRP1, *doa4 Δ::HIS3, YPQ1-GFP::KAN*	this study

YML556	*vps4*Δ, *YPQ1-GFP*	6210.1, *vps4*Δ::*TRP1*, *YPQ1-GFP*::*HIS3*	this study
YML605	*ssh4* Δ, *YPQ1-nGFP*, *VPS23-cGFP*,	6210.1, *YPQ1-nGFP*::*TRP1*, *VPS23-cGFP*::*HIS3*, *ssh4* Δ::*TRP1*	this study
YCY119	*vps27*Δ, *YPQ1-GFP*	6210, *vps27*Δ::HIS3, *YPQ1-GFP*::*TRP1*	this study
YCY120	*vps23* Δ, *YPQ1-GFP*	6210, *vps23*Δ::*HIS3*, *YPQ1-GFP*::*KAN*	this study
YCY121	*snf7*Δ, *YPQ1-GFP*	6210, *snf7*Δ::*TRP1*, *YPQ1-GFP*::*KAN*	this study
DYY1003	*vma3* Δ	6210, *vma3* Δ::*LEU2*	this study
CBY16	*pep12* Δ	6210, *pep12* Δ::*LEU2*	(Burd et al., 1997)
GOY3	*apm3* Δ	6210, *apm3* Δ::*HIS3*	(Cowles et al., 1997)
MBY45	*doa4*Δ	6210, *doa4* Δ::*HIS3*	(Katzmann et al., 2001)

S. cerevisiae expression plasmids

vector	***name***	***description***	***reference/source***
pRS416	*YPQ1-GFP*	endogenous promoter, c-terminal GFP	this study
pCM189	*YPQ1-GFP*	tet-off vector, c-terminal GFP	this study
pRS426	*Pcu-Myc-UBI*	Copper promoter, Myc-tagged Ubiquitin	this study
pRS416	*SSH4-3XHA*	endogenous promoter, c-terminal 3xHA tag	this study
pRS416	*ssh4- py1*-3XHA	endogenous promoter, first PY motif mutated to PAAA c-terminal 3xHA tag	this study
pRS416	*ssh4- py2*-3XHA	endogenous promoter, second PY motif mutated to PARA c-terminal 3xHA tag	this study
pRS416	*Padh1-SSH4*	For Ssh4 over-expression	this study
pRS416	*Padh1-ssh4-*$^{py1+2}$	For *ssh4-*$^{py1+2}$ over-expression	this study
pRS416	*Padh1-EAR1*	For Ear1 over-expression	this study
pRS416	*YPQ1-pHluorin*	endogenous promoter, c-terminal pHluorin	this study
pRS416	*ZRT3-pHluorin*	endogenous promoter, c-terminal pHluorin	this study
pRS416	*ypq1*^{diL}-GFP	endogenous promoter, c-terminal GFP, di-leucine motif mutated	this study

Supplemental References

Breslow, D. K., Collins, S. R., Bodenmiller, B., Aebersold, R., Simons, K., Shevchenko, A., Ejsing, C. S., and Weissman, J. S. (2010). Orm family proteins mediate sphingolipid homeostasis. Nature *463*, 1048-1053.

Helliwell, S. B., Losko, S., and Kaiser, C. A. (2001). Components of a ubiquitin ligase complex specify polyubiquitination and intracellular trafficking of the general amino acid permease. J Cell Biol *153*, 649-662.

Hettema, E. H., Valdez-Taubas, J., and Pelham, H. R. (2004). Bsd2 binds the ubiquitin ligase Rsp5 and mediates the ubiquitination of transmembrane proteins. Embo J *23*, 1279-1288.

Imai, K., Noda, Y., Adachi, H., and Yoda, K. (2007). Peculiar protein-protein interactions of the novel endoplasmic reticulum membrane protein Rcr1 and ubiquitin ligase Rsp5. Biosci Biotechnol Biochem *71*, 249-252.

Kota, J., Melin-Larsson, M., Ljungdahl, P. O., and Forsberg, H. (2007). Ssh4, Rcr2 and Rcr1 affect plasma membrane transporter activity in Saccharomyces cerevisiae. Genetics *175*, 1681-1694.

Leon, S., Erpapazoglou, Z., and Haguenauer-Tsapis, R. (2008). Ear1p and Ssh4p are new adaptors of the ubiquitin ligase Rsp5p for cargo ubiquitylation and sorting at multivesicular bodies. Mol Biol Cell *19*, 2379-2388.

Lin, C. H., MacGurn, J. A., Chu, T., Stefan, C. J., and Emr, S. D. (2008). Arrestin-related ubiquitin-ligase adaptors regulate endocytosis and protein turnover at the cell surface. Cell *135*, 714-725.

MacDonald, C., Stringer, D. K., and Piper, R. C. (2012). Sna3 is an Rsp5 adaptor protein that relies on ubiquitination for its MVB sorting. Traffic *13*, 586-598.

Yashiroda, H., Kaida, D., Toh-e, A., and Kikuchi, Y. (1998). The PY-motif of Bul1 protein is essential for growth of Saccharomyces cerevisiae under various stress conditions. Gene *225*, 39-46.

Zhao, Y., Macgurn, J. A., Liu, M., and Emr, S. (2013). The ART-Rsp5 ubiquitin ligase network comprises a plasma membrane quality control system that protects yeast cells from proteotoxic stress. Elife (Cambridge) *2*, e00459.

Burd, C. G., Peterson, M., Cowles, C. R., and Emr, S. D. (1997). A novel Sec18p/NSF-dependent complex required for Golgi-to-endosome transport in yeast.

Mol Biol Cell *8*, 1089-1104.

Cowles, C. R., Odorizzi, G., Payne, G. S., and Emr, S. D. (1997). The AP-3 adaptor complex is essential for cargo-selective transport to the yeast vacuole. Cell *91*, 109-118.

Katzmann, D. J., Babst, M., and Emr, S. D. (2001). Ubiquitin-dependent sorting into the multivesicular body pathway requires the function of a conserved endosomal protein sorting complex, ESCRT-I. Cell *106*, 145-155.

Result

Vacuole Membrane Protein Can be Triggered for Degradation inside the Vacuole

We set out to understand how cells regulate the composition and abundance of lysosomal membrane proteins using Saccharomyces cerevisiae as a model. We reasoned that manipulating their substrate concentration in the growth media might trigger changes in transporter levels at the vacuole membrane. Therefore, we chose five different vacuolar membrane transporters, including Vph1 (v-type ATPase subunit), Ypq1 (cationic amino acid transporter), Vba4 (another cationic amino acid transporter), Pmc1 (Ca2+ transporter), and Fth1 (Fe2+ transporter). We tested if changing pH (Vph1), cationic amino acid levels (Ypq1 and Vba4), Ca2+ (Pmc1), or Fe2+ (Fth1) concentration in the growth media can trigger degradation of the corresponding vacuolar transporters.

We found that when yeast cells were shifted from a lysine-replete to lysine-depleted medium, the Ypq1-GFP fusion protein was sorted into the lumen of the vacuole (Figures 3.1A–3.1C). In contrast, Vph1 and Pmc1 were stable on the vacuole

membrane under the same treatment (Figures 3.1A–3.1F), indicating that Ypq1 internalization is a highly selective process. Western blot analysis confirmed that Ypq1-GFP was degraded, while the levels of Vph1 and another cytosolic protein, G6PDH, remained unchanged (Figures 3.1G and 3.1H). To avoid aggregation due to boiling of multi-spam transmembrane proteins like Ypq1-GFP, we solubilized yeast membranes at a lower temperature (37°C) for SDS-PAGE. As a result, Ypq1-GFP sometimes migrated as a pair of bands on the PAGE gel, with one band at ~55 kDa and the second band at ~65 kDa, presumably because the protein is not fully denatured in SDS at 37°C. The GFP moiety, which is resistant to vacuolar proteases, accumulated (Figures 3.1G and 3.1H). Ypq1 has two close paralogues in budding yeast, Ypq2 and Ypq3 (Jézégou et al., 2012). All three proteins are localized to the vacuole membrane. However, only Ypq1 exhibited regulated degradation by lysine withdrawal (data not shown). Thus, we focused on Ypq1 to analyze the mechanism of signal-mediated vacuole membrane protein degradation. As for other transporters (Vph1, Vba4, Pmc1, and Fth1), we did not find a condition to trigger their internalization into the vacuolar lumen (data not shown).

The selectivity of Ypq1 internalization was further demonstrated by the observation that the sorting was only triggered by lysine withdrawal. Removing other amino acids, including leucine, tryptophan, or even histidine and arginine, did not trigger a similar response (Figure 3.1I).

Ypq1 is predicted to be a 7-transmembrane helical protein, with its C terminus located on the cytoplasmic side of the vacuole membrane (Jézégou et al., 2012). Indeed, when Ypq1 was C-terminally tagged with pHluorin, a pH-sensitive GFP variant (Miesenböck et al., 1998), the chimera could be visualized by fluorescence microscopy (Figures 3.2A and 3.2B), indicating that the C terminus of the Ypq1 faces the cytoplasm. In contrast, when pHluorin was fused to the C terminus of another vacuolar transporter, Zrt3, containing 8-transmembrane domains with the C terminus inside the vacuole lumen (MacDiarmid et al., 2000), the green fluorescence was quenched (Figure 3.2B). The loss of fluorescence was due to the low pH (~5.5) within the vacuole lumen. The green fluorescence was restored in a vma3Δ strain defective for the V-ATPase function (vacuole pH ~7). Taken together, we concluded that the C terminus of Ypq1 is on the cytosolic side of the vacuole membrane.

Therefore, the degradation of Ypq1-GFP and accumulation of free GFP is likely due to a process that selectively delivered Ypq1-GFP to the vacuole lumen following lysine withdrawal.

To confirm that Ypq1-GFP degradation is due to vacuolar proteases, we deleted the PEP4 gene that encodes a key vacuolar protease, which cleaves and activates other vacuolar enzymes. This blocked the degradation of Ypq1-GFP even after an extended 6-hr incubation. Ypq1-GFP was still internalized into the vacuolar lumen in pep4Δ mutant cells (Figures 3.1J and 3.1K). This further demonstrated that Ypq1 is degraded in the vacuolar lumen by the luminal proteases.

To confirm that the pre-existing pool of Ypq1 on the vacuole membrane is degraded, we expressed Ypq1-GFP under the control of a Tet-off promoter. As shown in Figure 3.3, withdrawing lysine in the presence of doxycycline (2 μg/ml, added 30 min before lysine withdrawal) still triggered the internalization and degradation of Ypq1-GFP. The degradation took ~8 hr to complete, probably due to a higher

expression level of Ypq1-GFP under the Tet-off promoter. Nevertheless, these data indicate that pre-existing Ypq1-GFP is targeted for degradation in the vacuole lumen after lysine withdrawal.

Newly Synthesized Ypq1 Is Sorted to the Vacuole via the AP3 Pathway

As an initial step to understand the mechanism of Ypq1 trafficking, we set out to determine the pathway for Ypq1 delivery to the vacuole. Two conserved pathways have been described for vacuolar protein targeting from the late Golgi. The VPS (vacuolar protein sorting) pathway transports vacuolar proteases such as CPY, Pep4, and Prb1 to the vacuole via an intermediate endosomal compartment marked by the Pep12 SNARE protein (Bowers and Stevens, 2005). It is also responsible for transporting ubiquitinated cargoes from the late Golgi such as CPS to the vacuole lumen via the ESCRT-mediated sorting of ubiquitinated CPS into ILVs at the endosome (Katzmann et al., 2001). Furthermore, the VPS pathway is responsible for transporting ubiquitinated PM proteins to the vacuole lumen for degradation. The VPS pathway can be blocked at an early stage by deleting PEP12, encoding the t-

SNARE protein on the pre-vacuolar endosome (Burd et al., 1997).

The AP3 pathway transports another subset of vacuolar membrane proteins from the Golgi, such as alkaline phosphatase (ALP) to the vacuole. These membrane proteins typically contain an acidic di-leucine targeting motif, which can be recognized at the late Golgi by the AP3 adaptor complex for sorting into carrier vesicles that then target and fuse with the vacuole. Mutants lacking subunits in the AP3 complex are defective for the trafficking of AP3 cargoes, causing a partial accumulation of these cargoes in the Golgi or other pre-vacuolar compartments (Bowers and Stevens, 2005; Darsow et al., 1998; Odorizzi et al., 1998). As shown in Figure 3.4B, deleting the PEP12 gene did not affect the trafficking of Ypq1-GFP to the vacuole membrane, indicating that Ypq1 can utilize the AP3 pathway to reach the vacuole. In contrast, deleting the APM3 gene, encoding the μ subunit of the AP3 complex, results in a partial accumulation of Ypq1-GFP outside the vacuole. The localization of Ypq1-GFP in pep12Δ and apm3Δ mutants is very similar to GFP-ALP (Figure 3.4C), indicating that Ypq1 is a cargo for the AP3 pathway. Examining the Ypq1 protein sequence revealed a putative acidic di-leucine motif (EQQPLL) within

the second cytosolic loop. This motif is conserved among all three yeast Ypq1 paralogues (Figure 3.4A). When mutated to AQQPAA (ypq1diL), the trafficking of ypq1diL-GFP to the vacuole was blocked, and numerous punctae accumulated in the pep12Δ cells (Figure 3.4B). Together, these data indicated that Ypq1-GFP is normally sorted to the vacuole via the AP3 pathway.

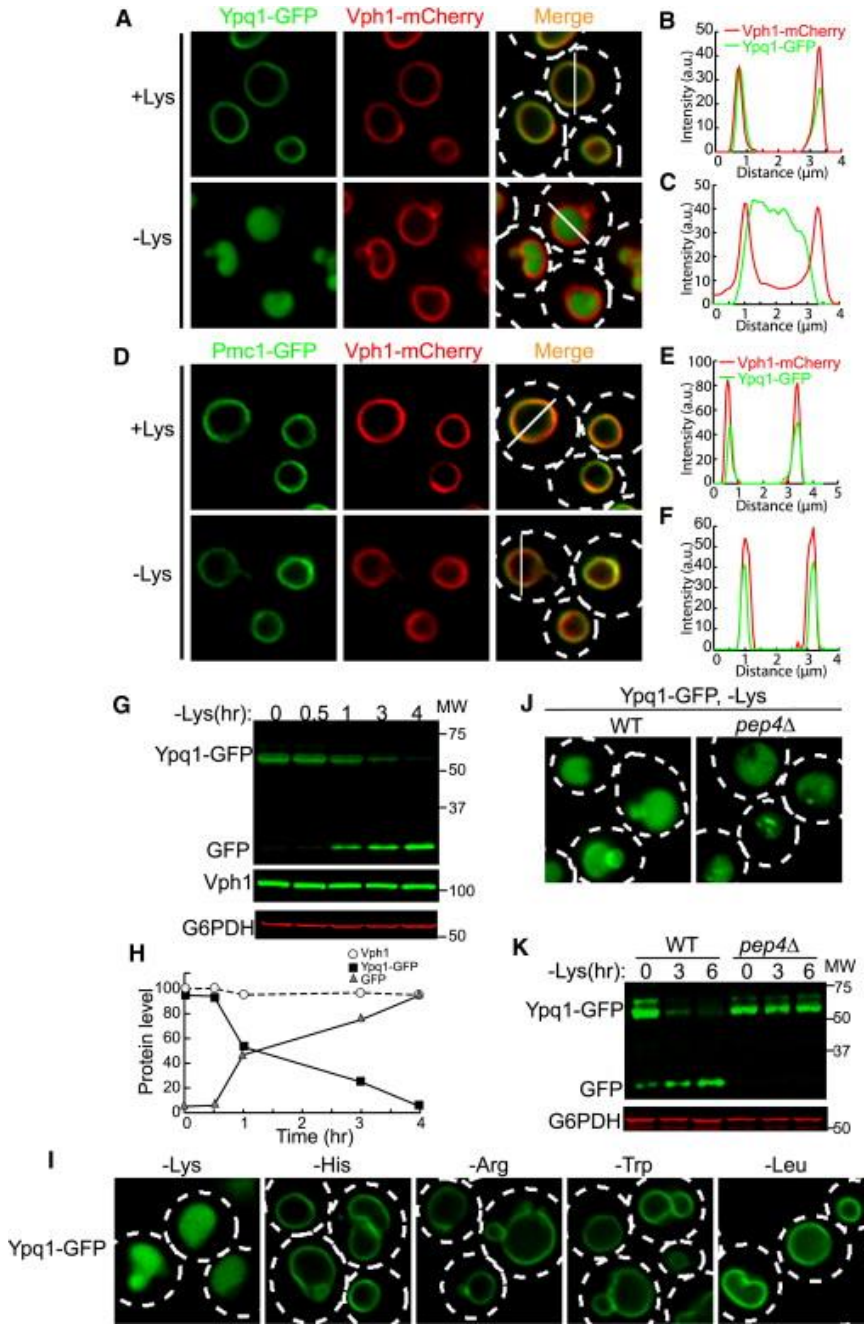
A
Ypq1-GFP
Vph1-mCherry
Merge
+Lys
-Lys
B
Vph1-mCherry
Ypq1-GFP
Intensity (a.u.)
Distance (μm)
C
D
Pmc1-GFP
Vph1-mCherry
Merge
+Lys
-Lys
E
Vph1-mCherry
Ypq1-GFP
Intensity (a.u.)
Distance (μm)
F
G
-Lys(hr): 0 0.5 1 3 4
MW
Ypq1-GFP
GFP
Vph1
G6PDH
75
50
37
100
50
H
Vph1
Ypq1-GFP
GFP
Protein level
Time (hr)
J
Ypq1-GFP, -Lys
WT
pep4Δ
K
WT
pep4Δ
-Lys(hr): 0 3 6 0 3 6
MW
Ypq1-GFP
GFP
G6PDH
I
-Lys
-His
-Arg
-Trp
-Leu
Ypq1-GFP

Figure 3.1

Figure 3.1. Ypq1-GFP Is Selectively Internalized and Degraded inside the Vacuole after Lysine Withdrawal

(A) Localization of Ypq1-GFP and Vph1-mCherry before (+Lys) and after (−Lys) lysine withdrawal (4 hr). Vacuoles chosen for line-scan analysis are highlighted by white lines.

(B) Line-scan analysis of Figure 3.1A, upper panel.

(C) Line-scan analysis of Figure 3.1A, lower panel.

(D) Localization of Pmc1-GFP and Vph1-mCherry before (+Lys) and after (−Lys) lysine withdrawal (4 hr). Vacuoles chosen for line-scan analysis are highlighted by white lines.

(E) Line-scan analysis of Figure 3.1D, upper panel.

(F) Line-scan analysis of Figure 3.1D, lower panel.

(G) Western blot analysis of Ypq1-GFP degradation kinetics. After lysine withdrawal, yeast cells stably expressing Ypq1-GFP were collected at five time points (0, 0.5, 1, 3, 4 hr), and whole-cell lysates were probed with GFP, Vph1, and

G6PDH antibodies.

(H) Normalized (to G6PDH) protein levels of Vph1, Ypq1-GFP, and GFP in Figure 3.1G.

(I) Localization of Ypq1-GFP after withdrawing Lys, His, Arg, Trp, or Leu (6 hr).

(J) Localization of Ypq1-GFP in WT and pep4Δ strains after lysine withdrawal (6 hr).

(K) Comparison of Ypq1-GFP degradation kinetics in WT and pep4Δ strains after lysine withdrawal. See also Figures 3.2–3.4.

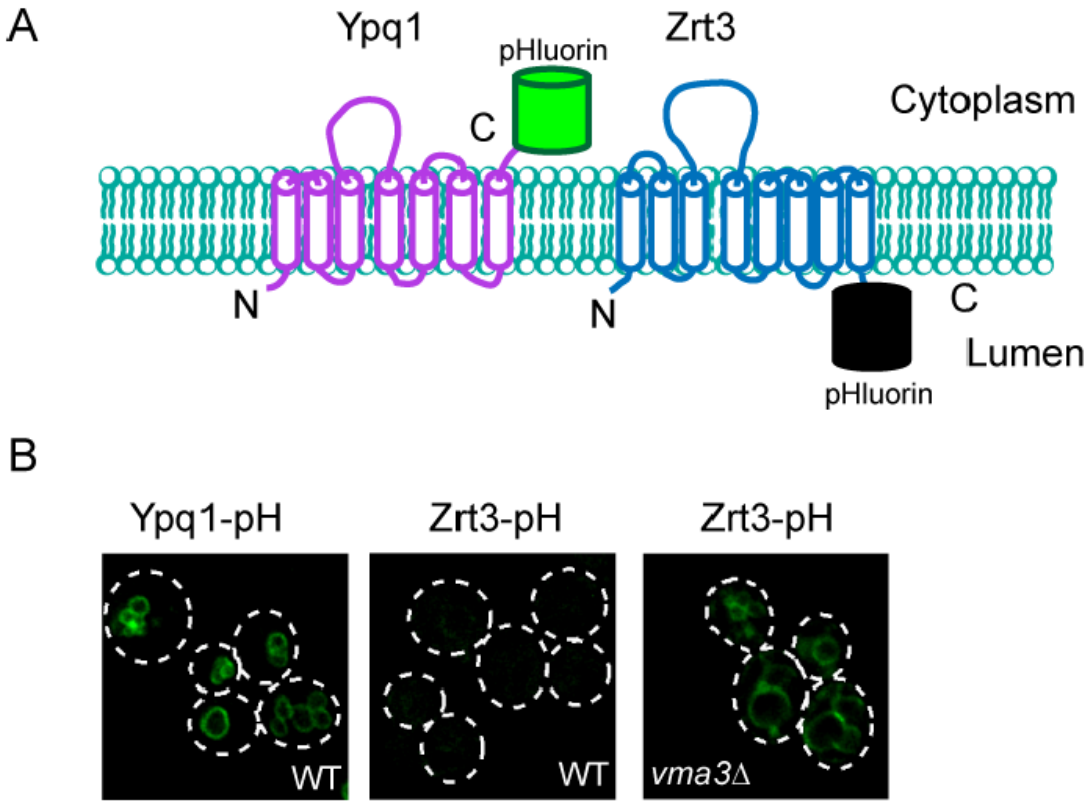
A
Ypq1
pHluorin
Zrt3
Cytoplasm
C
N
N
C
Lumen
pHluorin
B
Ypq1-pH
Zrt3-pH
Zrt3-pH
WT
WT
vma3Δ

Figure 3.2

Figure 3.2 (related to figure 3.1)

The C-terminus of Ypq1 is in the cytoplasm. **A)** Cartoon schematic showing predicted membrane orientation of Ypq1 and Zrt3. **B)** Fluorescent imaging of Ypq1-pHluorin in WT cell, Zrt3-pHluorin in both WT cell and *vma3*Δ cell.

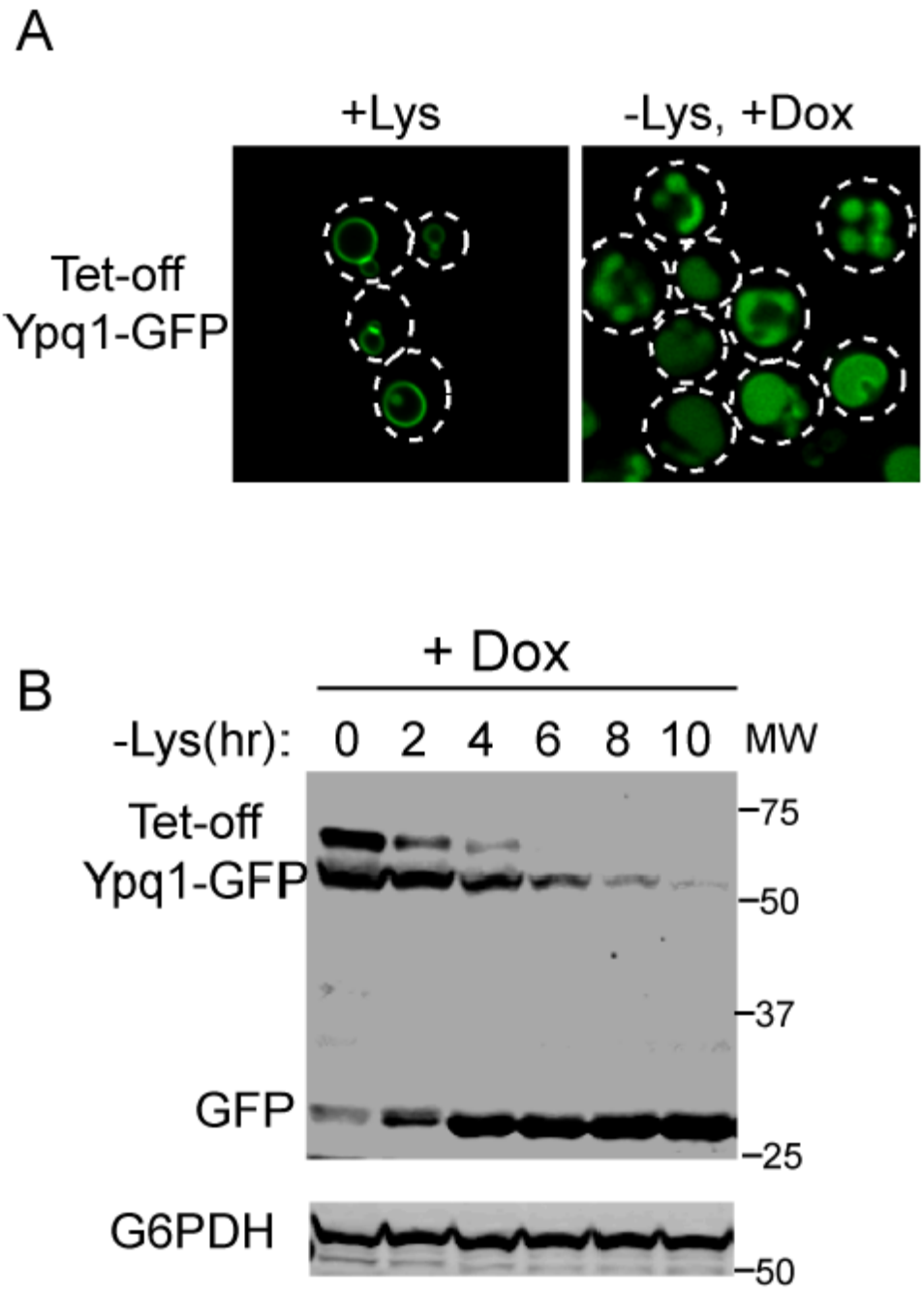
A
+Lys
-Lys, +Dox
Tet-off
Ypq1-GFP
B
+ Dox
-Lys(hr): 0 2 4 6 8 10 MW
Tet-off
Ypq1-GFP
GFP
G6PDH
75
50
37
25
50

Figure 3.3

Figure 3.3 (related to figure 3.1)

Lysine withdrawal triggers the degradation of the pre-existing Ypq1-GFP. **A)** Ypq1-GFP expressed under a Tet-off promoter was internalized after 8 hours of lysine withdrawal. The cells were pre- treated with 2 µg/ml doxycycline for 30 minutes to stop the synthesis of Ypq1-GFP. **B)** Degradation kinetics of the Tet-off Ypq1-GFP after addition of 2 µg/ml doxycycline and lysine withdrawal.

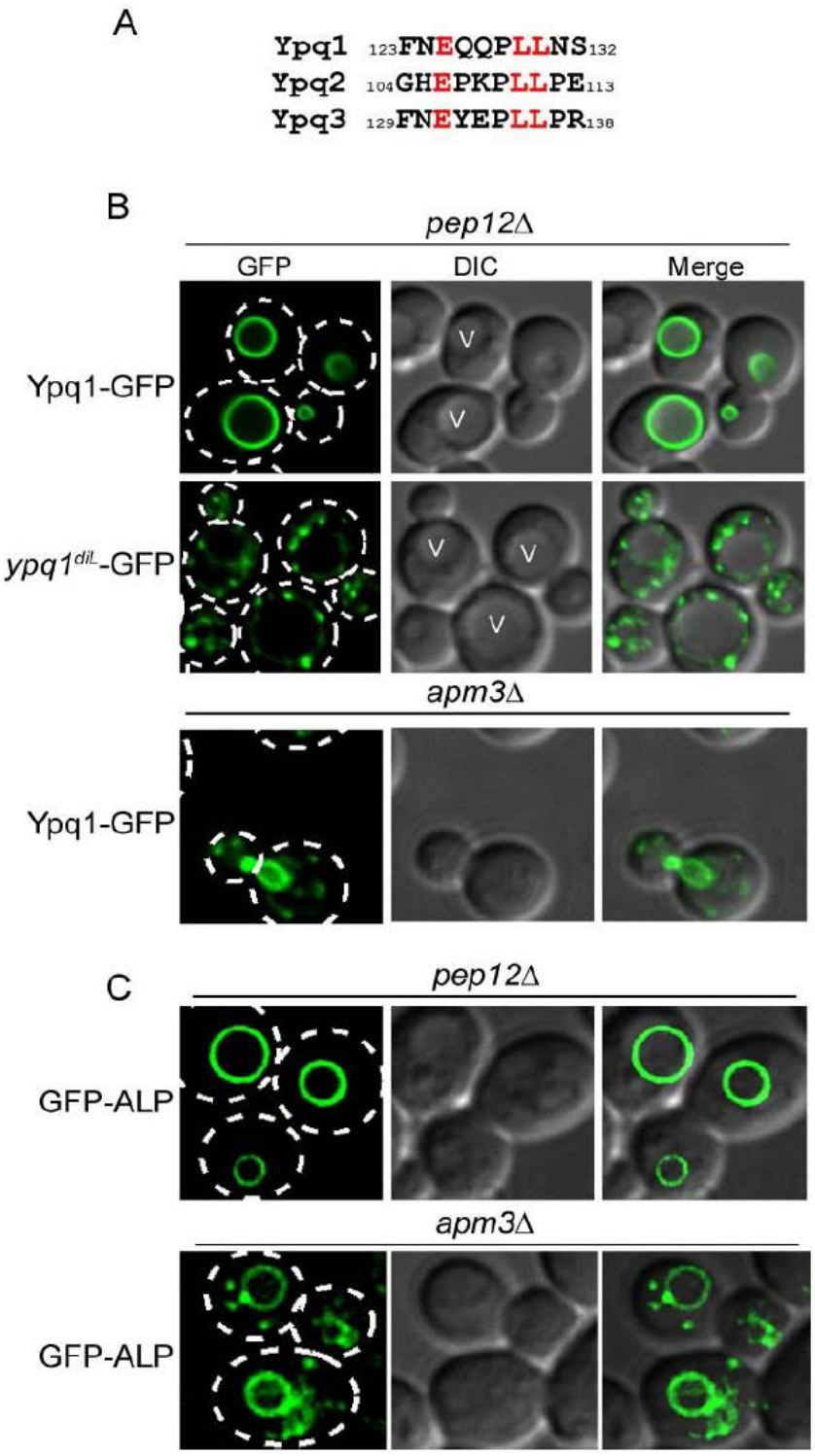
A
Ypq1 123FNEQQPLLNS132
Ypq2 104GHEPKPLLPE113
Ypq3 129FNEYEPLLPR138
B
pep12Δ
GFP
DIC
Merge
Ypq1-GFP
ypq1dil-GFP
apm3Δ
Ypq1-GFP
C
pep12Δ
GFP-ALP
apm3Δ
GFP-ALP

Figure 3.4

Figure 3.4 (related to figure 3.1)

Newly synthesized Ypq1 is sorted to the vacuole via the AP3 pathway. A) An alignment of Ypq1, Ypq2, and Ypq3 sequences, the conserved acidic di-leucine motif is highlighted in red. B) Localization of Ypq1-GFP and its di-leucine motif mutant (ypq1diL-GFP) in pep12Δ and apm3Δ cells. "V" highlights the location of the vacuole in the DIC images. C) Localization of GFP-ALP in pep12Δ and apm3Δ cells.

The ESCRT Machinery, but Not the Autophagy Machinery, Is Required for Ypq1-GFP Sorting to the Vacuole Lumen

There are two major pathways in yeast for sorting proteins into the vacuolar lumen for degradation, autophagy and the ESCRT pathway. Autophagy, including both macroautophagy and microautophagy, is responsible for delivering cytosolic proteins and organelles into the vacuole (He and Klionsky, 2009; Levine and Klionsky, 2004). To test if autophagy plays a role in sorting Ypq1-GFP into the vacuole lumen, we tested if deletion of essential genes for autophagy (ATG1, ATG5, and ATG7) blocks Ypq1 sorting (Levine and Klionsky, 2004). As shown in Figure 3.5A, deleting the ATG1 gene did not affect the internalization of Ypq1. Deletion of other essential genes for autophagy, including ATG5 and ATG7, also did not affect the internalization process. Western blot analysis further confirmed that the kinetics of Ypq1 degradation was unchanged in these deletion mutants (Figure 3.5B). Together, these results indicated that autophagy is not responsible for the internalization or degradation of vacuole membrane proteins.

We next tested if the ESCRT machinery is responsible for the internalization of Ypq1. To this end, we systematically deleted key components of each ESCRT sub-complex, including VPS27 (ESCRT-0), VPS23 (ESCRT-I), VPS36 (ESCRT-II), SNF7 (ESCRT-III), and VPS4 (AAA-ATPase). As shown in Figure 3.5C, deleting any of these components blocked the delivery of Ypq1 to the lumen of the vacuole, Ypq1-GFP remained on the vacuole membrane, with a fraction of Ypq1-GFP trapped in the post-vacuolar structures that are attached to the vacuole, possibly corresponding the class E compartment that accumulates in ESCRT mutants (Figure 3.5C, arrows). Western blot analysis further confirmed that Ypq1 degradation was blocked in ESCRT mutants even after an extended incubation (6 hr) in lysine minus media (Figure 3.5D).

To rule out the possibility that a component important for Ypq1 sorting and degradation is mis-sorted in the ESCRT mutants and therefore blocks the Ypq1 degradation indirectly, we performed the degradation assay in a vps4ts strain (Babst et al., 1997). At 26°C, the degradation of Ypq1 occurred normally (Figures 3.5E and 3.5F); however, when shifted to the non-permissive temperature (37°C),

Ypq1-GFP degradation was blocked (Figures 3.5E and 3.5F). The protein was mostly stabilized on the vacuole membrane, supporting that the ESCRT machinery directly participates in the turnover process of Ypq1-GFP.

We next investigated if the ESCRT machinery directly interacts with Ypq1 during the turnover process. To this end, we adopted a split-GFP assay that has been widely used to detect protein-protein interactions (Hu and Kerppola, 2003). The enhanced GFP (eGFP) molecule was split between Q158 and K159. The N-terminal half of the eGFP (nGFP) was chromosomally tagged to the C terminus of Ypq1 protein (Ypq1-nGFP), while the C-terminal half (cGFP) was chromosomally tagged to the C terminus of Vps23 (Vps23-cGFP, Figure 3.6A). The resulting strain only had a faint background fluorescence signal when grown in lysine-replete media (Figure 3.6B, +Lys). When shifted to lysine-minus media, we observed no fluorescent signal on the vacuole membrane, but we did detect formation of 1–4 weakly fluorescent punctae within the cell (average 2.4 punctate/cell, Figures 3.6B–3.6D), indicating a direct interaction between Ypq1 and Vps23. 21% (n = 236, Figure 3.6D) of the punctae appeared to be detached from the vacuole membrane. Intriguingly, the

induced punctae were reminiscent of the localization of Vps23 on endosomes. Moreover, the fact that we did not observe fluorescence on the vacuole surface indicates that Ypq1 might be first sorted off the vacuole membrane into an endosome-like structure before being recognized by Vps23. Importantly, the formation of these punctae was eliminated if SSH4, a gene that is essential for the Ypq1 ubiquitination, was deleted (Figures 3.6B and 3.6D, see below).

Taken together, we concluded that the ESCRT machinery is critical for the turnover of Ypq1.

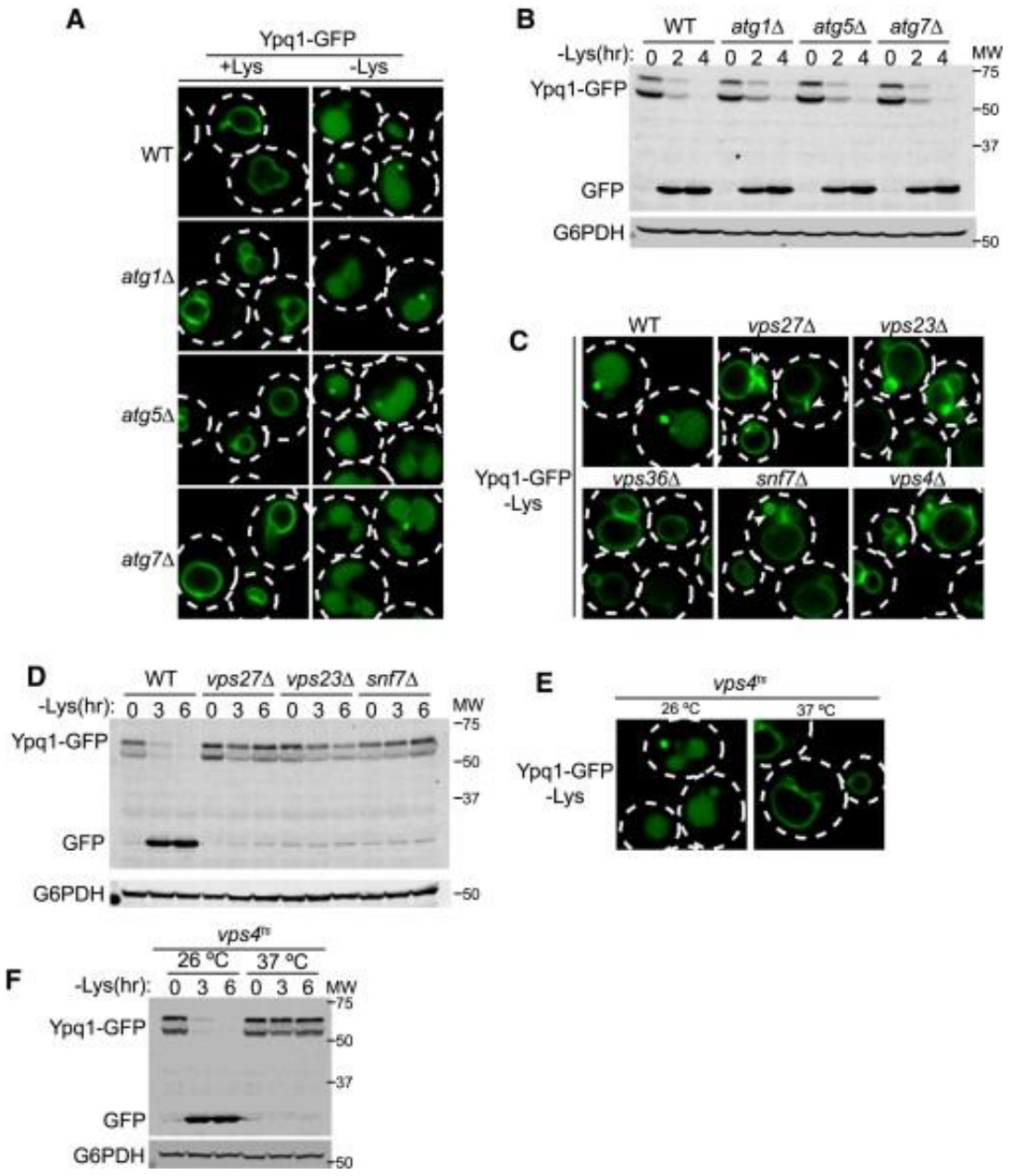
A
Ypq1-GFP
+Lys
-Lys
WT
atg1Δ
atg5Δ
atg7Δ
B
WT
atg1Δ
atg5Δ
atg7Δ
-Lys(hr): 0 2 4 0 2 4 0 2 4 0 2 4
MW
Ypq1-GFP
GFP
G6PDH
75
50
37
50
C
WT
vps27Δ
vps23Δ
Ypq1-GFP
-Lys
vps36Δ
snf7Δ
vps4Δ
D
WT
vps27Δ
vps23Δ
snf7Δ
-Lys(hr): 0 3 6 0 3 6 0 3 6 0 3 6
MW
Ypq1-GFP
GFP
G6PDH
75
50
37
50
E
vps4ts
26 °C
37 °C
Ypq1-GFP
-Lys
F
vps4ts
26 °C
37 °C
-Lys(hr): 0 3 6 0 3 6
MW
Ypq1-GFP
GFP
G6PDH
75
50
37
50

Figure 3.5

Figure 3.5. Ypq1-GFP Degradation Requires the ESCRT Machinery, but Not the Autophagy Machinery

(A) Localization of Ypq1-GFP before (+Lys) and 4 hr after (−Lys) lysine withdrawal. Ypq1-GFP was chromosomally expressed in all strains.

(B) Comparison of Ypq1-GFP degradation kinetics in WT, atg1Δ, atg5Δ, and atg7Δ strains. Whole-cell lysates from 0, 2, and 4 hr were probed with GFP and G6PDH antibodies.

(C) Localization of Ypq1-GFP after lysine withdrawal (6 hr). Ypq1-GFP was chromosomally expressed in all strains. Arrows highlight the class E compartments.

(D) Comparison of Ypq1-GFP degradation kinetics in WT and ESCRT deletion strains.

(E) Ypq1-GFP localization in vps4ts strain at both 26°C and 37°C. Images were obtained after 6-hr lysine withdrawal.

(F) Comparison of degradation kinetics of Ypq1-GFP between 26°C and 37°C in the vps4ts strain. See also Figure S4.

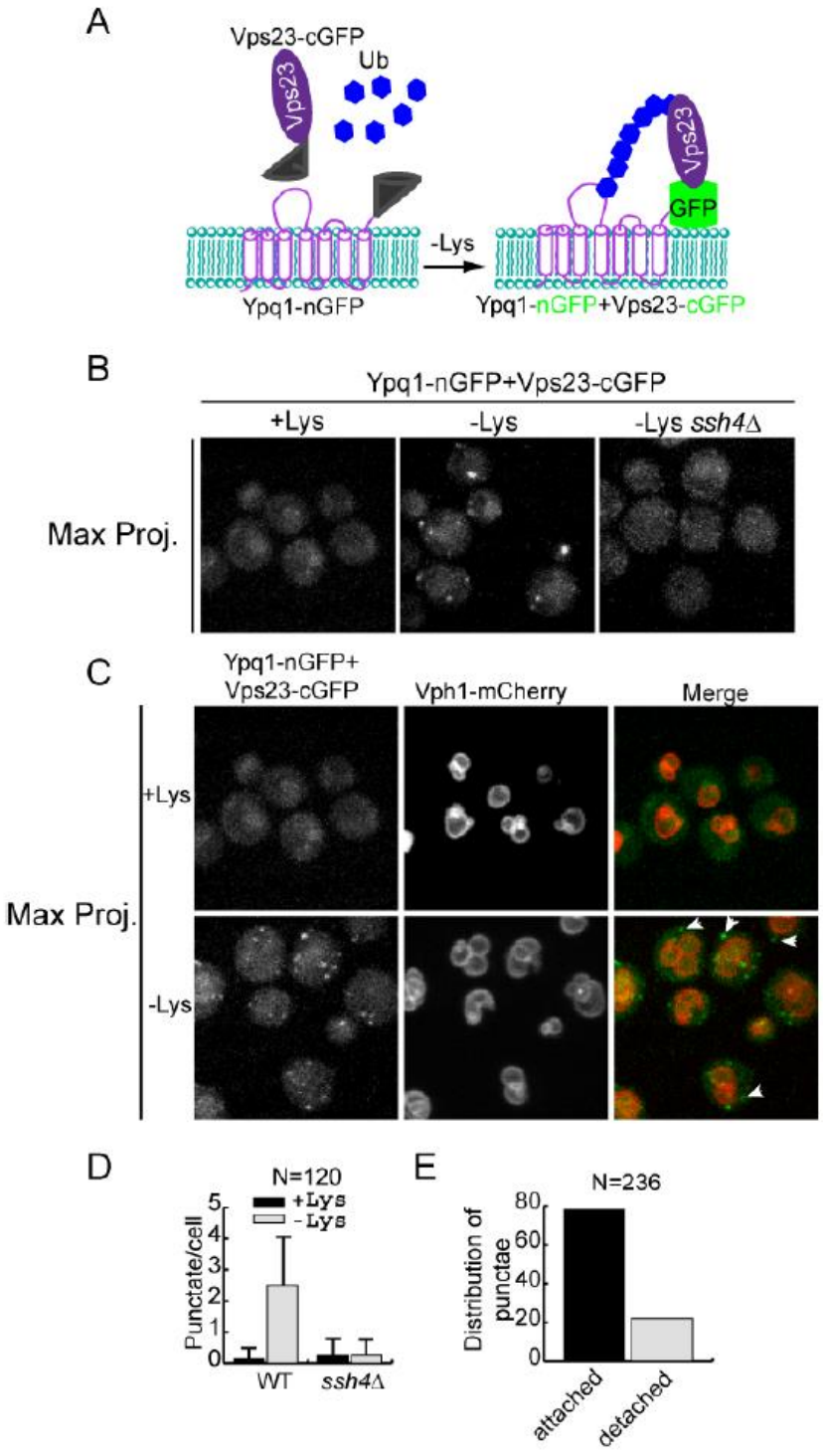
A
Vps23-cGFP
Ub
Vps23
GFP
-Lys
Ypq1-nGFP
Ypq1-nGFP+Vps23-cGFP
B
Ypq1-nGFP+Vps23-cGFP
+Lys
-Lys
-Lys ssh4Δ
Max Proj.
C
Ypq1-nGFP+
Vps23-cGFP
Vph1-mCherry
Merge
+Lys
-Lys
Max Proj.
D
N=120
+Lys
-Lys
Punctate/cell
WT
ssh4Δ
E
N=236
Distribution of punctae
attached
detached

Figure 3.6

Figure 3.6 (related to figure 3.5)

Vps23 directly interacts with Ypq1 during its degradation process. A) Cartoon schematic showing a split-GFP assay to probe the interaction between Vps23 and ubiquitinated Ypq1. B) Lysine withdrawal triggers interaction between Ypq1-nGFP and Vps23-cGFP, as indicated by the formation of several punctae in cells. C) A fraction of induced punctae is detached from the vacuole membrane. D) Quantification of the number of punctae per cell. Error bars represent standard deviation. E) Quantification of the vacuole-attached and detached punctae.

Ypq1 Is Ubiquitinated by Rsp5

Cargo ubiquitination is a prerequisite for recognition by the ESCRT machinery. Several key ESCRT components, including Vps27, Vps36, Vps23, and Hse1, have specific domains that directly interact with ubiquitin. To test if Ypq1 is itself ubiquitinated, we expressed a Myc-tagged ubiquitin in a Ypq1-GFP strain (YML522, Table 3.1). We then deleted the DOA4 gene, the major de-ubiquitinase in the endomembrane system, in order to stabilize any ubiquitinated Ypq1 (Amerik et al., 2000; Richter et al., 2007; Swaminathan et al., 1999). Following lysine withdrawal, we carried out an immunoprecipitation (IP) assay using the GFP-TRAP antibody. The IP reaction was probed with a Myc antibody, and a high molecular weight smear was detected, indicating that Ypq1-GFP was poly-ubiquitinated (Figure 3.7A). Ubiquitinated Ypq1-GFP could be detected 30 min after lysine withdrawal, and the ubiquitination level further increased after 2 hr of lysine withdrawal (Figure 3.7A), a time point when Ypq1-GFP was actively degraded.

Rsp5, the Nedd4 family E3 ligase, is responsible for the ubiquitination of numerous

membrane cargoes before they are delivered to the vacuole for degradation (Belgareh-Touzé et al., 2008). To test if Rsp5 is also responsible for the ubiquitination of Ypq1-GFP, a temperature-sensitive mutant of RSP5, rsp5-1, was used. At the non-permissive temperature (37°C), the degradation of Ypq1-GFP was blocked in rsp5-1, while the degradation was normal in the wild-type (WT) strain (Figure 3.7B). Ypq1-GFP remained on the vacuole membrane (Figure 3.7C), indicating that ubiquitination by Rsp5 is required for Ypq1 sorting and degradation.

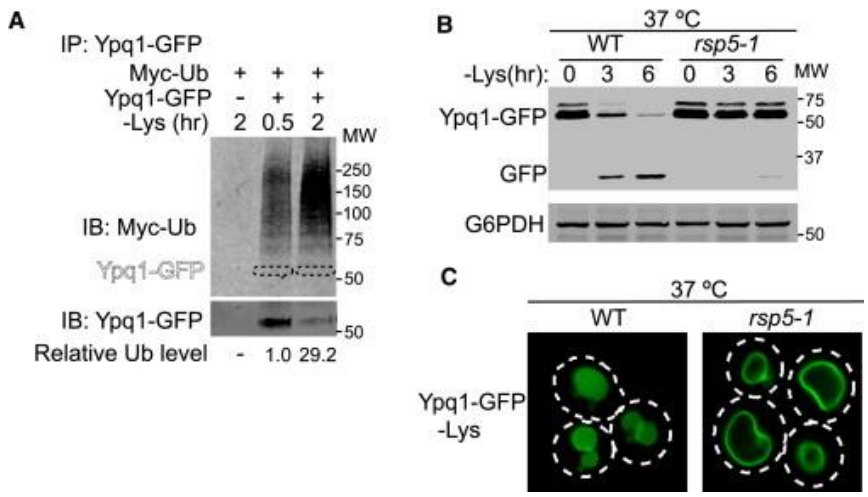
A
IP: Ypq1-GFP
Myc-Ub + + +
Ypq1-GFP - + +
-Lys (hr) 2 0.5 2
MW
250
150
100
75
50
IB: Myc-Ub
Ypq1-GFP
IB: Ypq1-GFP
50
Relative Ub level - 1.0 29.2
B
37 °C
WT
rsp5-1
-Lys(hr): 0 3 6 0 3 6 MW
Ypq1-GFP
75
50
GFP
37
G6PDH
50
C
37 °C
WT
rsp5-1
Ypq1-GFP
-Lys

Figure 3.7

Figure 3.7. The E3 Ubiquitin Ligase Rsp5 Is Required for Ypq1-GFP Degradation

(A) Ypq1-GFP was immunoprecipitated from a doa4Δ strain (YML522) co-expressing Myc-ubiquitin either 0.5 or 2 hr after lysine withdrawal. The IP reaction was probed with both GFP and Myc antibodies. A doa4Δ strain (MBY45) only expressing Myc-ubiquitin was included as a negative control (left lane). The relative ubiquitin level was normalized to the Ypq1-GFP level. The dashed circles highlight the positions of non-ubiquitinated Ypq1-GFP.

(B) A comparison of Ypq1-GFP degradation kinetics between WT and rsp5-1 strains at 37°C.

(C) A comparison of Ypq1-GFP localization between WT and rsp5-1 strains at 37°C. Images were obtained after 6 hr of lysine withdrawal.

Ypq1 Degradation Requires a PY Motif-Containing Adaptor, Ssh4

Rsp5 contains three WW domains that interact with PY motifs (X1PX2Y, where X1 is often a P). This WW-PY interaction is important for recruiting Rsp5 to different locations within the cell. Examining the Ypq1 protein sequence did not reveal any PY motifs, suggesting a PY-motif-containing adaptor may be required to recruit Rsp5 to the vacuole. In order to identify this adaptor, we screened a total of 17 genes that encode proteins containing one or more PY motifs (Table 3.2). Each of these proteins has been shown to associate with the Rsp5 ubiquitin ligase by either co-immunoprecipitation, proteomics, or yeast two-hybrid studies (Gupta et al., 2007; Hettema et al., 2004; Imai et al., 2007; Lin et al., 2008). Deletion mutants for each of these genes were tested for Ypq1-GFP sorting and degradation. Only one mutant, ssh4Δ, was found to block the degradation (Table 3.2, Figures 3.8B and 3.8C). The Ypq1 protein was no longer ubiquitinated after lysine withdrawal (Figure 3.8H), and it was stabilized on the vacuole membrane (Figure 3.8B). Ssh4 has two PY motifs at amino acid residues 426–429 (PPAY) and 447–450 (PPRY) (Figure 3.8A). In addition, it also has a SPRY domain (166–352) that normally acts as a scaffold to mediate protein-protein interactions (Figure 3.8A). Intriguingly, over 100

genes are present in the human genome that encode the SPRY domain-containing proteins, half of which are important for protein ubiquitination, either as E3 ligases or as adaptors to recruit E3 ligases (Kuang et al., 2010; Perfetto et al., 2013). Mutating either PY motif (py1, PAAA; py2, PARA) blocked Ypq1 degradation, underscoring the importance of both PY motifs (Figures 3.8D and 3.8E). To confirm that Ssh4 directly interacts with Rsp5, we performed a co-immunoprecipitation experiment, using the GFP-TRAP antibody, from a whole-cell lysate expressing both GFP-Rsp5 and Ssh4-HA. Indeed, Ssh4 could be co-immunoprecipitated with Rsp5 (Figure 3.8G), while the interaction was diminished in an ssh4 mutant lacking both PY motifs (ssh4py1+2, 6% of WT).

Ssh4 has a paralogue, Ear1, in budding yeast (Figure 3.8A). These two proteins are considered to be functionally redundant (Léon et al., 2008). They have been proposed to be adaptors for Rsp5 on endosomes. However, deleting EAR1 did not affect the Ypq1 internalization and degradation (Figures 3.8B and 3.8C). Furthermore, the assumption that Ssh4 functions on the endosome is inconsistent with its role in Ypq1 degradation. To address this issue, we chromosomally tagged

both SSH4 and EAR1 with GFP. As shown in Figure 3.8F, while Ear1 localized to endosomes as reported (Léon et al., 2008), Ssh4 localized to the vacuole surface. This observation was consistent with another indirect immunofluorescence study showing that Ssh4 localizes to the vacuole membrane (Kota et al., 2007). A small amount of both proteins also localized to the vacuole lumen, presumably because they could be ubiquitinated by Rsp5 and sent to the vacuole for degradation (Léon et al., 2008). To directly test if Ssh4 can recruit Rsp5 to the vacuole membrane, we overexpressed Ssh4 (~6-fold, data not shown) under the ADH1 promoter. Strikingly, under this condition, most of the GFP-Rsp5 was recruited to the vacuole membrane (Figure 3.8I). This recruitment depended on the PY motifs in Ssh4 since a PY motif mutant (ssh4py1+2) lost the ability to recruit Rsp5 (Figure 3.8I). Furthermore, the Rsp5 recruitment to the vacuole membrane caused a significant amount of Ypq1-GFP to be degraded constitutively, bypassing the requirement of lysine withdrawal (Figures 3.8I and 3.8J). In contrast, overexpressing Ear1 recruited Rsp5 to punctae (endosomes), and this did not result in the degradation of Ypq1-GFP (Figures 4I and 4J) (Léon et al., 2008). Together, our data indicated that Ssh4 is functionally distinct from Ear1, despite the sequence similarity between these two

proteins. Ssh4 is localized at the vacuole membrane, where it could recruit Rsp5 to selectively ubiquitinate vacuole membrane proteins.

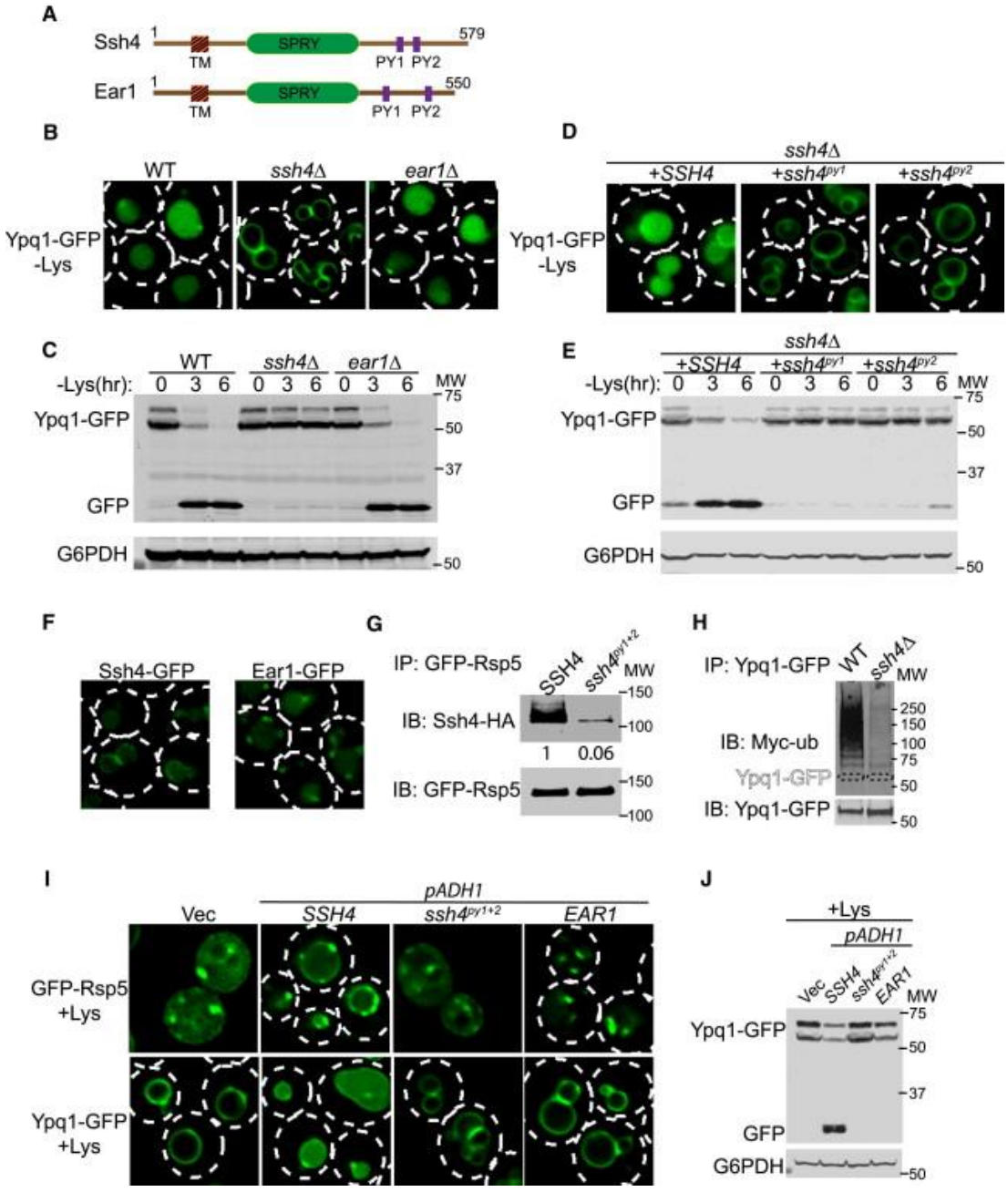
A
Ssh4
1
579
TM
SPRY
PY1 PY2
Ear1
1
550
TM
SPRY
PY1 PY2
B
WT
ssh4Δ
ear1Δ
Ypq1-GFP
-Lys
D
ssh4Δ
+SSH4
+ssh4py1
+ssh4py2
Ypq1-GFP
-Lys
C
WT
ssh4Δ
ear1Δ
-Lys(hr): 0 3 6 0 3 6 0 3 6
MW
Ypq1-GFP
GFP
G6PDH
75
50
37
50
E
ssh4Δ
+SSH4
+ssh4py1
+ssh4py2
-Lys(hr): 0 3 6 0 3 6 0 3 6
MW
Ypq1-GFP
GFP
G6PDH
75
50
37
50
F
Ssh4-GFP
Ear1-GFP
G
IP: GFP-Rsp5
SSH4
ssh4py1+2
MW
IB: Ssh4-HA
150
100
1
0.06
IB: GFP-Rsp5
150
100
H
IP: Ypq1-GFP
WT
ssh4Δ
MW
IB: Myc-ub
Ypq1-GFP
IB: Ypq1-GFP
250
150
100
75
50
50
I
pADH1
Vec
SSH4
ssh4py1+2
EAR1
GFP-Rsp5
+Lys
Ypq1-GFP
+Lys
J
+Lys
pADH1
Vec
SSH4
ssh4py1+2
EAR1
MW
Ypq1-GFP
GFP
G6PDH
75
50
37
50

Figure 3.8

Figure 3.8. Ssh4 Is the Vacuolar Membrane Adaptor to Recruit Rsp5

(A) Cartoon schematic showing the domain architecture of Ssh4 and Ear1.

(B) Comparison of Ypq1-GFP localization among WT, ssh4Δ, and ear1Δ cells after 6 hr of lysine withdrawal.

(C) Comparison of Ypq1-GFP degradation kinetics among WT, ssh4Δ, and ear1Δ strains after lysine withdrawal.

(D) Comparison of Ypq1-GFP localization in the ssh4Δ strain expressing either SSH4 or its PY motif mutants (ssh4py1 and ssh4py2). Images were obtained after 6 hr of lysine withdrawal.

(E) Comparison of Ypq1-GFP degradation kinetics in the ssh4Δ strain expressing either SSH4 or its PY motif mutants (ssh4py1 and ssh4py2) after lysine withdrawal.

(F) Localization of chromosomally tagged Ssh4-GFP and Ear1-GFP.

(G) Mutating of both PY motifs (ssh4py1+2) dramatically reduces its interaction with Rsp5 (to 6%).

(H) Ypq1-GFP poly-ubiquitination is abolished in ssh4Δ strain. The IP reaction was

performed after 2 hr of lysine withdrawal. The dashed circles highlight the positions of non-ubiquitinated Ypq1-GFP.

(I) Localization of GFP-Rsp5 (upper panel) and Ypq1-GFP (lower panel) after overexpressing Ssh4, ssh4py1+2, and Ear1 under the ADH1 promoter. The empty vector was also included as a control. Images were taken in the presence of lysine.

(J) Western blot analysis of Ypq1-GFP abundance after overexpressing Ssh4, ssh4py1+2, or Ear1. Cells were collected in the presence of lysine. See also Table 3.2.

Table 3.2. (related to Figure 3.8) Tested genes encoding PY-motif containing proteins

Gene deleted	*Predicted PY motifs*	*Block Ypq1 sorting /degradation?*	*Previous studies*
ART1	2	No*	(Lin et al., 2008)
ART2	7	No	(Lin et al., 2008)
ART3	2	No	(Lin et al., 2008)
ART4	4	No	(Lin et al., 2008)
ART5	3	No	(Lin et al., 2008)
ART6	4	No	(Lin et al., 2008)
ART7	3	No	(Lin et al., 2008)
ART1-7[1]	/	No*	(Zhao et al., 2013)
ART8	8	No	(Lin et al., 2008)
ART9	3	No	(Lin et al., 2008)
BSD2	2	No	(Hettema et al., 2004)
BUL1	1	No	(Helliwell et al., 2001; Yashiroda et al., 1998)
BUL2	2	No	(Helliwell et al., 2001; Yashiroda et al., 1998)
BUL1-2[2]	/	No	(Helliwell et al., 2001)
EAR1	2	No	(Leon et al., 2008)
RCR1	2	No	(Imai et al., 2007; Kota et al., 2007)
RCR2	2	No	(Kota et al., 2007)
SNA3	1	No	(MacDonald et al., 2012)
SSH4	2	Yes	(Leon et al., 2008)

*: Has a kinetic delay.

[1]: ART1 to ART7 deleted.

[2]: Both BUL1 and BUL2 deleted.

Ypq1 Is Selectively Sorted off the Vacuole Membrane during Its Degradation

It has been well established that the ESCRTs function on endosomes to internalize ubiquitinated membrane proteins into ILVs before they are delivered to the vacuole lumen for degradation (Henne et al., 2011). Our discovery that vacuole membrane proteins can be triggered for degradation within the vacuole lumen in an ESCRT-dependent manner raises an interesting question: how does the endosome-localized ESCRT machinery meditate the internalization of vacuole membrane proteins?

Two hypotheses can provide an explanation. First, vacuoles are marked with PI3P and ubiquitinated membrane proteins (Cheever et al., 2001), two prerequisites for recruiting the ESCRT machinery (Henne et al., 2011). The ESCRT machinery may therefore be directly recruited to the vacuole membrane and mediate the internalization of ubiquitinated cargoes locally (hereafter referred as the direct vacuole membrane invagination hypothesis). Alternatively, vacuolar membrane proteins that are ubiquitinated may be trafficked away from the vacuole into a transport intermediate (vesicle or membrane tube) that delivers them to an

endosome-like compartment where the ESCRTs can sort them into ILVs (hereafter referred as the vacuole membrane recycling and degradation [vRed] hypothesis). Many published studies of the ESCRT machinery (Babst et al., 2000, 2002; Katzmann et al., 2003) and our split GFP results with Ypq1-nGFP and Vps23-cGFP indicate that the ESCRT machinery does not directly localize to the vacuole membrane (Figure 3.5H). Instead, they exist as distinct punctae that may correspond to a post-vacuolar endosome-like compartment.

It is known that endosomal structures are tethered to the vacuole surface by the HOPS complex, and fusion between the two organelles is mediated by a SNARE complex (Kümmel and Ungermann, 2014). We reasoned that if the recycling hypothesis is correct, compromising the function of the HOPS complex or SNARE complex could block the degradation of Ypq1. In contrast, Ypq1 degradation should not be affected if the ESCRT machinery can be directly recruited to the vacuole surface. To differentiate between these two hypotheses, we performed the Ypq1 degradation assay in either a vps18ts (HOPS) or a vam3ts (SNARE) mutant strain (Darsow et al., 1997; Rieder and Emr, 1997). At 26°C, Ypq1 degradation was

unaffected (Figures 3.9A and 3.9B). However, Ypq1 degradation was blocked at the non-permissive temperature (37°C), underscoring the importance of tethering ESCRT-containing structures to the vacuole surface (Figures 3.9A and 3.9B). Surprisingly, Ypq1GFP remained on the vacuole membrane, indicating that the HOPS/SNARE machinery may, in addition to tethering the putative Ypq1 degradation intermediates to the vacuole membrane, have other roles in the pathway. Nevertheless, these observations made the direct invagination hypothesis unlikely and suggested that Ypq1 might be sorted from the vacuole to a distinct endosome-like compartment that is tethered to the vacuole by the HOPS complex.

To directly test if the recycling hypothesis is correct, we used a strain (YYR36, Table 3.1) co-expressing Ypq1-GFP and Vph1-mCherry from the chromosome to investigate if lysine withdrawal can trigger a selective sorting of Ypq1-GFP. Indeed, after lysine withdrawal, we observed selective sorting of Ypq1-GFP into a compartment that did not co-localize with Vph1-mCherry (Figure 3.10A). Many of these vacuole membrane-attached compartments appeared to be tethered by the HOPS complex, as indicated by the colocalization of Ypq1-GFP with Vps18-mCherry

and their movement together on the vacuole surface (Figures 3.9C and 3.9D and Movie 3.1).This was consistent with the essential role of Vps18 for Ypq1 degradation and further suggested that tethering the Ypq1-GFP compartment to the vacuole is a critical intermediate step.

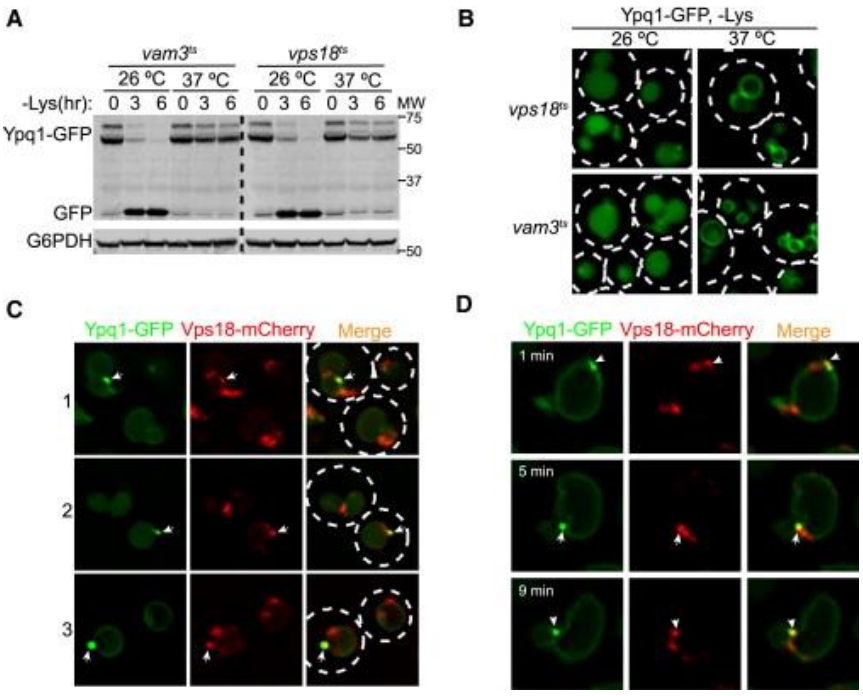
A
vam3ts
vps18ts
26 °C 37 °C
26 °C 37 °C
-Lys(hr): 0 3 6 0 3 6 0 3 6 0 3 6 MW
Ypq1-GFP
GFP
G6PDH
75
50
37
50
B
Ypq1-GFP, -Lys
26 °C
37 °C
vps18ts
vam3ts
C
Ypq1-GFP Vps18-mCherry Merge
1
2
3
D
Ypq1-GFP Vps18-mCherry Merge
1 min
5 min
9 min

Figure 3.9

Figure 3.9. The Fusion Machineries to the Vacuole Are Important for Ypq1 Degradation

(A) Comparison of Ypq1-GFP degradation kinetics between 26°C and 37°C in vam3ts and vps18ts strains.

(B) Comparison of Ypq1-GFP localization between 26°C and 37°C in vam3ts and vps18ts strains. Images were obtained after 6 hr of lysine withdrawal.

(C) Vps18-mCherry colocalizes with the Ypq1-GFP intermediate compartments. Three independent images are shown.

(D) Vps18-mCherry moves together with the Ypq1-GFP compartment along the vacuole surface. Three time points are shown. See also Movie 3.1.

We grouped our fluorescence images into three degradation stages (early, middle, late) based on the ratio of GFP signal between the vacuolar lumen and membrane (Figure 3.10A). The Ypq1-GFP compartments were observed at all three stages of the degradation (Figure 3.10A). At the early stage, when almost no luminal GFP signal could be detected, the Ypq1 intermediate compartments appeared as bright green tubes or punctae (Figure 3.10A, early stage), indicating that sorting of Ypq1-GFP to this compartment is an intermediate step prior to the delivery of internalized Ypq1-GFP into the vacuolar lumen. As the degradation proceeded to the middle stage, the GFP signal in the lumen increased, while the signal on the vacuole membrane decreased (Figure 3.10A). Importantly, unlike the vacuole membrane, the GFP intensity in the compartments did not decrease, which was consistent with the hypothesis that ubiquitinated Ypq1-GFP is sorted and concentrated into these compartments before being internalized by the ESCRT machinery.

While most of these compartments were attached to the vacuole membrane, we also observed some compartments that were detached from the vacuole surface (18%, n = 50; Figures 3.10B and 3.10D and Movies 3.2, 3.3, and 3.4), indicating that sorted

Ypq1-GFP could bud off the vacuole membrane into a distinct post-vacuolar intermediate compartment.

After 2 hr of lysine withdrawal, about 13% of the cells contained the post-vacuolar Ypq1-GFP compartments (Figure 3.10C). After 4 hr of lysine withdrawal, only 6% of the cells contained these putative transport intermediates. By this time point, most of the Ypq1-GFP was sorted into the vacuole lumen and degraded, consistent with the loss of the intermediates. Furthermore, deleting the SSH4 gene dramatically reduced the number of punctae, underscoring the importance of protein ubiquitination for selective sorting of Ypq1-GFP (Figure 3.10C).

The fact that only 13% of the cells contained the intermediate sorting compartments at the 2-hr time point suggested that these structures were transient intermediate in the sorting process. Therefore, we tested if these compartments could be stabilized by slowing down the degradation process. As shown in Figure 3.11A, the pep12ts mutant exhibited a delay in Ypq1 degradation at the non-permissive

temperature (37°C). While in the wild-type strain, the degradation at 37°C can be completed within ~2 hr, it took about 5–6 hr to complete the degradation in the pep12ts mutant (Figure 3.11A). This kinetic delay resulted in a 4-fold increase (53% at 3 hr) in the number of the cells that contained the Ypq1intermediate compartments (Figures 3.11B and 3.11C). This ratio decreased at 6 hr, when Ypq1 degradation was nearly completed.

Our data indicate that ubiquitinated Ypq1 is selectively sorted into an intermediate compartment before being delivered to the vacuole lumen for degradation. To directly test this hypothesis, we labeled Ypq1 with nGFP (Ypq1-nGFP) and ubiquitin with cGFP (cGFP-Ub) and co-expressed them in a Vph1-mCherry strain (Figure 3.12A). In the presence of lysine, only weak background fluorescence was observed. In contrast, lysine withdrawal triggered the formation of several punctae in cells (4/cell; Figures 3.12B and 3.12C). 17% of the induced punctae (n = 235; Figures 3.12B and 3.12D) were detached from the vacuole membrane. Deletion of SSH4 abolished the formation of these punctae (Figure 3.12B). Together, our data strongly support the vReD hypothesis as the mechanism for Ypq1 degradation and the

existence of intermediate compartments during its degradation process.

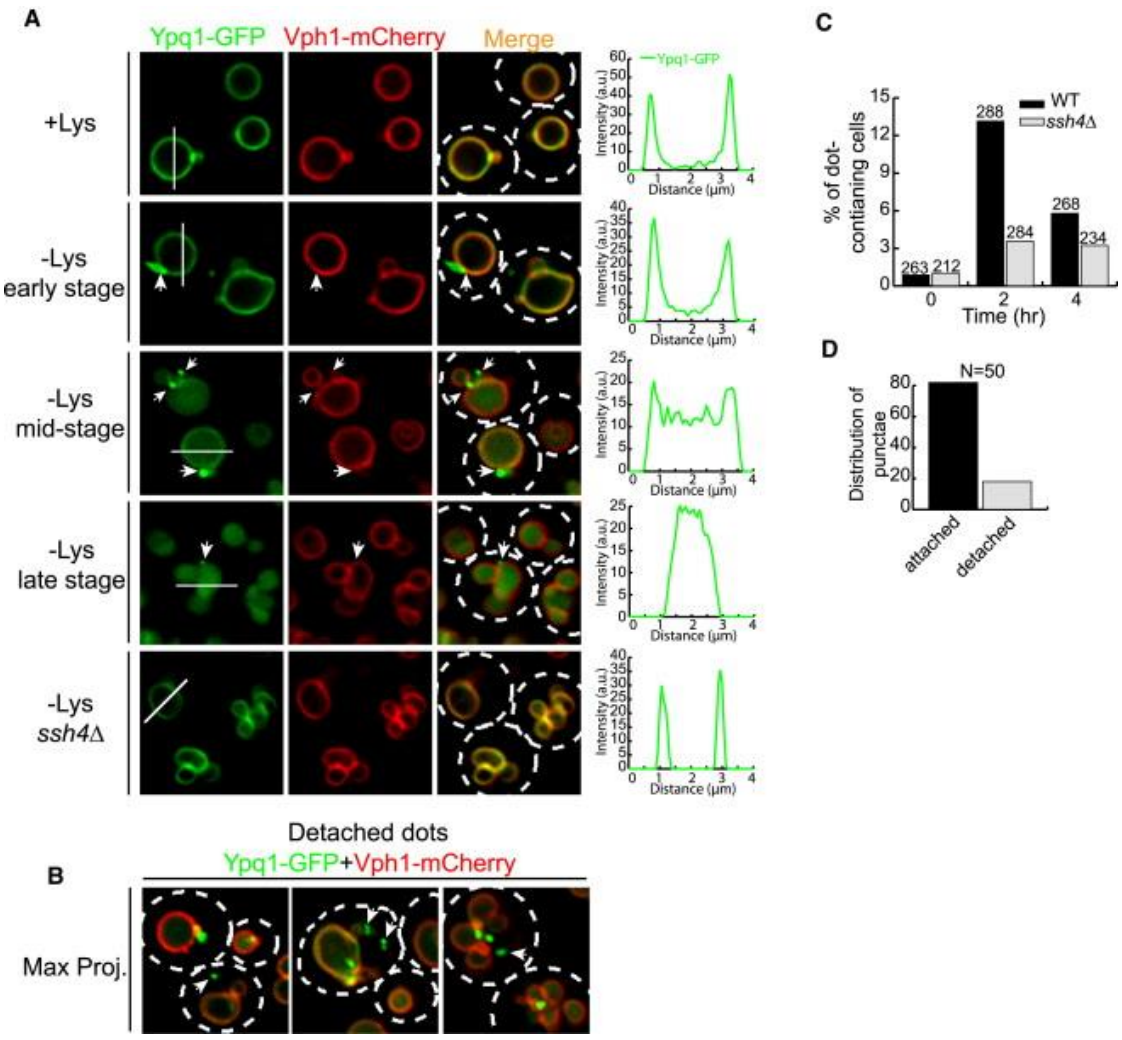
A
Ypq1-GFP
Vph1-mCherry
Merge
+Lys
-Lys early stage
-Lys mid-stage
-Lys late stage
-Lys ssh4Δ
Intensity (a.u.)
Distance (μm)
B
Detached dots
Ypq1-GFP+Vph1-mCherry
Max Proj.
C
% of dot-containing cells
WT
ssh4Δ
288
284
268
234
263
212
Time (hr)
D
N=50
Distribution of punctae
attached
detached

Figure 3.10

Figure 3.10. Ypq1-GFP Is Selectively Sorted into an Intermediate Compartment during Its Degradation Process

(A) Lysine withdrawal triggered a selective sorting of Ypq1-GFP into compartments that do not colocalize with Vph1-mCherry (indicated by arrows). Deletion of SSH4 abolished the selective sorting process. Line-scan analysis of Ypq1-GFP intensity was also included in the corresponding panel.

(B) Detached intermediate compartments from the vacuole membrane (indicated by arrows). See Movies 3.2, 3.3, and 3.4 for 3D reconstructions.

(C) Quantification of the intermediate compartment-containing cells in WT and ssh4Δ strains at 0, 2, and 4 hr. The numbers above each column are the total number of counted cells.

(D) Quantification of the intermediate compartments that are either attached or detached from the vacuole membrane. N indicates the total number of the counted compartments. See also Figures 3.11 and 3.12 and Movies 3.2, 3.3, and 3.4.

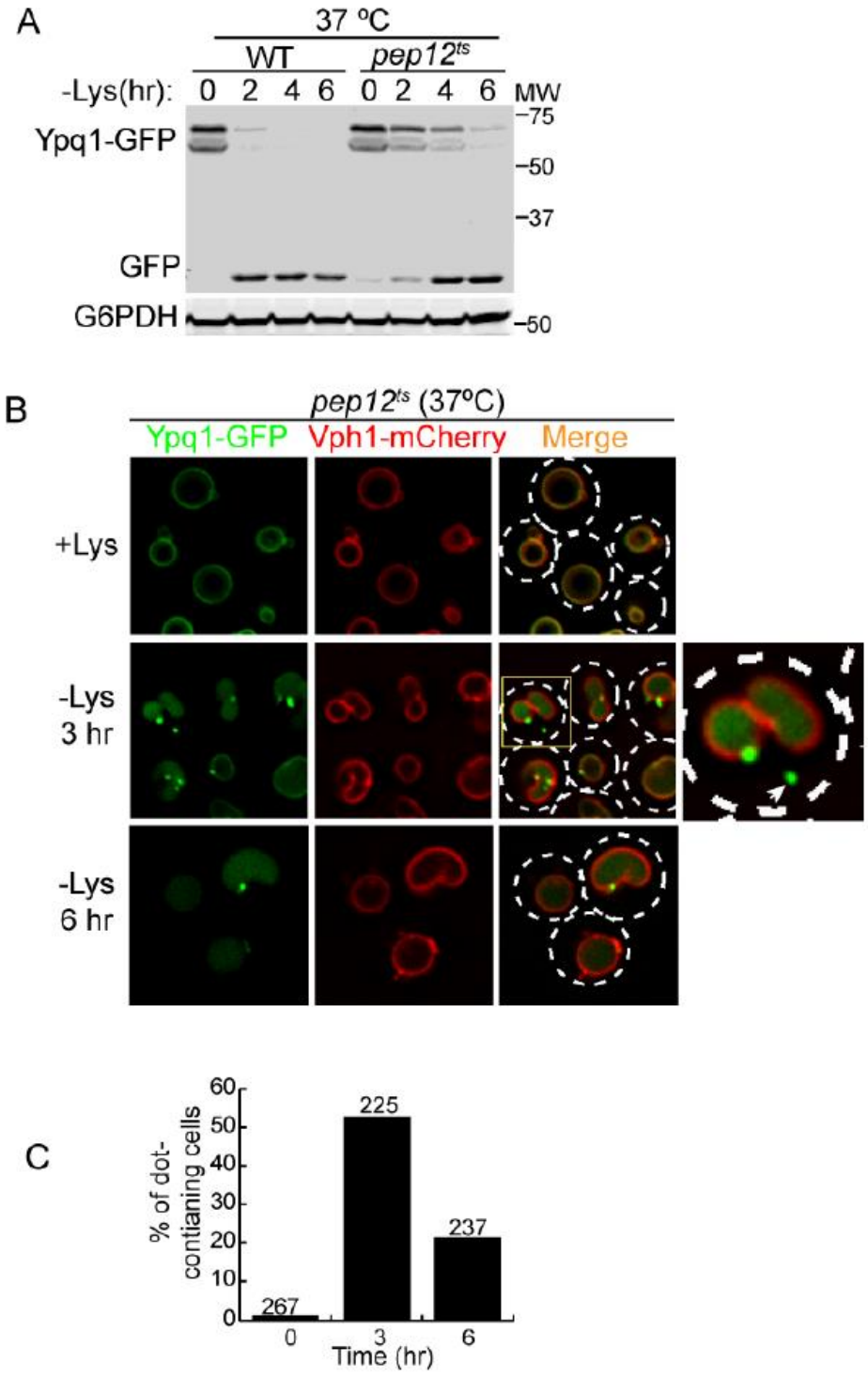
A
37 °C
WT
pep12ts
-Lys(hr): 0 2 4 6 0 2 4 6 MW
Ypq1-GFP
GFP
G6PDH
75
50
37
50
B
pep12ts (37°C)
Ypq1-GFP
Vph1-mCherry
Merge
+Lys
-Lys 3 hr
-Lys 6 hr
C
% of dot-contianing cells
60
50
40
30
20
10
0
225
237
267
0
3
6
Time (hr)

Figure 3.11

Figure 3.11 (related to figure 3.10)

pep12^{ts} cells accumulate more intermediate compartments at 37 ° C. **A)** Comparison of Ypq1-GFP degradation kinetics between WT and *pep12^{ts}* strains at 37 ° C. **B)** More cells accumulate the Ypq1-GFP intermediate compartments at 37 ° C. The enlarged panel highlights a detached intermediate compartment (arrow). **C)** Quantification of the intermediate compartment-containing cells. The numbers above each column are the total number of counted cells.

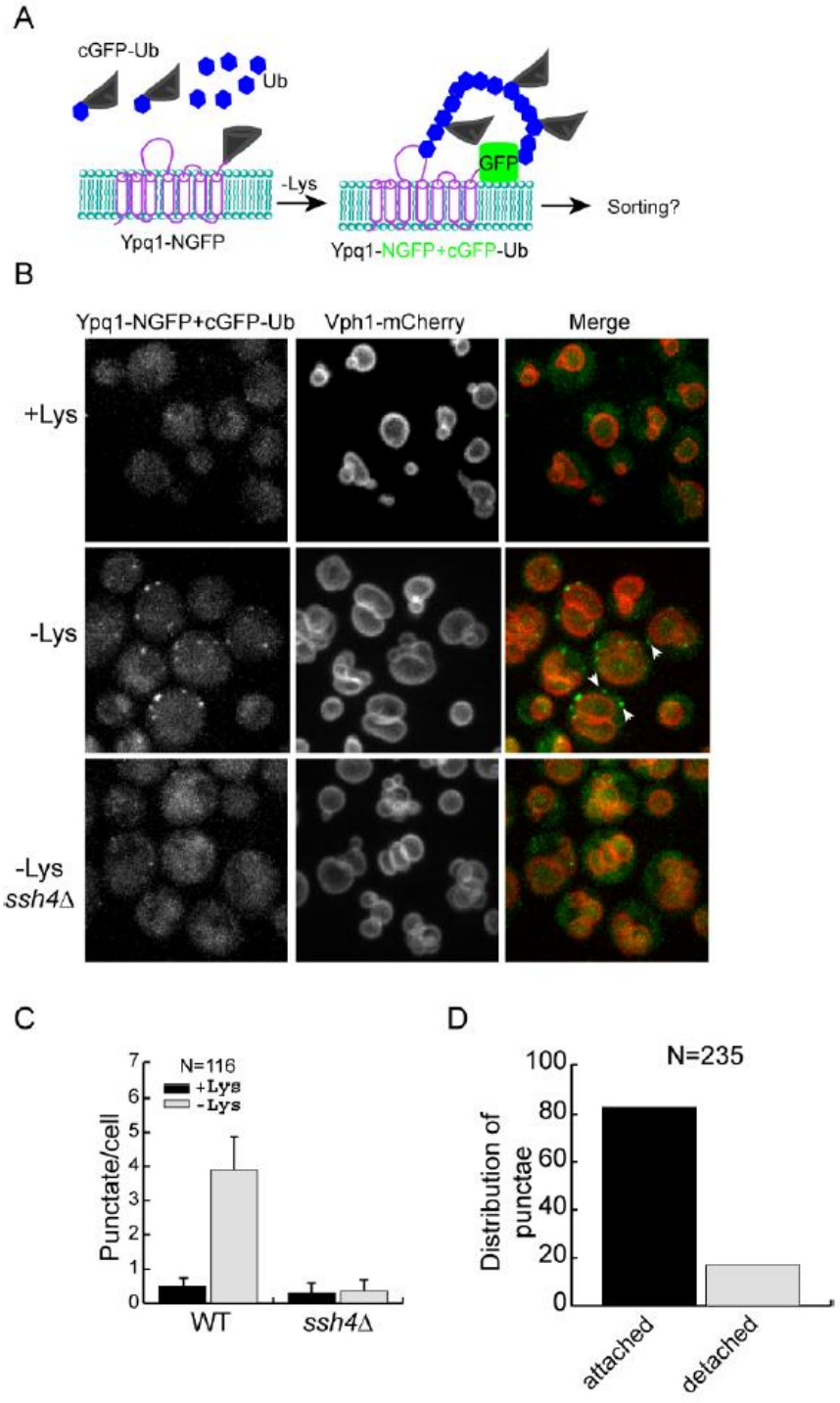
A
cGFP-Ub
Ub
-Lys
GFP
Sorting?
Ypq1-NGFP
Ypq1-NGFP+cGFP-Ub
B
Ypq1-NGFP+cGFP-Ub
Vph1-mCherry
Merge
+Lys
-Lys
-Lys
ssh4Δ
C
N=116
+Lys
-Lys
Punctate/cell
WT
ssh4Δ
D
N=235
Distribution of punctae
attached
detached

Figure 3.12

Figure 3.12. (related to figure 3.10)

Ubiquitinated Ypq1 is selectively sorted into intermediate compartments after lysine withdrawal. **A)** Cartoon schematic showing a split-GFP assay to monitor the trafficking of ubiquitinated Ypq1. **B)** Ubiquitinated Ypq1 is selectively sorted and concentrated into the intermediate compartments after lysine withdrawal. **C)** Quantification of the number of punctae per cell in WT and *ssh4*Δ strains. Error bars represent standard deviation. **D)** Quantification of the vacuole-attached and detached punctae.

Discussion

Eukaryotic cells are highly compartmentalized with an elaborate system of distinct membrane-enclosed organelles. The coordination of intracellular transport and metabolic processes requires communication among these organelles, which is mediated by integral membrane proteins, vesicles, and inter-organelle contact sites, etc. In humans, about 25% the genome encodes transmembrane proteins (Fagerberg et al., 2010). Regulation of these membrane proteins in response to changes in environmental and intracellular cues is essential for the normal growth and division of cells. Therefore, understanding how cells regulate the quantity and quality of their membrane proteins is of fundamental importance. The lysosomal membrane is composed of ~120 integral membrane proteins (Braulke and Bonifacino, 2009), about half of which are membrane transporters. These transporters, together with their PM counterparts, are key regulators of cytoplasmic nutrient and ion homeostasis. Changes in cytosolic nutrient levels trigger membrane remodeling at both the PM and the lysosomal membrane. Numerous studies have been carried out on the regulation of PM transporters, and now we have a detailed understanding of the mechanisms by which PM protein levels are regulated (via

secretion, endocytosis, and lysosomal degradation) (Doherty and McMahon, 2009; Weinberg and Drubin, 2012). However, little is known about the regulation of lysosomal membrane proteins. In fact, the lysosome is often considered a static terminal compartment of the endo-membrane trafficking system.

In this study, we demonstrated that lysosomal membrane proteins are under strict regulation in response to changes in the environment (such as nutrient starvation). As an initial step to address the underlying mechanisms, we focused our analysis on one vacuolar membrane protein, the lysine transporter Ypq1. Our results uncovered a ubiquitin and ESCRT-dependent membrane trafficking pathway that regulates the composition and function of the vacuole membrane. As summarized in Figure 3.13, we speculate that the sorting and turnover of Ypq1 requires the following: (I) activation of the vacuole-anchored ubiquitin ligase (VAcUL-1) complex, composed of the integral membrane adaptor protein Ssh4 and the E3 ligase Rsp5 (Figures 3.7 and 3.8); (II) sorting and packaging of the ubiquitinated Ypq1 into a vacuolar membrane domain (Figure 3.10); (III) vacuole membrane deformation and budding of a post-vacuolar intermediate compartment (e.g., vesicles) (Figure 3.10); (IV) ESCRT-

mediated internalization of ubiquitinated Ypq1 into ILVs, possibly after mixing with endocytic and biosynthetic cargoes in a common late endosome (Figure 3.5); and (V) docking and fusion of the intermediate compartment with the vacuole, thereby delivering the Ypq1 containing ILVs into the vacuole lumen for degradation (Figure 3.9).

Because of the extensive conservation of lysosomal functions between yeast and mammals, many yeast vacuolar membrane proteins have homologs in mammalian lysosomes. It seems likely that a similar ubiquitin-dependent surveillance system exists in mammalian cells. Indeed, similar to Ssh4, humans have over 100 SPRY domain-containing genes. Several of these genes encode proteins with architecture similar to Ssh4. In addition, many of the human SPRY domain-containing proteins have been shown to function in protein ubiquitination, either as E3 ligases or as adaptors to recruit E3 ligases (Kuang et al., 2010; Perfetto et al., 2013). It is possible that this family of proteins will play a role in the downregulation of lysosomal membrane proteins.

Our study provides insights into the mechanism for ubiquitination of Ypq1, and we show imaging data that maps out the trafficking itinerary for Ypq1-GFP degradation. However, as one might expect, our analysis of this vacuolar recycling and degradation (vReD) pathway raises many new and interesting questions. Some of the steps, such as vesicle budding and ESCRT-mediated ILV formation, are still speculative. Furthermore, the identity of the intermediate compartments still needs to be clarified. Whether these intermediate compartments fuse with prevacuolar endosomes prior to ESCRT-mediated sorting is still an open question. Additionally, we cannot rule out the possibility that there are smaller and undetected Ypq1-containing vesicles that bud off the vacuole membrane and traffic to the intermediate compartments.

Another key question is how the ubiquitinated Ypq1 is recognized on the vacuole surface? We did not observe recruitment of the ESCRTs to the vacuole even though the ESCRTs contain several ubiquitin binding domains. There are many other

proteins with ubiquitin binding domains (UBD) in the yeast genome, some of which are involved in the sorting and trafficking of ubiquitinated membrane cargoes (Dixit et al., 2014; Lauwers et al., 2010). Determining whether some of these proteins are important for the sorting of ubiquitinated Ypq1 will require further analysis.

Another protein complex that is capable of retrieving membrane proteins is the retromer complex (Seaman et al., 1997; Seaman et al., 1998). This complex normally functions in the endosome-to-Golgi recycling pathway. The retromer complex is composed of the sorting nexin sub-complex (Vps5 and Vps17) and the cargo recognition sub-complex (Vps26, Vps29, and Vps35) (Seaman, 2012). The cargo recognition sub-complex is an effector of Rab7. In yeast, the interaction between the cargo recognition sub-complex and Ypt7 (yeast Rab7) can recruit the sub-complex to vacuole surface (Liu et al., 2012; Seaman, 2012). However, the function for the vacuole-localized cargo recognition complex is unknown. Although the retromer complex has no known UBDs, it might function together with other ubiquitin binding proteins to sort vacuole membrane cargoes. Our initial tests of the retromer mutant cells indicate that the retromer is not required for Ypq1 sorting. However, a kinetic delay in Ypq1 degradation was observed (M.L. and S.D.E., unpublished data).

Further analysis will be required to investigate the role of the retromer.

Our findings indicate that the vacuole is dynamic and its membrane proteins can be sorted off the vacuole membrane if an appropriate sorting signal is present. We have uncovered a ubiquitin surveillance system on the vacuole membrane (VAcUL-1) that regulates the abundance of resident vacuolar membrane proteins in response to environmental cues. What are other functions of the vReD pathway? Lysosomal membrane proteins are constantly susceptible to damage/cleavage by luminal hydrolyases, presenting a challenge for the cell to clear out these damaged membrane proteins. Moreover, autophagy and the endomembrane trafficking systems constantly deliver exogenous membrane proteins and lipids to the vacuole membrane during vesicle fusion reactions. These membranes and proteins must be recycled or degraded to maintain the proper size, composition, and function of the vacuole. The existence of a ubiquitin-dependent vacuole quality control system could provide a rapid response system to recycle and degrade damaged membrane proteins and excessive lipids, thereby maintaining the integrity of the vacuole.

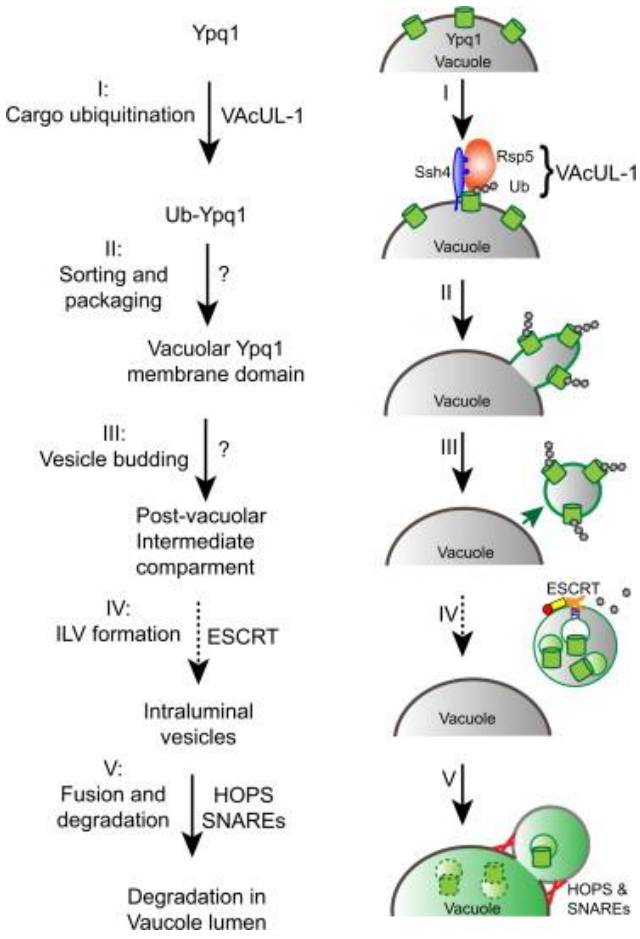
Ypq1
I:
Cargo ubiquitination
VAcUL-1
Ub-Ypq1
II:
Sorting and
packaging
?
Vacuolar Ypq1
membrane domain
III:
Vesicle budding
?
Post-vacuolar
Intermediate
comparment
IV:
ILV formation
ESCRT
Intraluminal
vesicles
V:
Fusion and
degradation
HOPS
SNAREs
Degradation in
Vaucole lumen
Ypq1
Vacuole
I
Rsp5
Ssh4
Ub
VAcUL-1
Vacuole
II
Vacuole
III
Vacuole
ESCRT
IV
Vacuole
V
Vacuole
HOPS &
SNAREs

Figure 3.13

Figure 3.13. A Tentative Working Model for the Vacuole Membrane Recycling and Degradation Pathway

The vacuole membrane recycling and degradation (vReD) pathway, as represented here using Ypq1, includes the following steps: (I) activation of the VAcUL-1 complex, composed of Ssh4 and Rsp5, to ubiquitinate Ypq1; (II) sorting and packaging of the ubiquitinated Ypq1 on the vacuole membrane; (III) budding of the intermediate compartment; (IV) ESCRT-mediated internalization of ubiquitinated Ypq1 into ILVs; and (V) fusion with the vacuole and Ypq1 degradation in the vacuole lumen. The dashed line at step IV highlights additional transport events that may exist (e.g., delivery to a late endosome prior to the ESCRT-mediated internalization).

Acknowledgments

We thank members of the Emr laboratory, especially W.M. Henne and S. Tang, for helpful discussion and comments about the manuscript. We are grateful to J.C. Fromme and W.J. Brown for many helpful discussions and critical reading of the manuscript. We also thank R. Williams from the Cornell BRC Imaging Facility for help with the Olympus spinning-disc confocal microscopy (supported by NIH1S10OD010605-01A). Y.-S.C. is supported by a scholarship from the Taiwanese Ministry of Education. The work was supported by a Cornell University Research Grant (S.D.E.).

References

Amerik, A.Y., Nowak, J., Swaminathan, S., and Hochstrasser, M. (2000). The Doa4 deubiquitinating enzyme is functionally linked to the vacuolar proteinsorting and endocytic pathways. Mol. Biol. Cell 11, 3365–3380.

Babst, M., Sato, T.K., Banta, L.M., and Emr, S.D. (1997). Endosomal transport function in yeast requires a novel AAA-type ATPase, Vps4p. EMBO J. 16, 1820–1831.

Babst, M., Odorizzi, G., Estepa, E.J., and Emr, S.D. (2000). Mammalian tumor susceptibility gene 101 (TSG101) and the yeast homologue, Vps23p, both function in late endosomal trafficking. Traffic 1, 248–258.

Babst, M., Katzmann, D.J., Snyder, W.B., Wendland, B., and Emr, S.D. (2002).

Endosome-associated complex, ESCRT-II, recruits transport machinery for protein sorting at the multivesicular body. Dev. Cell 3, 283–289.

Bar-Peled, L., and Sabatini, D.M. (2014). Regulation of mTORC1 by amino acids. Trends Cell Biol. 24, 400–406.

Belgareh-Touzé, N., Léon, S., Erpapazoglou, Z., Stawiecka-Mirota, M., Urban-Grimal, D., and Haguenauer-Tsapis, R. (2008). Versatile role of the yeast ubiquitinligase Rsp5p in intracellular trafficking. Biochem. Soc. Trans. 36, 791–796.

Bowers, K., and Stevens, T.H. (2005). Protein transport from the late Golgi to the vacuole in the yeast Saccharomyces cerevisiae. Biochim. Biophys. Acta 1744, 438–454.

Braulke, T., and Bonifacino, J.S. (2009). Sorting of lysosomal proteins. Biochim. Biophys. Acta 1793, 605–614.

Bryant, N.J., Piper, R.C., Weisman, L.S., and Stevens, T.H. (1998). Retrograde traffic out of the yeast vacuole to the TGN occurs via the prevacuolar/endosomal compartment. J. Cell Biol. 142, 651–663.

Burd, C.G., Peterson, M., Cowles, C.R., and Emr, S.D. (1997). A novel Sec18p/ NSF-dependent complex required for Golgi-to-endosome transport in yeast. Mol. Biol. Cell 8, 1089–1104.

Cheever, M.L., Sato, T.K., de Beer, T., Kutateladze, T.G., Emr, S.D., and Overduin, M. (2001). Phox domain interaction with PtdIns(3)P targets the Vam7 t-SNARE to vacuole membranes. Nat. Cell Biol. 3, 613–618.

Darsow, T., Rieder, S.E., and Emr, S.D. (1997). A multispecificity syntaxin homologue, Vam3p, essential for autophagic and biosynthetic protein transport to the vacuole. J. Cell Biol. 138, 517–529.

Darsow, T., Burd, C.G., and Emr, S.D. (1998). Acidic di-leucine motif essential for AP-3-dependent sorting and restriction of the functional specificity of the Vam3p vacuolar t-SNARE. J. Cell Biol. 142, 913–922.

Dixit, G., Baker, R., Sacks, C.M., Torres, M.P., and Dohlman, H.G. (2014). Guanine nucleotide-binding protein (Ga) endocytosis by a cascade of ubiquitin binding domain proteins is required for sustained morphogenesis and proper mating in yeast. J. Biol. Chem. 289, 15052–15063.

Doherty, G.J., and McMahon, H.T. (2009). Mechanisms of endocytosis. Annu. Rev. Biochem. 78, 857–902.

Fagerberg, L., Jonasson, K., von Heijne, G., Uhlén, M., and Berglund, L. (2010). Prediction of the human membrane proteome. Proteomics 10, 1141–1149.

Gupta, R., Kus, B., Fladd, C., Wasmuth, J., Tonikian, R., Sidhu, S., Krogan, N.J., Parkinson, J., and Rotin, D. (2007). Ubiquitination screen using protein microarrays for comprehensive identification of Rsp5 substrates in yeast. Mol. Syst. Biol. 3, 116.

He, C., and Klionsky, D.J. (2009). Regulation mechanisms and signaling pathways of autophagy. Annu. Rev. Genet. 43, 67–93.

Henne, W.M., Buchkovich, N.J., and Emr, S.D. (2011). The ESCRT pathway. Dev. Cell 21, 77–91.

Hettema, E.H., Valdez-Taubas, J., and Pelham, H.R. (2004). Bsd2 binds the ubiquitin ligase Rsp5 and mediates the ubiquitination of transmembrane proteins. EMBO J. 23, 1279–1288.

Hu, C.D., and Kerppola, T.K. (2003). Simultaneous visualization of multiple protein interactions in living cells using multicolor fluorescence complementation analysis. Nat. Biotechnol. 21, 539–545.

Imai, K., Noda, Y., Adachi, H., and Yoda, K. (2007). Peculiar protein-protein interactions of the novel endoplasmic reticulum membrane protein Rcr1 and ubiquitin ligase Rsp5. Biosci. Biotechnol. Biochem. 71, 249–252.

Jézégou, A., Llinares, E., Anne, C., Kieffer-Jaquinod, S., O'Regan, S., Aupetit, J., Chabli, A., Sagné, C., Debacker, C., Chadefaux-Vekemans, B., et al. (2012). Heptahelical protein PQLC2 is a lysosomal cationic amino acid exporter underlying the action of cysteamine in cystinosis therapy. Proc. Natl. Acad. Sci. USA 109, E3434–E3443.

Katzmann, D.J., Babst, M., and Emr, S.D. (2001). Ubiquitin-dependent sorting into the multivesicular body pathway requires the function of a conserved endosomal protein sorting complex, ESCRT-I. Cell 106, 145–155.

Katzmann, D.J., Stefan, C.J., Babst, M., and Emr, S.D. (2003). Vps27 recruits ESCRT machinery to endosomes during MVB sorting. J. Cell Biol. 162, 413–423.

Kota, J., Melin-Larsson, M., Ljungdahl, P.O., and Forsberg, H. (2007). Ssh4, Rcr2 and Rcr1 affect plasma membrane transporter activity in Saccharomyces cerevisiae. Genetics 175, 1681–1694.

Kuang, Z., Lewis, R.S., Curtis, J.M., Zhan, Y., Saunders, B.M., Babon, J.J., Kolesnik, T.B., Low, A., Masters, S.L., Willson, T.A., et al. (2010). The SPRY domain-containing SOCS box protein SPSB2 targets iNOS for proteasomal degradation. J. Cell Biol. 190, 129–141.

Kümmel, D., and Ungermann, C. (2014). Principles of membrane tethering and fusion in endosome and lysosome biogenesis. Curr. Opin. Cell Biol. 29, 61–66.

Laplante, M., and Sabatini, D.M. (2009). mTOR signaling at a glance. J. Cell Sci. 122, 3589–3594.

Lauwers, E., Erpapazoglou, Z., Haguenauer-Tsapis, R., and André, B. (2010). The ubiquitin code of yeast permease trafficking. Trends Cell Biol. 20, 196–204.

Léon, S., Erpapazoglou, Z., and Haguenauer-Tsapis, R. (2008). Ear1p and Ssh4p are

new adaptors of the ubiquitin ligase Rsp5p for cargo ubiquitylation and sorting at multivesicular bodies. Mol. Biol. Cell 19, 2379–2388.

Levine, B., and Klionsky, D.J. (2004). Development by self-digestion: molecular mechanisms and biological functions of autophagy. Dev. Cell 6, 463–477.

Lin, C.H., MacGurn, J.A., Chu, T., Stefan, C.J., and Emr, S.D. (2008). Arrestinrelated ubiquitin-ligase adaptors regulate endocytosis and protein turnover at the cell surface. Cell 135, 714–725.

Liu, T.T., Gomez, T.S., Sackey, B.K., Billadeau, D.D., and Burd, C.G. (2012). Rab GTPase regulation of retromer-mediated cargo export during endosome maturation. Mol. Biol. Cell 23, 2505–2515.

MacDiarmid, C.W., Gaither, L.A., and Eide, D. (2000). Zinc transporters that regulate

vacuolar zinc storage in Saccharomyces cerevisiae. EMBO J. 19, 2845–2855.

Miesenböck, G., De Angelis, D.A., and Rothman, J.E. (1998). Visualizing secretion and synaptic transmission with pH-sensitive green fluorescent proteins. Nature 394, 192–195.

Odorizzi, G., Cowles, C.R., and Emr, S.D. (1998). The AP-3 complex: a coat of many colours. Trends Cell Biol. 8, 282–288.

Perfetto, L., Gherardini, P.F., Davey, N.E., Diella, F., Helmer-Citterich, M., and Cesareni, G. (2013). Exploring the diversity of SPRY/B30.2-mediated interactions. Trends Biochem. Sci. 38, 38–46.

Platt, F.M., Boland, B., and van der Spoel, A.C. (2012). The cell biology of disease: lysosomal storage disorders: the cellular impact of lysosomal dysfunction. J. Cell

Biol. 199, 723–734.

Ramirez-Montealegre, D., and Pearce, D.A. (2005). Defective lysosomal arginine transport in juvenile Batten disease. Hum. Mol. Genet. 14, 3759–3773.

Richter, C., West, M., and Odorizzi, G. (2007). Dual mechanisms specify Doa4-mediated deubiquitination at multivesicular bodies. EMBO J. 26, 2454–2464.

Rieder, S.E., and Emr, S.D. (1997). A novel RING finger protein complex essential for a late step in protein transport to the yeast vacuole. Mol. Biol. Cell 8, 2307–2327.

Seaman, M.N. (2012). The retromer complex - endosomal protein recycling and beyond. J. Cell Sci. 125, 4693–4702.

Seaman, M.N., Marcusson, E.G., Cereghino, J.L., and Emr, S.D. (1997). Endosome to

Golgi retrieval of the vacuolar protein sorting receptor, Vps10p, requires the function of the VPS29, VPS30, and VPS35 gene products. J. Cell Biol. 137, 79–92.

Seaman, M.N., McCaffery, J.M., and Emr, S.D. (1998). A membrane coat complex essential for endosome-to-Golgi retrograde transport in yeast. J. Cell Biol. 142, 665–681.

Shimazu, M., Sekito, T., Akiyama, K., Ohsumi, Y., and Kakinuma, Y. (2005). A family of basic amino acid transporters of the vacuolar membrane from Saccharomyces cerevisiae. J. Biol. Chem. 280, 4851–4857.

Stearman, R., Yuan, D.S., Yamaguchi-Iwai, Y., Klausner, R.D., and Dancis, A. (1996). A permease-oxidase complex involved in high-affinity iron uptake in yeast. Science 271, 1552–1557.

Swaminathan, S., Amerik, A.Y., and Hochstrasser, M. (1999). The Doa4 deubiquitinating enzyme is required for ubiquitin homeostasis in yeast. Mol. Biol. Cell 10, 2583–2594.

Urbanowski, J.L., and Piper, R.C. (1999). The iron transporter Fth1p forms a complex with the Fet5 iron oxidase and resides on the vacuolar membrane. J. Biol. Chem. 274, 38061–38070.

Weinberg, J., and Drubin, D.G. (2012). Clathrin-mediated endocytosis in budding yeast. Trends Cell Biol. 22, 1–13.

Chapter IV

Conclusions

A Bipartite Sequence for Specific Retromer Recognition

Retromer-mediated endosome-to-Golgi retrograde transport is important for many proteins to function normally. How so many proteins are precisely recognized by the retromer is unclear. Here, we show that a bipartite recycling signal can be used to ensure the specificity and diversity of cargo recognition by the retromer complex. We found that the vacuole hydrolase receptor Vps10 contains an FGEIRL motif and a YSSL motif. The FGEIRL motif plays a major role in Vps10 recycling, while the YSSL motif acts as an accessory role for the recycling. In addition to Vps10, the E3 ubiquitin ligase Rsp5 adaptor Ear1 also has a similar pattern. Ear1 has a PPGFEF motif and an INL motif, which are equally important for the recycling. Furthermore, we show that Vps26 is the major subunit in the retromer complex responsible for cargo recognition. Vps26 utilizes a universal site to recognize each cargo as well as specific sites to recognize different cargos. Vps26 uses F334 and L285 to recognize Vps10, and I251/F368 and L285 to recognize Ear1. Thus, our results show that the

retromer recognizes cargos differentially, providing insight into how so many cargos are precisely recognized for recycling.

Lysosomal Membrane Protein Degradation

The lysosome is an important organelle for degradation and nutrient storage. Nutrients are transported across the lysosome membrane by transporters. Mutations in those lysosomal membrane transporters could lead to the abnormal accumulation of specific nutrients, which contribute to lysosomal storage diseases. It is thus essential to understand the mechanism by which the normal turnover of the lysosomal membrane proteins is regulated. In this thesis, we have used the lysosomal lysine transporter Ypq1 as a model to show that, upon stimulation for degradation, lysosomal membrane proteins are ubiquitinated by an E3 ubiquitin ligase complex, composed of Rsp5 and Ssh4. The ubiquitinated membrane transporters then recruit the ESCRT machinery to promote the direct invagination into the lysosome lumen (Zhu et al., 2017). This is the first study of lysosomal membrane protein degradation.

Future Directions

Investigate the mechanism of cargo recognition by the retromer complex

In Chapter II, we've shown that Vps26-F334/L285 is required to recognize Vps10, presumably through the FGEIRL-YSSL motif. However, how Vps26 interacts with Vps10 recycling motifs is still elusive. A structure-based model will be required to explain the details of cargo recognition in the future. Interestingly, we have shown that the first 30 residues of the Vps10 c-tail are important for recycling. In addition to the FGEIRL motif, multiple residues are implicated in Vps10 recycling, including I1419, I1439, N1442, and D1445 (Fig. 5.1). How do multiple residues contribute to the recognition by the retromer? There are two models to explain this phenotype. In the first model, all those residues *in trans* physically bind to Vps26 at different sites. In this case, single mutations in those residues cannot completely block the recycling and only shows a partial phenotype, which is very different from the Ear1 case. In the second model, those residues bind to each other *in cis* to form a specific structure, such as a global domain, which can then interact with a pocket in Vps26. More research will be required to examine these two models in the future.

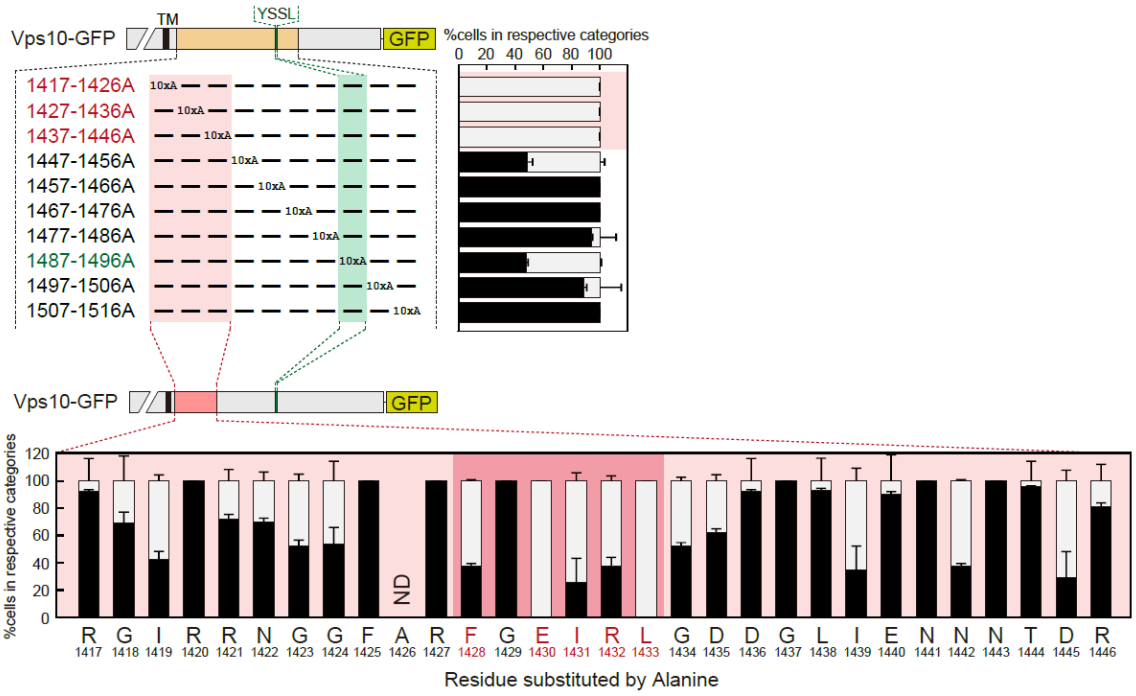
Vps10-GFP
TM
YSSL
GFP
%cells in respective categories
0 20 40 60 80 100
1417-1426A
1427-1436A
1437-1446A
1447-1456A
1457-1466A
1467-1476A
1477-1486A
1487-1496A
1497-1506A
1507-1516A
10xA
Vps10-GFP
GFP
%cells in respective categories
120
100
80
60
40
20
0
ND
R G I R R N G G F A R F G E I R L G D D G L I E N N N T D R
1417 1418 1419 1420 1421 1422 1423 1424 1425 1426 1427 1428 1429 1430 1431 1432 1433 1434 1435 1436 1437 1438 1439 1440 1441 1442 1443 1444 1445 1446
Residue substituted by Alanine

Figure 4.1

Figure 4.1. Multiple residues contribute to Vps10 recycling.

In the first 30 residues, many of them contribute to Vps10 recycling, especially including I1419, I1439, N1442, and D1445. Those residues might work synergistically in cargo recognition by the retromer complex.

Investigate the mechanism of retromer complex formation

Retromer is composed of cargo selective complex (Vps35, Vps29, and Vps26) and sorting nexins (Vps5 and Vps17). However, how the subunits interact with each other to form a complex is still unclear. Furthermore, in the case of Ear1 recycling, Vps17 is not required. Every component in retromer can be phosphorylated or ubiquitinated, but it is still unknown whether post-translational modifications play a role in regulating retromer. It is possible that those modifications might affect the association and dissociation of the retromer components and thus regulate cargo recycling. For example, phosphorylation at serine 226 of sorting nexin 5 (SNX5) is found to regulate the dimerization with SNX1 or SNX2, suggesting that phosphorylation of retromer components might regulate membrane trafficking and cargo recycling (Itai et al., 2018). Future studies will focus on the mechanism of retromer complex formation.

Vps26-mediated cargo recognition in mammalian cells

Our study has shown that Vps26 is the major subunit for cargo recognition. In

humans, VPS26 is the only component of the core complex which has been found to have three paralogues, VPS26a, VPS26b, and VPS26c, and studies imply that the expression level of VPS26b might be differential in the brain (Small et al., 2015). Interestingly, a previous study has shown that the FANSHY motif of sorLA, the sorting receptor for amyloid precursor protein, has been found to be recognized by VPS26 for recycling (Fjorback et al., 2012). However, it is still unclear how sorLA is recognized by VPS26. Future studies will focus on this direction to identify the details of retromer recognition.

Lysosomal membrane protein degradation in mammalian cells

Our study of lysosomal membrane protein degradation has shown that the major complexes in this pathway include the E3 ubiquitin ligase complex Rsp5/Ssh4 and the ESCRT machinery (Zhu et al., 2017). However, it is still unclear how lysosomal membrane protein degradation in mammalian cells is regulated. Besides, it remains unknown how this pathway is implicated in human diseases, such as lysosomal storage diseases. Future studies should provide more information about those

mechanisms.

Applications of the RapiDeg system

In the current study, we used the RapiDeg system to study lysosomal membrane protein degradation. In addition, we found that the RapiDeg system can be used to target membrane proteins on other organelles, such as PM, endosome, and the Golgi. In the future, we could try to apply this strategy for targeted protein degradation in mammalian cells for the purpose of disease treatments. Further studies will be required to establish an effective RapiDeg system in mammalian cells.

Recycling model for lysosomal membrane protein degradation

Our study has shown that ESCRT-mediated direct invagination is the major pathway for lysosomal membrane protein degradation (Zhu et al., 2017). However, we have not yet ruled out the possibility that cargos might be budded off from the vacuole to form a vesicle, which forms an MVB by the ESCRTs and then recycles back to the lysosome for degradation. Previously our lab has shown that the transmembrane

autophagy protein Atg27 can be recycled from the vacuole membrane to the Golgi by two steps: the Snx4 complex regulates the recycling of Atg27 from the lysosome to the endosome, and the retromer complex regulates the recycling of Atg27 from the endosome to the Golgi (Suzuki and Emr, 2018). It is possible that after cargo ubiquitination, other ubiquitin-binding proteins recognize and bind the cargo to follow the recycling model. Indeed, previously I have performed a screening to identify potential proteins implicated in the recycling model. In this screen, I focus on 39 proteins containing ubiquitin-binding domains, such as UBA, UBX, UIM, NZF, GAT, CUE, and UVE (Fig. 5.2). Specifically, I utilized pHluorin, the pH-sensitive version of GFP, to generate the Ypq1-pHluorin construct. I then transformed this construct into the 39 mutants lacking the gene encoding ubiquitin-binding proteins in the BY4741 collection, a set of deletion strains derived from S288C strain background. Ypq1 degradation was then triggered by lysine withdrawal and examined by flow cytometry to determine the fluorescence signal of each group. In WT cells, Ypq1-pHluorin was internalized into the vacuole lumen, so that the pHluorin signal was weak. In *ssh4*Δ, Ypq1-pHluorin was blocked on the vacuole membrane, so that the pHluorin signal was strong. The signal in *ssh4*Δ was set as a

positive control and that in WT cells as a negative control. By comparing the fluorescence signals with the signals in *ssh4*Δ and WT cells, I was able to identify other genes implicated in Ypq1 degradation pathway. Interestingly, I found that the guanine exchange factor Vps9 showed a good signal. Vps9 is a CUE domain-containing protein which can bind ubiquitinated cargos on the endosome to promoter vesicle maturation. I further examined the phenotype in *vps9*Δ by fluorescent microscopy and found that Ypq1 degradation was slowed down in *vps9*Δ after lysine withdrawal, coupled with Ypq1-GFP puncta in the cytosol (Fig. 5.2). This result was consistent with the recycling model. Furthermore, I found that more Ypq1-GFP puncta were observed in *vps9-ts* in the non-permissive temperature, suggesting that Ypq1-GFP intermediates might be blocked in the cytosol in this condition (Fig. 5.3). Consistent with this, in Chapter II, we have shown evidence to propose a recycling model. We found that numerous Ypq1-GFP puncta appear after lysine withdrawal at non-permissive temperature in *pep12-ts* (Fig. 3.11). Also, by using the split-GFP method to detect protein-protein interactions, we have shown that Ypq1 colocalized with ubiquitin or the ESCRT subunit Vps23 in the cytosol, suggesting that ubiquitinated Ypq1 recruits the ESCRT machinery in the cytosol

after lysine withdrawal (Fig. 3.6 and 3.12). These results imply that Ypq1 might form an intermediate in the cytosol after lysine withdrawal condition and thus support the recycling model. Future studies will be required to further examine this model, especially focusing on characterizing the identity of the cytosolic Ypq1 puncta.

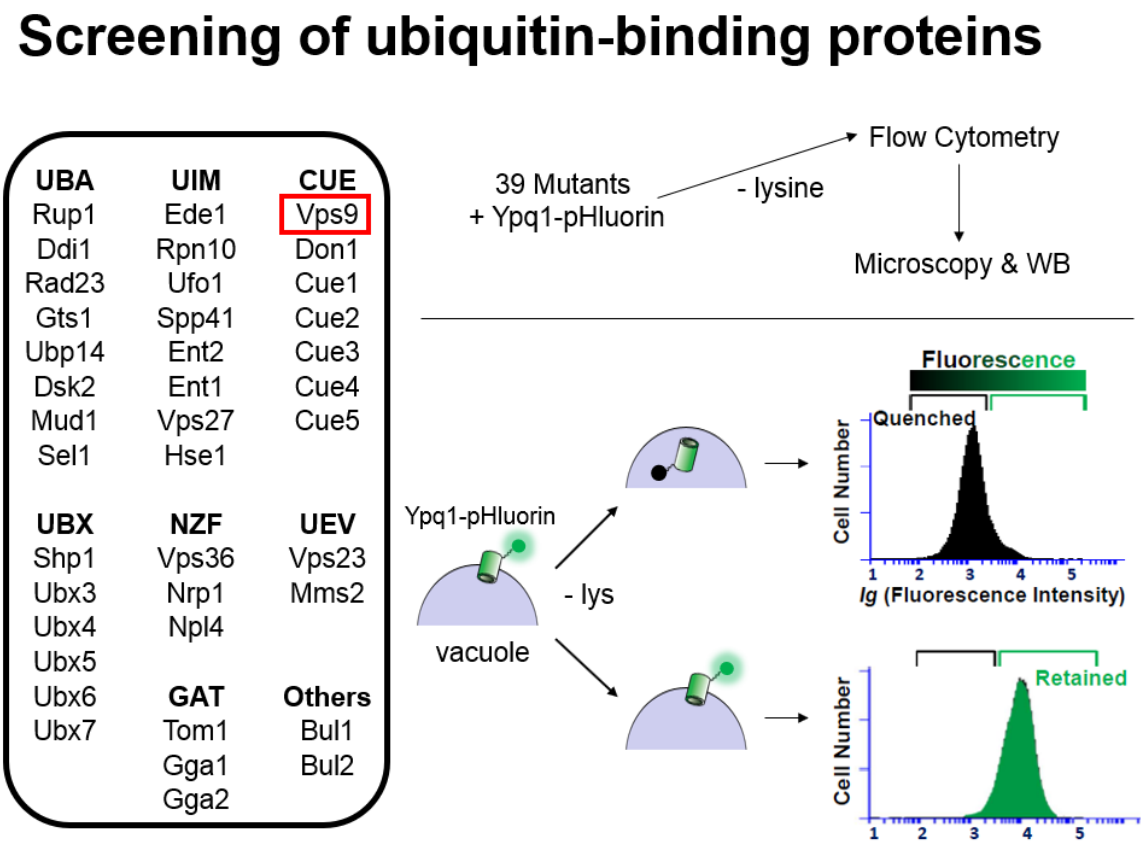
Screening of ubiquitin-binding proteins
UBA
Rup1
Ddi1
Rad23
Gts1
Ubp14
Dsk2
Mud1
Sel1
UIM
Ede1
Rpn10
Ufo1
Spp41
Ent2
Ent1
Vps27
Hse1
CUE
Vps9
Don1
Cue1
Cue2
Cue3
Cue4
Cue5
UBX
Shp1
Ubx3
Ubx4
Ubx5
Ubx6
Ubx7
NZF
Vps36
Nrp1
Npl4
GAT
Tom1
Gga1
Gga2
UEV
Vps23
Mms2
Others
Bul1
Bul2
39 Mutants
+ Ypq1-pHluorin
- lysine
Flow Cytometry
Microscopy & WB
Ypq1-pHluorin
- lys
vacuole
Fluorescence
Quenched
Cell Number
lg (Fluorescence Intensity)
Retained
Cell Number

Figure 4.2

Figure 4.2. Screening of ubiquitin-binding proteins in Ypq1 degradation. 39 ubiquitin-binding proteins are selected to examine their roles in Ypq1 degradation by flow cytometry.

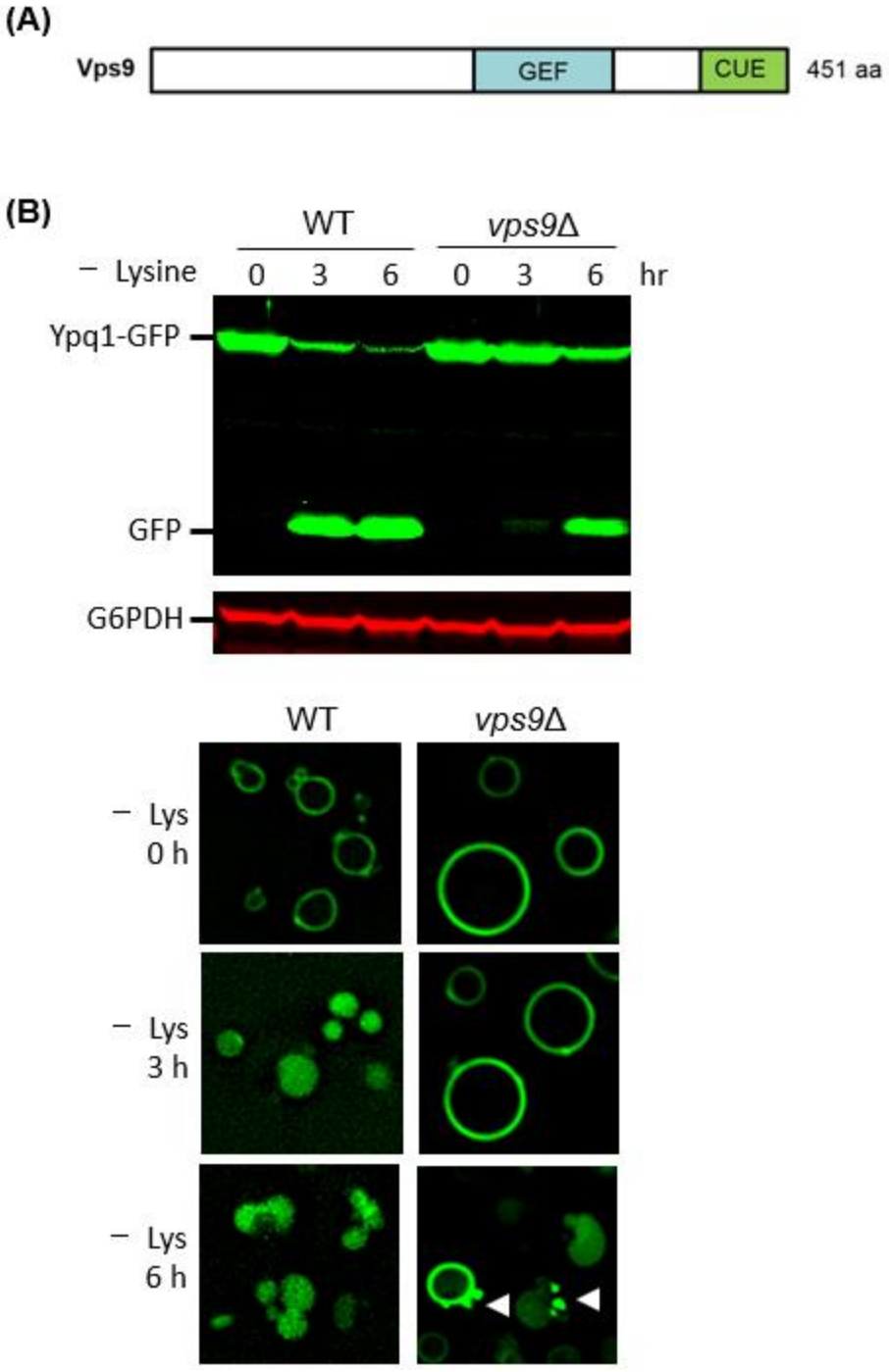
(A)
Vps9
GEF
CUE
451 aa
(B)
WT
vps9Δ
– Lysine
0 3 6 0 3 6 hr
Ypq1-GFP
GFP
G6PDH
WT
vps9Δ
– Lys 0 h
– Lys 3 h
– Lys 6 h

Figure 4.3

Figure 4.3. Ypq1 degradation is defective in *vps9*Δ. (A) The diagram of Vps9, which has a GEF domain and a CUE domain. (B) Ypq1-GFP degradation is slowed down in *vps9*Δ. Ypq1-GFP puncta are generated in *vps9*Δ during lysine withdrawal.

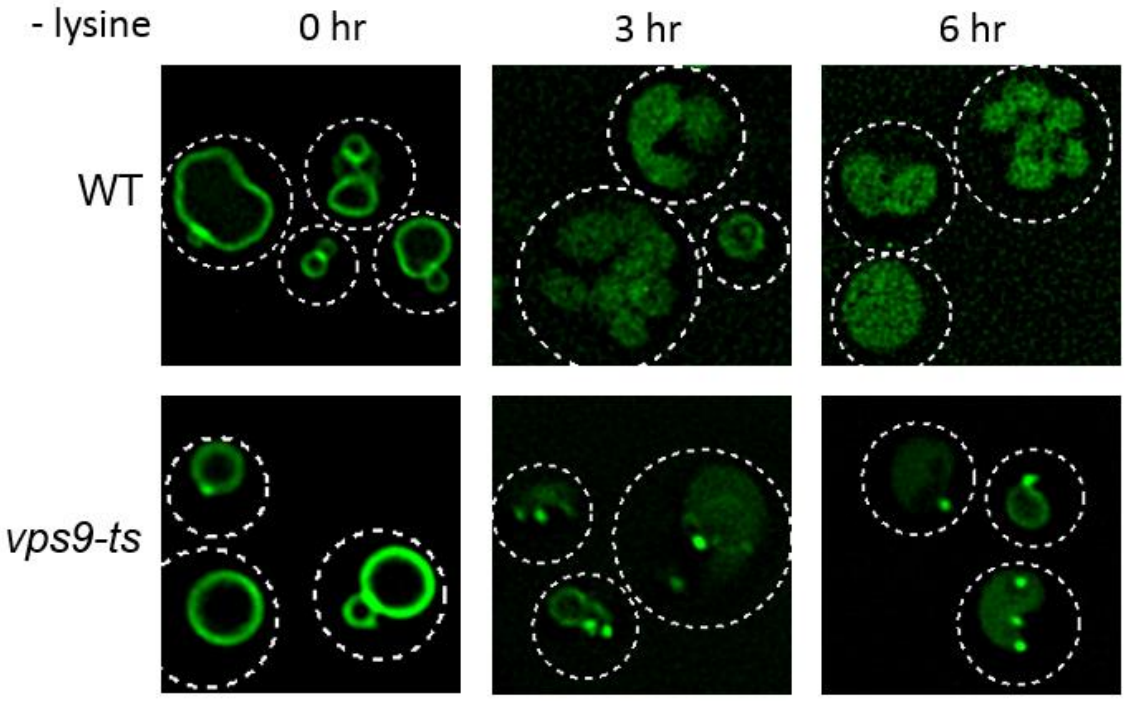

Figure 4.4

Figure 4.4. Ypq1 puncta are observed in *vps9-ts*. Ypq1-GFP degradation is triggered at non-permissive temperature (37℃) by lysine withdrawal and multiple Ypq1-GFP puncta are observed in the cytosol.

References

D'Cruz AA, Babon JJ, Norton RS, Nicola NA, Nicholson SE. Structure and function of the SPRY/B30.2 domain proteins involved in innate immunity. Protein Sci. 2013 Jan;22(1):1-10. doi: 10.1002/pro.2185.

Fjorback AW, Seaman M, Gustafsen C, Mehmedbasic A, Gokool S, Wu C, Militz D, Schmidt V, Madsen P, Nyengaard JR, Willnow TE, Christensen EI, Mobley WB, Nykjær A, Andersen OM. Retromer binds the FANSHY sorting motif in SorLA to regulate amyloid precursor protein sorting and processing. J Neurosci. 2012 Jan 25;32(4):1467-80. doi: 10.1523/JNEUROSCI.2272-11.2012.

Itai N, Shimazu T, Kimura T, Ibe I, Yamashita R, Kaburagi Y, Dohi T, Tonozuka T, Takao T, Nishikawa A. The phosphorylation of sorting nexin 5 at serine 226 regulates retrograde transport and macropinocytosis. PLoS One. 2018 Nov 12;13(11):e0207205. doi: 10.1371/journal.pone.0207205. eCollection 2018.

Small SA, Petsko GA. Retromer in Alzheimer disease, Parkinson disease and other neurological disorders. Nat Rev Neurosci. 2015 Mar;16(3):126-32. doi: 10.1038/nrn3896. Epub 2015 Feb 11.

Suzuki SW, Emr SD. Membrane protein recycling from the vacuole/lysosome membrane. J Cell Biol. 2018 May 7;217(5):1623-1632. doi: 10.1083/jcb.201709162. Epub 2018 Mar 6.

Zhu L, Jorgensen JR, Li M, Chuang YS, Emr SD. ESCRTs function directly on the lysosome membrane to downregulate ubiquitinated lysosomal membrane proteins. Elife. 2017 Jun 29;6. pii: e26403. doi: 10.7554/eLife.26403.

Appendix

This appendix includes the response to reviewers' comments in Chapter II: A bipartite sorting signal ensures specificity of retromer complex in membrane protein recycling. This part has important information which has not been shown in Chapter II.

Reviewer #1 (Comments to the Authors (Required)):

The cargo selective complex of retromer (CSC) is comprised of Vps26, Vps29 and Vps35. This complex works together with a SNX-BAR dimer of Vps5 and Vps17. In this thorough analysis, Emr and colleagues identify a new sorting motif that adds cargo selectivity to retromer cargo recognition.

Previously]F/Y/W/]X[L/M/V] was considered to represent the recognition seqeuence, but its presence in non retromer cargoes suggested there was more.

Through extensive mutagenesis combined with localization in yeast cells, the authors identify YSSL and FGEIRL in Vps10 as being important, and sufficient to localize a distinct cargo protein. In Ear1, they identify PPGFEF and INL. They go on to show that CSC is needed for sorting of both cargoes; Vps10 also needed Vps5 and Vps17, but Ear1 only needed Vps5. Both cargoes need the same complexes as determined from competition experiments. They show that Vps10 and Ear1 engage different binding sites in Vps26 and more specifically than

previously thought, due to coincidence detection.

Overall this represents a lot of work that will be of interest to readers of JCB, and the story should be accepted without delay but would benefit from more discussion about other cargoes and how much additional diversity might be anticipated in other cargoes and whether mutation of Vps26 has indicated selective recycling issues for one cargo and not another.

Thank you! We also tested Kex2 localization in *vps26* mutants (Fig. Rev. 1). Kex2-GFP was mislocalized in I251E/F368E or L285E, but not in F334E, suggesting that I251/F368 recognized at least Ear1 and Kex2. Because of the space restriction for the report format, we decided not to include this data in the revised manuscript.

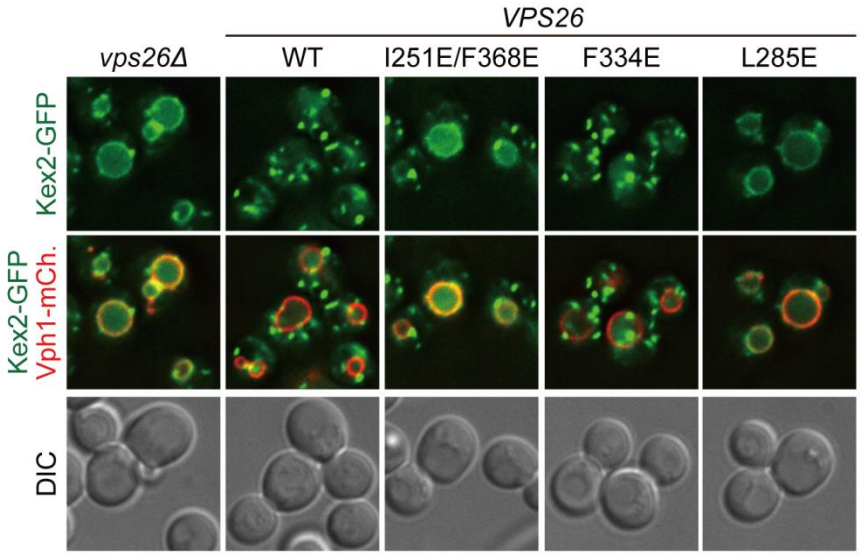
VPS26
vps26Δ
WT
I251E/F368E
F334E
L285E
Kex2-GFP
Kex2-GFP
Vph1-mCh.
DIC

Fig. Rev. 1

Page 6 bottom-- Rsp5?

Thanks for pointing this out. We have corrected it in the manuscript to avoid confusion (Page 6, paragraph 1, lane 16).

Reviewer #2 (Comments to the Authors (Required)):

This paper contains a lot of solid and well presented data, but there are no real mechanistic insights, and the authors have a tendency to gloss over inconsistencies. The study is based on the premise that because the best characterized retromer sorting signal, ΦX[L/M/V] (where Φ is F, Y, or W), can be found in nearly all proteins, retromer cargo proteins are likely to have additional sorting signals. The authors use truncations and alanine scanning mutagenesis to dissect two retromer cargo proteins, Vps10 and Ear1, and they identify two motifs on each that contribute to their recycling away from the vacuole. They also mutate the Vps26 subunit of the retromer complex and show that individual

mutations can have different effects on the localization of Vps10 and Ear1. From this they conclude that there are at least three cargo binding sites on Vps26, one of which is shared by Vps10 and Ear1, while the other two sites interact with one but not the other. This is illustrated in their final figure, 5F.

My main reservation is that the authors present no real evidence for a direct interaction between any of their sorting signals and Vps26, so their model is extremely speculative.

In the revised manuscript, we have included the biochemical evidence for the cargo binding of retromer (Fig. 2E, 4E, 4F, 5E, 5F, S2E, and S2F were added in the revised manuscript). We believe these new data strengthen our conclusion.

Moreover, although the paper starts off with the idea that there are other sorting signals in addition to ΦX[L/M/V], in fact none of the motifs they analyse is actually a ΦX[L/M/V].

Thanks for pointing this out. In the initial manuscript, we used ΦX[L/M/V] as a consensus motif defined by the mammalian retromer cargos (Cullen and Steinberg., 2018). However, when we listed all identified yeast recycling sequences (Fig. S1A was added in the revised version), we realized that that 4 out of 8 identified recycling signals such as YSSL of Vps10, FQFND of Ste13, YEF of Kex2, and WKY of Stv1 do not follow this rule. It could be that yeast recycling signals and mammalian recycling signals are different. The only common feature of yeast recycling signals is the presence of hydrophobic residues. In the revised manuscript, we addressed this in the text (Page 3, paragraph 3, line 3).

The Introduction and the first two sentences of the Results make much of this motif, but then the authors go on to examine the YSSL sequence in Vps10, presumably with the assumption that it fits the consensus. Yet there are two residues rather than one residue between the Y and the L, which means not only

that the key residues would be spaced further apart than in a ΦX[L/M/V] motif, but also that they would be pointing in different directions. So it is difficult to imagine how a ΦX[L/M/V] motif and a YSSL motif could be binding to the same site.

Our study proposes that the retromer has multiple binding sites. Currently, we don't have any evidence regarding which binding site binds to which sequence. However, how the different recycling sequences bind to the retromer complex will be the focus of our investigation in the future.

In fact, YSSL looks like a motif for the AP (adaptor protein) complexes. Can the authors rule out the possibility that YSSL binds to AP-1, which also facilitates endosome-to-Golgi retrieval?

We tested Vps10-GFP localization in AP-1 mutants (*apl2*Δ cells) (Fig. Rev. 2). However, it still localized on punctate structures similar to WT cells, suggesting

that AP-1 does not facilitate Vps10 recycling. Also, consistent with our interpretation, a recent study reports that AP-1 is required for intra-Golgi recycling, not endosome-to-Golgi retrieval (Casler et al., JCB 2019).

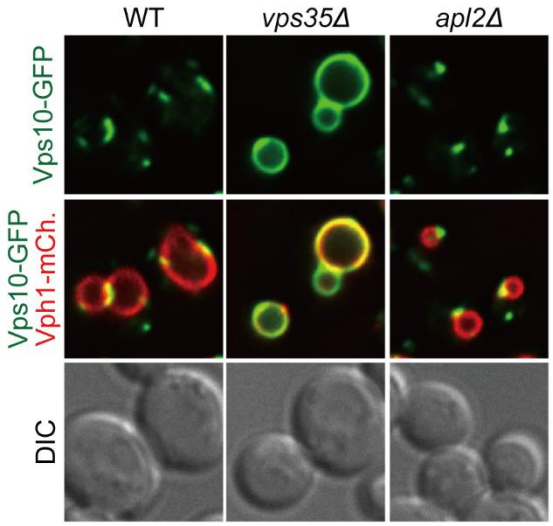

Fig. Rev. 2

Interestingly, a 1995 study from the Emr lab, making use of deletion mutants, pinpointed the sequence FYVF, which does fit the ΦX[L/M/V] consensus, as a key retrieval signal on Vps10. However, the FYVF motif is not discussed, presumably because a subsequent 1996 study from the Stevens lab, which was the first to investigate the YSSL motif, showed by alanine scanning mutagenesis that the FYVF sequence is not strictly necessary for Vps10 retrieval.

Consistent with a 1996 study from the Stevens lab, both 1447-1456A and 1457-1466A mutants which include the sequence 1456-FYVF-1459 did not exhibite striking phenotype (Fig. 1F). Accordingly, we revised the text in the manuscript (Page 4, paragraph 1, line 7).

However, that study, and the present study as well, show that YSSL isn't essential either, so it is not clear to me why they focus so exclusively on the

YSSL motif.

Indeed, Cooper and Stevens showed YSSL is not essential. However, they observed 36% of CPY is missorted in Y1492A mutants (described as $Y_{77}A$ in Figure 8A in Cooper and Stevens., 1996). From this data, they concluded “a tyrosine-based signal ($YSSL_{80}$) within the cytosolic domain enables vps10p to cycle between the late-Golgi and prevacuolar/endosomal compartments” (Cooper and Stevens., 1996). Based on this data and our study, we believe the YSSL motif is important for recycling.

A second concern is that, although the authors propose that Vps10 and Ear1 share a binding site on Vps26, the motifs they identify (YSSL plus FGEIRL on Vps10, and INL plus PPGFEF on Ear1) not only don't conform to the ΦX[L/M/V] motif, but also don't appear to share any other consensus sequences. Thus, it is difficult to imagine how two of these sequences (they don't specify which two) could make use of a common binding site.

As mentioned above, yeast recycling motifs do not share any clear consensus motif (Fig. S1A in the revised manuscript). Determination of the genuine consensus motif for retromer binding is an important question in the field. However, to answer this, structural analysis will ultimately be required. We feel this is beyond the scope of the current manuscript. We hope that we will be able to answer this in future studies.

It is also not clear why the authors assume that the interactions must be with the Vps26 subunit, rather than with the Vps35 subunit and/or the associated SNX/BAR proteins, all of which have also been implicated in cargo retrieval. Their rationale seems to come from their Vps26 mutagenesis experiments.

Thanks for pointing this out. In the revised manuscript, we examined cargo binding to the retromer in each retromer subunit mutant (Fig. 4E, 4F, S2E, and S2F were added in the revised manuscript) and show that cargo binding of

retromer requires both Vps26 and Vps35. There were two reasons to investigate cargo-binding by Vps26, firstly it is an arrestin-type protein and therefore a good candidate for cargo-binding by analogy with other arrestin proteins and secondly the crystal structure of cargo-bound to Vps26 has been reported (Lucas et al., 2016), thus enabling predictions based on the structural data. How Vps35 interacts with the cargos will be the focus of future studies.

Initially they mutated I251 and F368, based on the 2016 X-ray crystallography structure of a partial mammalian retromer complex that was co-crystalized with a peptide derived from a cargo protein, which contains a ΦX[L/M/V] motif, YLL. The structure showed that I251 and F368 are in contact with the YLL motif, suggesting that they help to form the cargo binding site. However, in September 2018, a new retromer structure was solved by cryo-EM tomography (PubMed 27889239).The authors do not cite that study, but it is extremely relevant to their own work, not least because it is of a fungal complex. An important difference between fungi (including yeast) and mammals is that in fungi, the SNX/BAR proteins are stably associated with the Vps26-Vps29-Vps35 core. Interestingly, in

the fungal structure, the SNX/BAR protein Vps5 occludes the putative cargo-binding pocket in Vps26. Thus, there is a strong possibility that the mutations the authors made in Vps26 prevented the binding of Vps5, and thus that effects on cargo recognition are indirect. The authors go on to make additional mutations in Vps26, but the same caveat applies: these mutations could also affect cargo recognition indirectly.

As suggested by the reviewer, we performed CoIP analysis and confirmed that the Vps5-Vps26 interaction was unaffected in the *vps26* mutants (Fig. 5E was added to the revised version.). We have also discussed the differences with the Cryo-EM structure in the text.

The authors end by concluding that retromer cargo proteins have bipartite recycling signals, making their recognition more specific. This is a sensible conclusion, but it is not a new one: over 20 years ago, Cooper and Stevens proposed that Vps10 has more than one retrieval signal (PubMed 8636229).

Cooper and Stevens showed that $Y_{77}A/F_{106}A$ mutants exhibited a stronger CPY missorting phenotype than $Y_{77}A$ ($Y_{77}A/F_{106}A$: 49%, $Y_{77}A$: 36%). From this result, they concluded "Y_{77} and F_{106} signal plays a major role in the membrane trafficking of Vps10p yet other residues are likely to contribute". We directly examined Vps10-GFP localization of these mutants. We found that $Y_{77}A$ (Y1492A) mutants showed a partial recycling defect (Fig. Rev. 3). However, we could not see a clear difference between $Y_{77}A$ (Y1492A) and $Y_{77}A/F_{106}A$ (Y1492A/F1521A) mutants.

In our study, we found that 1428-FGEIRL-1433 and 1492-YSSL-1495 motifs of Vps10 are required for retromer recognition. Importantly, when we mutated both motifs (FGEIRL>AAAAAA and YSSL>AAAA), this double mutant did not show any detectable punctate structures (Fig. 2C), suggesting that these two motifs are major recycling motifs for Vps10 (Fig. 2C and Fig. 2D). Also, the other retromer cargo, Ear1, also has two discontinuous motifs, 453-PPGFEF-458 and

473-INL-475, sufficient for its recycling mediated by the retromer complex.

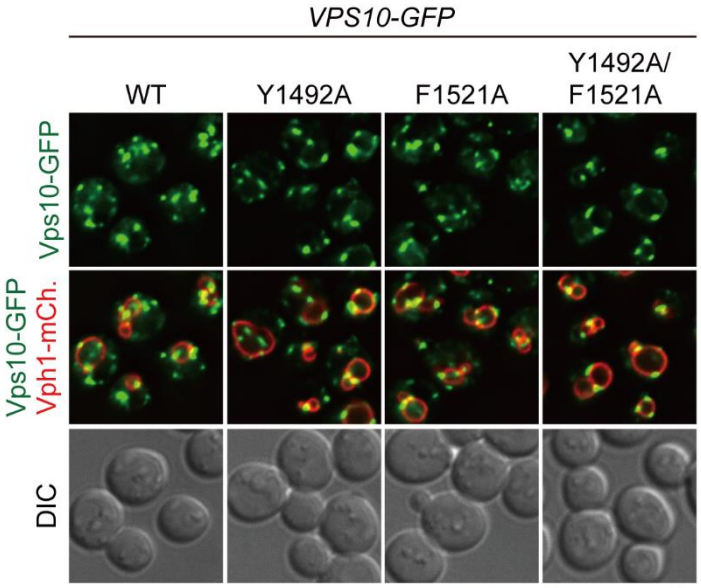
VPS10-GFP
WT
Y1492A
F1521A
Y1492A/
F1521A
Vps10-GFP
Vps10-GFP
Vph1-mCh.
DIC

Fig. Rev. 3

They then point out that the AP-1 and AP-2 complexes can recognize both YXXΦ motifs and [D/E]XXXL[L/I] motifs, and they suggest that bipartite signal recognition may be a general mechanism in membrane trafficking. However, this is not really a good comparison, because YXXΦ motifs and [D/E]XXXL[L/I] motifs can act in isolation (PubMed 20214754 and 28003333). Moreover, YXXΦ sequences are almost as common as ΦX[L/M/V] sequences, but for them to act as sorting signals, they need to be within an unstructured cytoplasmic domain of a transmembrane protein, and this is a lot less common. In addition, although coincidence detection is certainly important in membrane trafficking pathways, the coincidences do not have to be within the cytoplasmic domain of a single membrane protein. Interactions with phosphoinositides and small GTPases are important for getting the trafficking machinery onto the right membrane in the first place, where it can then find its cargo, and this applies equally well to retromer and to AP complexes.

We know that YXXΦ motifs and [D/E]XXXL[L/I] motifs can act in isolation. However, there are examples of membrane proteins containing both signals

(Kozik et al., 2010) and the conformational change induced in AP2 when it binds D/ExxLL motifs could facilitate further binding to YxxL. To avoid confusion, we have deleted this discussion.

In summary, the authors have generated some useful data, and future studies will no doubt show how the sequences they have identified actually function. But the present study is more of a collection of observations than an insight into actual mechanisms.

If the authors are invited to submit a revised version, these are the most important points to be addressed:

1. Clarify what is and what isn't supposed to be a canonical ΦX[L/M/V].

As mention earlier, we used ΦX[L/M/V] as a consensus motif defined by the

mammalian retromer cargos (Cullen and Steinberg, 2018). However, we realized that 4 out of 8 identified recycling signals in yeast such as YSSL of Vps10, FQFND of Ste13, YEF of Kex2, and WKY of Stv1 do not follow this rule (Fig. S1A was added in the revised version). Hence, the yeast recycling sequence does not follow the ΦX[L/M/V] consensus. Defining the consensus sequence will be the focus of our future investigations.

2. Take the new cryo-EM structure into account.

Collins lab with others recently solved the Cryo-EM structure of *C. thermophilum* Vps5-Vps5-Vps26-Vps29-Vps35 complex (Kovtun et al., 2018). However, we believe that this Cryo-EM structure and the yeast retromer structure are different for the following reasons. In the Cryo-EM structure, the CSC (Vps26-Vps29-Vps35 complex) and the SNX-BAR dimers (Vps5-Vps17 complex) form a complex through the Vps5-Vps26 interaction, which is a sole contact between CSC and SNX-BAR dimers. Vps29 and Vps35 do not interact with the SNX-BAR

dimer, which suggests that Vps29 and Vps35 require Vps26 to interact with the SNX-BAR dimer. However, it has been reported that SNX-BAR (Vps5) still interacts with Vps29 and Vps35 in vps26Δ cells (Reddy and Seaman, 2001; Seaman and Williams, 2002). Also, in the Cryo-EM structure, Vps26 directly interacts with SNX-BAR (Vps5), which would mean that Vps26 does not require Vps29 or Vps35 for the interaction with SNX-BAR (Vps5). However, Collins himself previously reported that Vps26 requires Vps29 to interact with SNX-BAR (Vps17) (Collins et al., 2005). Also, the Seaman lab has reported that Vps26 fails to interact with SNX-BAR (Vps5) in vps29Δ (Reddy and Seaman, 2001; Seaman and Williams., 2002). Importantly, in the Cryo-EM structure (Kovtun et al., 2018), this L252 residue of Vps29, which is required for binding to the SNX-BAR dimer (Collins et al., 2005), does not face towards any of other retromer subunit including SNX-BAR dimer (Fig. Rev. 4A and 4B). Unfortunately, Kovtun et al. did not cite these previous observations in their Cryo-EM study (Kovtun et al., 2018). Also, they did not confirm whether Vps5 directly interacts with Vps26 in vivo (Kovtun et al., 2018). We examined the retromer complex formation in the revised manuscript to ask if the model suggested by the Cryo-EM structure fits

with the IP results (Fig Rev.5; IP results were added to the revised version as Fig. 4B). We tagged *VPS5* and *VPS17* at their endogenous locus with FLAG and HA epitopes, respectively. We confirmed that Vps10 is recycled in this strain, implying that Vps5-FLAG and Vps17-HA are functional. When we immunoprecipitated Vps5-FLAG from yeast cell lysates, Vps17-HA, Vps26, Vps29, and Vps35 co-precipitated. Strikingly, Vps17-HA, Vps29, and Vps35 still co-precipitated with Vps5-FLAG in vps26Δ cells. On the other hand, the association of Vps26 with Vps5-FLAG was abolished in vps29Δ or vps35Δ cells. These results strongly suggest that the CSC interacts with the SNX-BAR dimer through Vps29 and Vps35, and not through Vps26. This conclusion is consistent with the previously published results by Seaman's lab (Reddy and Seaman., 2001; Seaman and Williams., 2002) and Collins's lab (Collins et al., 2005), but inconsistent with the Cryo-EM structure (Kovtun et al., 2018). Based on this finding, we conclude that complex formation of yeast retromer and C. thermophilum Vps5-Vps5-Vps26-Vps29-Vps35 are probably different. Hence, we were unable to take the Cryo-EM data into account in our models. It is interesting to note also that a recent study from the Jackson Lab has indicated that retromer

can form more diverse structures than the Kovtun et al. study indicated and the angle of the CSC related to the SNX-BAR dimer is more variable hinting at a dynamic and/or flexible arrangement of the retromer subcomplexes (Kendal et al., 2019 -https://doi.org/10.1101/639575)

The recent Cryo-EM structure is also inconsistent with other previous observations. The retrieval of several cargos (i.e. Kex2, Ste13, Pep12, Ear1 etc.) is known to require Snx3 (Fig. Rev. 6). Snx3 interacts with retromer through Vps26 (Lucas et al., 2016). However, this Snx3 binding site on Vps26 is used for Vps5 binding (Kovtun et al., Nature 2018). Also, the DMT1-II (cargo) binding site determined by crystal structure and also confirmed by in vivo experiments is used for Vps5 binding (Kovtun et al., 2018). These inconsistencies support our interpretation that yeast retromer and the Cryo-EM structure are different.

Several possibilities may explain why assembly of the C. thermophilum Vps5-Vps5-Vps26-Vps29-Vps35 complex and the yeast retromer are different. It could

be because components of the Cryo-EM structure and yeast retromer complex are different. Yeast retromer complex consists of Vps5, Vps17, Vps26, Vps29, and Vps35. All of them have a 1:1:1:1:1 stoichiometry. On the other hand, Kovtun et al. used two Vps5, Vps26, Vps29, and Vps35. They did not use Vps17 and in essence therefore did not report the structure of 'retromer'. In yeast, Vps5 makes a heterodimer with Vps17 (Horazdovsky et al., 1997; Seaman et al., 1998). However, Kovtun et al. claimed (without evidence) "Vps17 is likely to be structurally homologous to Vps5, in which case a heterodimeric array of Vps5 and Vps17 would form through equivalent contacts". However, vps17Δ cells exhibit a strong CPY missorting phenotype like vps5Δ cells (Horazdovsky et al., 1997). Also, we confirmed that Vps5 is unable to interact with Vps5 even in the absence of Vps17 (Fig. Rev. 7). These facts strongly suggest that the Vps5-Vps5 interaction and Vps5-Vps17 interaction are different. To answer this question, solving the retromer structure consisting of Vps5, Vps17, Vps26, Vps29, and Vps35 is essential.

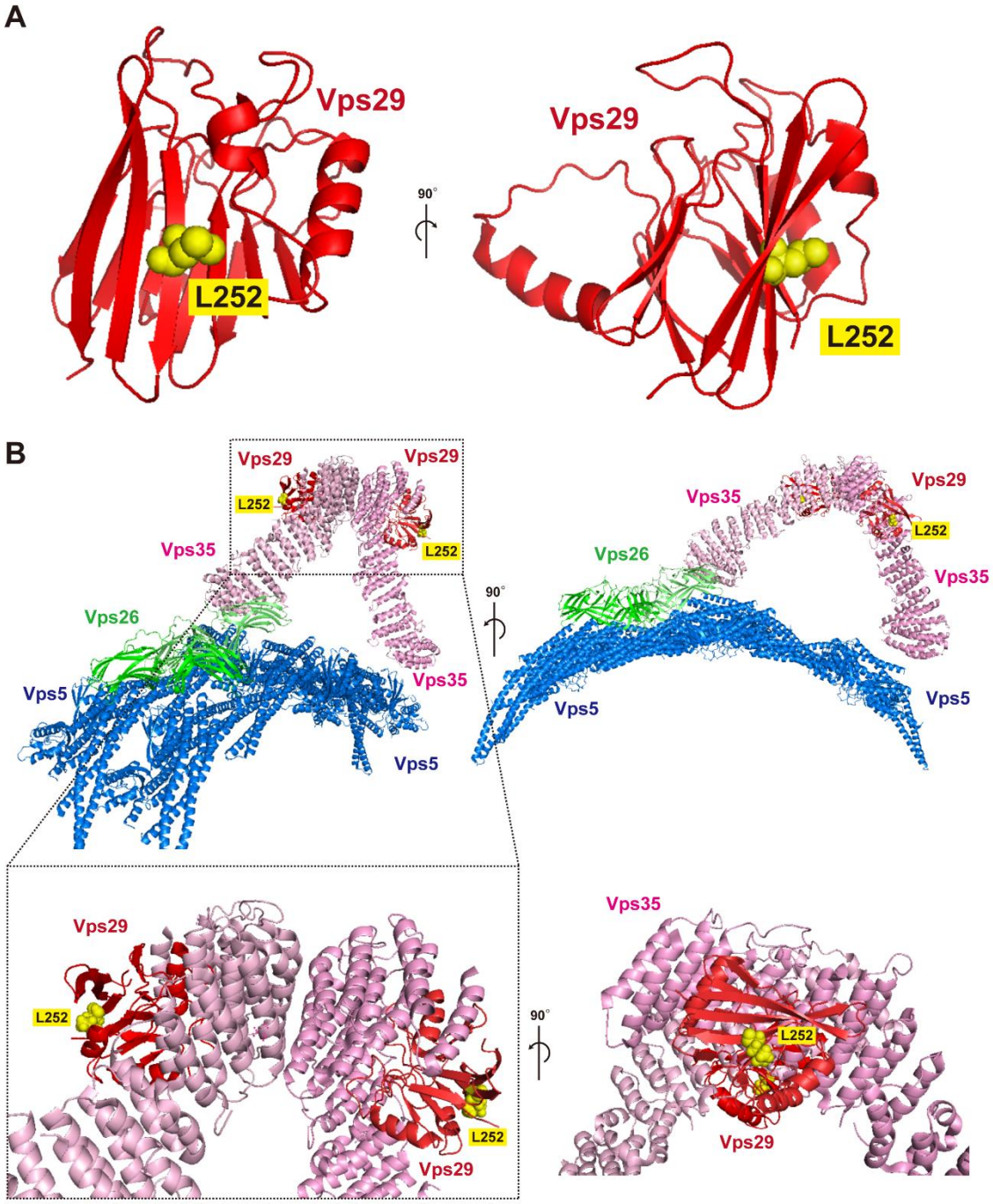
A
Vps29
L252
90°
Vps29
L252
B
Vps29
Vps29
L252
L252
Vps35
Vps26
Vps5
Vps35
Vps5
90°
Vps29
Vps35
L252
Vps26
Vps35
Vps5
Vps5
Vps29
L252
L252
Vps29
90°
Vps35
L252
Vps29

Fig. Rev. 4

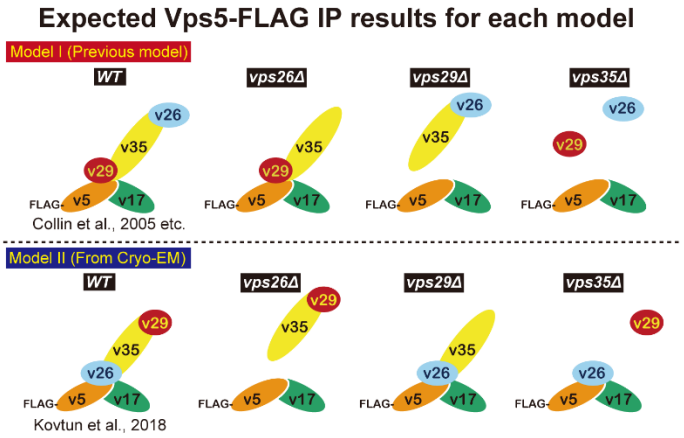

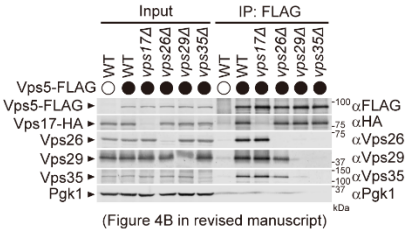

Fig. Rev. 5

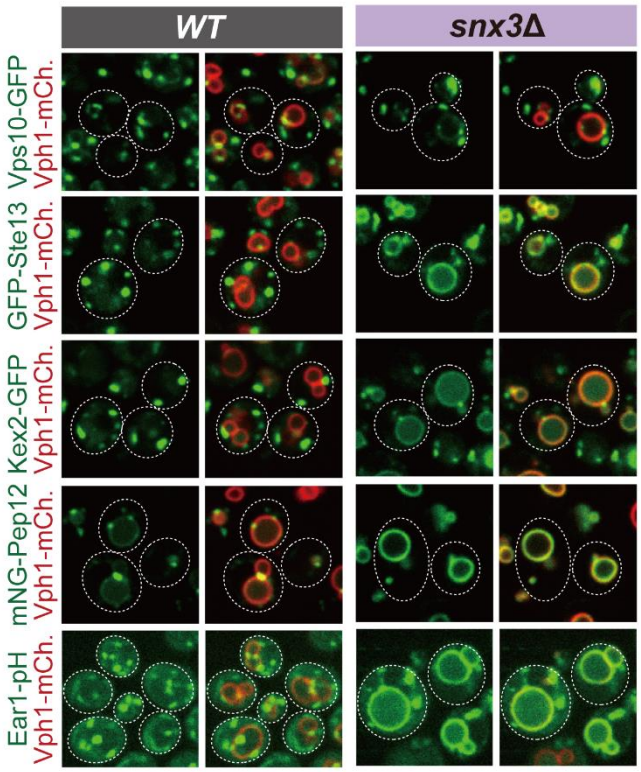

Fig. Rev. 6

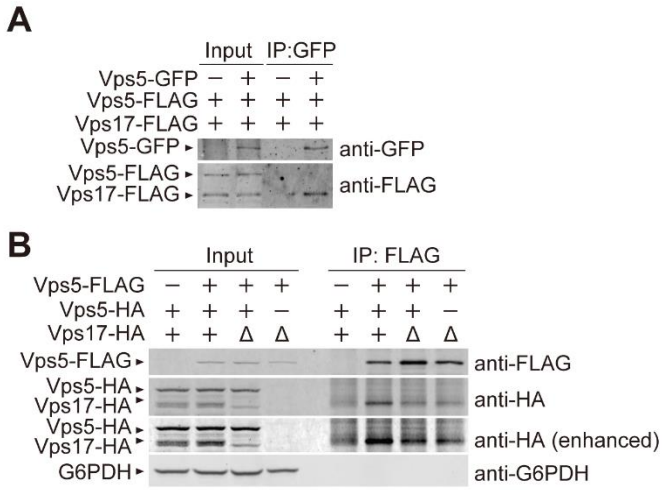

Fig. Rev. 7

3. Test by immunoprecipitation whether any of their Vps26 mutations affect assembly of the complex.

As mention above, we examined the retromer complex formation in our mutants and confirmed that our mutations do not affect it (Fig. 5E was added to the revised version.).

4. Provide evidence for a direct interaction between Vps26 and sorting signals.

To investigate this interaction, we examined Vps10 binding to the retromer complex by CoIP analysis (Fig. 2E was added in the revised manuscript). Wild-type Vps10-GFP was co-precipitated with Vps26-FLAG, but a Vps10 sorting signal mutant did not, suggesting that the sorting signal is required for the interaction with retromer. To determine whether this binding is mediated by Vps26, we tested this interaction in retromer subunit mutants (Fig. 4E, 4F, S2E, and S2F were added in the revised manuscript) and found that Vps26 is essential for cargo binding. Furthermore, we examined cargo binding of retromer in a Vps26(F334E) mutant. In this mutants, retromer is assembled normally (Fig. 5E was added in the revised manuscript), but cargo binding is impaired (Fig. 5F was added in the revised manuscript). Collectively, we propose that Vps26 directly interacts with the sorting signals.

Reviewer #3 (Comments to the Authors (Required)):

Review Suzuki et al., 2019, JCB

In the present study, Suzuki et al. investigate how the yeast hydrolase transporter, the Vps10 receptor, is recognized and retrogradely transported through the retromer complex. Using extensive mutagenesis and an imaging based sorting assay, they thoroughly dissect the sorting requirements for VPS10 (and Ear1) to conclude that retromer requires a complex, bipartite sequence to retrieve these receptors from the vacuolar pathway.

The mutagenesis and sorting data are clean, very convincing and leave little doubt about the identified sorting signal. Given that recent data on the mammalian retromer and the Vps10p equivalent CI-MPR has caused considerable confusion in the field, the study is also timely and of importance for the field. The report format is appropriate as the authors report a single finding

with considerable impact.

Thank you!

The only weakness of the study is the use of a single assay to identify and verify the sorting requirements. All the results are based on mutagenesis of either Vps10 or VPS26 and imaging based analysis of retrograde sorting. Given that the retromer associated SNX-BAR proteins have recently been shown to directly bind CI-MPR (Kvainickas et al., 2017/ Simonetti et al, 2017) it would be great if the authors could use a biochemical approach to verify that the Vps10 tail indeed binds to the core retromer trimer and not to the Vps5/Vps17 subunit. At present, the data do not fully exclude that Vps10 binds to Vps5 or Vps17 as the mutagenesis of VPS26 could also disrupt retromer function in an unspecific way. A binding assay between purified Vps10 tail and retromer components could then also be used to test whether the sorting motif within Vps10 that was identified through mutagenesis and imaging indeed mediates the binding. At least for the

mammalian proteins, the VPS29/VPS35/VPS26 and the SNX-BAR subcomplexes can be individually expressed and purified. In my opinion, it would really strengthen the study if the authors showed some form of binding assay with the wildtype and mutant Vps10 tail with the individual retromer subcomplexes. This could be a GST pulldown with recombinant and purified proteins or maybe even co-IPs from mammalian HEK293 cells if the proteins express poorly in bacteria.

As suggested by the reviewer, we first tried a GST pulldown assay by using recombinant proteins. However, we could not detect a Vps26-Vps10^{tail} interaction (Fig. Rev. 8). In this assay, we used GST-Chs3^{tail} as a control, because the Burd lab successfully detected the Vps26-Chs3 interaction by this vitro binding assay (Cui et al., 2017). However, although we used the same construct (GST-Chs3^{tail} construct from Fromme lab used in Cui et al., 2017), we could not detect the Vps26-Chs3 interaction. Hence, we tried to examine the cargo binding of retromer by in vivo CoIP analysis. We expressed Vps10-GFP and Vps26-FLAG, and performed immunoprecipitation experiments. Vps10-GFP efficiently co-

immunoprecipitated Vps26-FLAG (Fig. 2E added to the revised manuscript). However, sorting signal mutants (1428-1433A/1492-1495A double mutants) did not co-precipitate with Vps26-FLAG. Furthermore, cargo binding of retromer was observed in vps5Δ, vps17Δ, or vps29Δ, but it was not detected in vps26Δ or vps35Δ (Fig. 4E and 4F were added in the revised manuscript). These results suggest that the Vps10 sorting signal is required for the association with the retromer complex and that this association requires the CSC (Vps26 and Vps35), not the SNX-BAR dimer (Vps5 and Vps17).

To directly assess whether the SNX-BAR dimer interacts with cargo, we also examined the cargo binding of the SNX-BAR dimer in vps29Δ cells, because in this mutant, the SNX-BAR dimer is formed, but cannot interact with the CSC (Fig. 4B was added in the revised manuscript). In WT cells, SNX-BAR dimer (Vps5-FLAG) was able to interact with cargos (Vps10-GFP) (Fig. S2E and S2F was added in the revised manuscript). However, the Vps5-Vps10 interaction was abolished in vps29Δ cells. This data also strengthen our conclusion that the cargo is recognized by the CSC, not the SNX-BAR dimer.

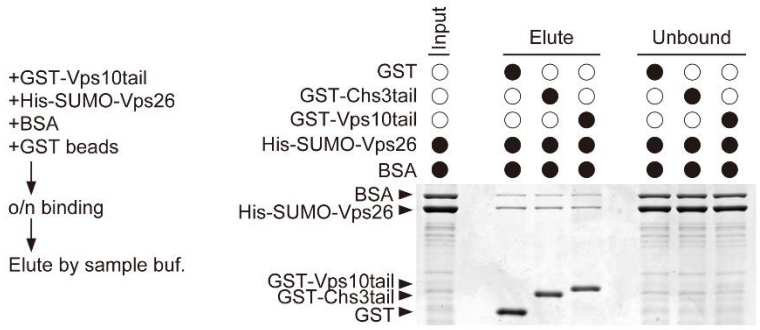

Fig. Rev. 8

Some additional minor points:

In the introduction, the authors state that the Parkinson associated VPS35-D620N mutant causes lysosomal dysfunction. I am not sure whether this has been conclusively shown. The data from the D620N knock-in mouse (Ishizu et al., 2016) strongly suggests that the D620N mutant is an extremely subtle loss of

function mutant even in D620N homozygous mice. It is unlikely to cause significant lysosomal dysfunction as it retains most cargo sorting functions.

Thanks for pointing this out. Indeed, Ishizu et al. did not observe any lysosomal dysfunction. However, Follett et al. and McGough et al. observed mislocalization of CatD or M6PR, respectively (Follett et al., 2013; McGough et al., 2014). We revised the manuscript to reflect this (Page 2, paragraph 2, line 13).

At the end of the results section, the authors state that SNX3 is recruited to the endosomal membrane via binding to VPS26. Given that SNX3 has intrinsic lipid binding capabilities through its PX domain and has been shown to mediate retromer recruitment together with RAB7-GTP (Harrison et al., 2014, PNAS), this is really surprising. The authors cite Lucas et al. in this context, but that study also only shows the recruitment of retromer via SNX3, not the other way around?

Thank you for pointing this out. Mammalian SNX3 is recruited to the endosomal

membrane in a PI3P dependent manner, allowing retromer recruitment on the endosome (Lucas et al., 2016). However, yeast Snx3 is also recruited to the endosomal membrane in a PI3P dependent manner (Strochlic et al., 2007), but this PI3P binding is not sufficient. The endosomal localization of Snx3 requires at least Vps26 (Fig. Rev. 9A). On the other hand, Vps26 localization to the endosome does not require Snx3 (Fig. Rev. 9B). Thus, yeast Snx3 requires both lipid binding and Vps26 binding for its recruitment to the endosome, but the endosomal localization of retromer does not require Snx3. This conclusion is consistent with the result that the retromer complex can recycle Vps10 even in snx3Δ cells (Fig. Rev 6). Collectively, the yeast retromer complex (Vps5-Vps17-Vps26-Vps29-Vps35 complex) is recruited onto the endosomal membrane in a Snx3 independent manner, whereas Snx3 is recruited onto the endosomal membrane through both Vps26 and PI3P binding.

In the original manuscript, we had examined Snx3-GFP localization to evaluate retromer complex formation in vps26 mutants. However, we have now directly assessed retromer complex formation by CoIP experiments (Fig. 5E was added

to the revised manuscript), and have included this in the revised manuscript.

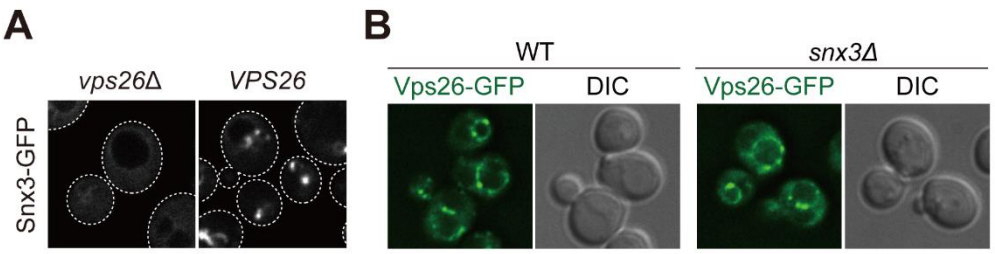

Fig. Rev. 9